University of Alberta

EXPRESSION PATTERNS OF GENES INVOLVED IN COPPER TRANSPORT

©

by

Steven D. P. Moore

A thesis submitted to the Faculty of Graduate Studies and Research in partial fulfillment of the requirements for the degree of Doctor of Philosophy

In

Medical Sciences - Medical Genetics

Edmonton, Alberta

Fall 2002

National Library of Canada
Acquisitions and Bibliographic Services
395 Wellington Street
Ottawa ON K1A 0N4
Canada

Bibliothèque nationale du Canada
Acquisitions et services bibliographiques
395, rue Wellington
Ottawa ON K1A 0N4
Canada

Your file Votre référence

Our file Notre référence

The author has granted a non-exclusive licence allowing the National Library of Canada to reproduce, loan, distribute or sell copies of this thesis in microform, paper or electronic formats.

The author retains ownership of the copyright in this thesis. Neither the thesis nor substantial extracts from it may be printed or otherwise reproduced without the author's permission.

L'auteur a accordé une licence non exclusive permettant à la Bibliothèque nationale du Canada de reproduire, prêter, distribuer ou vendre des copies de cette thèse sous la forme de microfiche/film, de reproduction sur papier ou sur format électronique.

L'auteur conserve la propriété du droit d'auteur qui protège cette thèse. Ni la thèse ni des extraits substantiels de celle-ci ne doivent être imprimés ou autrement reproduits sans son autorisation.

0-612-81245-6

Canada

University of Alberta

Library Release Form

Name of Author: Steven Dennis Pfau Moore

Title of Thesis: Expression Patterns of Genes Involved in Copper Transport

Degree: Doctor of Philosophy

Year of Degree Granted: 2002

Permission is hereby granted to the University of Alberta Library to reproduce single copies of this thesis and to lend or sell such copies for private, scholarly or scientific research purposes only.

The author reserves all other publication and other rights in association with the copyright in the thesis, and except as herein before provided, neither the thesis nor any substantial portion thereof may be printed or otherwise reproduced in any material form whatever without the author's prior written permission.

3412 Stearns Hill Road
Waltham, MA. USA
02451

August 20, 2002

University of Alberta

Faculty of Graduate Studies and Research

The undersigned certify that they have read and recommended to the Faculty of Graduate Studies and Research for acceptance a thesis entitled "Expression patternsof genes involved in copper transport" submitted by Steven D.P. Moore in partial fulfillment for the degree of Doctor of philosophy in Medical Sciences-Medical Genetics .

Diane W. Cox

Moira Glerum

Michael Walter

Martin Somerville

David Pilgrim

August 19, 2002

Seymour Packman

DEDICATION

I would like to dedicate this to my beautiful wife for her years of support and patience. From my first post-secondary exam to my thesis defense, she has stood by me through every delay and every success.

ABSTRACT

Copper is biologically important as an essential cofactor in many proteins. However, because of its oxidative potential, copper levels are tightly regulated. Wilson disease, associated with mutations in *ATP7B*, results from an accumulation of copper due to dysfunctional bile copper excretion. In contrast, Menkes disease, associated with mutations in *ATP7A*, is caused by copper deficiency due to a decrease in intestinal absorption of copper. I have chosen to use the mouse model system to investigate expression patterns of genes involved in copper homeostasis based on its similarity to the human system.

At the onset of this thesis project, some of the genes involved in mammalian copper transport had been identified. Additional genes had been identified from studies in yeast, leading to the identification of human and murine orthologues. In yeast, the chaperone for superoxide dismutase (CCS), which delivers copper to the free radical scavenger superoxide dismutase (SOD1), was identified in human, but was not yet identified in mice. Therefore, I isolated, sequenced, and mapped the mouse orthologue to *CCS* (*Ccsd*). In addition, I have shown that *Ccsd*/*CCS* are ubiquitously expressed.

Another gene implicated to have an important role in copper transport is *Atox1*. This mammalian protein was identified as a chaperone that is able to deliver copper to Atp7b and Atp7a. Its physiological roles in liver and kidney were not well defined. I have determined its pattern of expression in these tissues. In the liver, Atox1 is expressed in hepatocytes surrounding hepatic and central veins. Within the kidney, Atox1 co-localizes with the copper transporter Atp7b in the glomeruli and loops of Henle.

These studies have added to our knowledge of the role of specific proteins, particularly copper chaperones. In the kidney, the accumulation of copper in Wilson disease patients occurs downstream of ATOX1 and ATP7B expression. This suggests copper accumulates either by a localized transporter dysfunction in the glomeruli or an increase in copper associated low molecular weight substances that are capable of entering the glomerular sieve. Hepatic and renal expression of Atox1 overlaps with ATP7B, supporting the assumption that this is the chaperone for ATP7B.

ACKNOWLEDGEMENTS

In particular I would like to thank my supervisor, Dr. Diane Cox, for the opportunity to work in her lab and all her advice over the past years. She provided a research environment that has allowed me to develop independent scientific thought that will be instrumental for my future success.

I would also like to thank those people whose work contributed to my research: Dr. Heather McDermid for providing the adult mouse cDNA library, Dr. David McFayden for assistance with the radiation hybrid panels. I also thank Dr. David Rayner (University of Calgary) for his help in analysis of kidney and liver expression patterns, Dr. Derrick Rancourt for his assistance with the *in situ* hybridization protocol, and Karmon Helmle for assistance with mouse immunohistochemistry. I thank Dr. B. Sarkar and coworkers (Zang Xuefeng, Suree Narindrasorasak, and Dr. Eve Roberts), The Hospital for Sick Children, Toronto, for providing purified protein used in ATOX1 antibody production. I would also like to thank Dr. Joe Casey for protocols and reagents used for protein purification; Susan Kenney for automated LiCor sequencing, and the University of Alberta Health Sciences Laboratory Animal Services personnel for protocols and animal handling. I thank the numerous physicians and patients who provided samples for analysis.

Dr. Michael Walter and Dr. Moira Glerum, members of my supervisory committee, deserve my special gratitude for their extreme helpfulness and support during my research.

I would like to thank the National Sciences and Engineering Research Council and the Canadian Genetic Diseases Network for operating funding. I would especially like to thank the Canadian Liver Foundation and the Canadian Institutes of Health Research for doctoral research scholarships throughout my postgraduate training.

TABLE OF CONTENTS

CHAPTER 1: INTRODUCTION 1

1.1) MAMMALIAN COPPER TRANSPORT 2

1.1.1) Overview of the role of copper 2

1.1.2) Copper transport via the blood 6

1.2) YEAST COPPER TRANSPORT 8

1.3) COPPER TRANSPORTERS AND RELATED DISEASES 14

1.3.1) Menkes disease and animal models 14

1.3.2) Wilson disease and animal models 18

1.3.3) Canine copper toxicosis 25

1.3.4) Ctr1 and animal model 26

1.4) COPPER CHAPERONES AND THEIR POTENTIAL ROLES 27

1.4.1) ATOX1, putative copper chaperone for ATP7A and ATP7B 27

1.4.2) Ccsd and delivery to superoxide dismutase 32

1.4.3) Cox17 and delivery of copper to cytochrome c oxidase 35

1.5) TISSUE EXPRESSION OF GENES INVOLVED IN COPPER TRANSPORT 36

1.5.1) Distribution of Atp7a 36

1.5.2) Distribution of Atp7b 37

1.5.3) Distribution of Atox1 40

1.6) HYPOTHESES AND AIMS OF THESIS 42

1.7) REFERENCES 44

CHAPTER 2: COPPER CHAPERONE FOR SUPEROXIDE DISMUTASE (Ccsd) 62

2.1) INTRODUCTION 63

2.2) MATERIALS AND METHODS 64

2.2.1) Human CCS probe 64

2.2.2) Screening cDNA library 65

2.2.3) Subcloning and Sequencing 65

2.2.4) Mapping mouse Ccsd 66
2.2.5) Mapping human CCS 66
2.2.6) Northern blot analysis 66
2.3) RESULTS 67
2.3.1) Screening mouse cDNA library 67
2.3.2) Mapping CCS/Ccsd 71
2.3.3) Mouse/Human expression pattern 71
2.4) DISCUSSION 75
2.5) REFERENCES 76

CHAPTER 3: EXPRESSION IN MOUSE KIDNEY OF COPPER TRANSPORTERS Atp7a AND Atp7b 77
3.1) INTRODUCTION 78
3.2) METHODS AND MATERIALS 79
3.2.1) Construction of Atp7b probes 79
3.2.2) Probe characterization 80
3.2.3) Preparations of tissue sections 81
3.2.4) In situ hybridization 82
3.254) Immunohistochemistry 83
3.3) RESULTS 84
3.3.1) RNA probes 84
3.3.2) Non-radioactive in situ hybridization of Atp7b in mouse kidney 84
3.3.3) Immunohistochemistry of ATP7B.N60 in mouse kidney 91
3.4) DISCUSSION 91
3.5) REFERENCES 99

CHAPTER 4: STUDIES OF THE COPPER CHAPERONE ATOX1 101
4.1) INTRODUCTION 102
4.2) MATERIALS AND METHODS 103
4.2.1) ATOX1 cDNA construction 103
4.2.2) Antibody production 104

4.2.3) Tissue section preparation and immunohistochemistry 104
4.2.4) Tissue expression during mouse development 105
4.3) RESULTS 106
4.3.1) ATOX1 antibody 106
4.3.2) Immunohistochemistry 106
4.3.2) Mouse developmental northern blot 112
4.4) DISCUSSION 116
4.5) REFERENCES 120

CHAPTER 5: SEQUENCING FOR ATOX1 MUTATIONS IN SELECTED PATIENTS 122
5.1) INTRODUCTION 123
5.2) METHODS AND MATERIALS 123
5.2.1) ATOX1 BAC isolation and sequencing 123
5.2.2) Sequencing of ATOX1 in patients 124
5.3) RESULTS 125
5.3.1) BAC isolation 125
5.3.2) Sequencing of ATOX1 in selected patients 128
5.4) DISCUSSION 128
5.5) REFERENCES 131

CHAPTER 6: GENERAL DISCUSSION AND CONCLUSIONS 132
6.1) COPPER CHAPERONE FOR SUPEROXIDE DISMUTASE 134
6.2) ATOX1 EXPRESSION 136
6.2.1) Liver 136
6.2.1.1) Future directions 137
6.2.2) Kidney 137
6.2.2.1) Future directions 140
6.2.3) ATOX1 co-expression with ATP7A and ATP7B 140
6.2.3.1) Future directions 143
6.3) MODELS FOR RENAL COPPER HOMEOSTASIS 144

6.4) PLACENTA AND DEVELOPMENT 147
6.4.1) Developmental expression 147
6.4.2) Atox1 co-expression with ATP7B 147
6.4.3) Future directions 149
6.5) FINAL CONCLUSIONS 150
6.6) REFERENCES 152

APPENDICES 157
A.1) PRIMERS 158

A.2) PATIENT LIST FOR ATOX1 MUTATION SCREENING 160

LIST OF TABLES

Table 1-1: Copper dependent proteins 3

Table 1-2: Copper concentrations in Wilson and Menkes disease 9

LIST OF FIGURES

Figure 1-1: Chemical reactions 4

Figure 1-2: Copper absorption and distribution pathway 7

Figure 1-3: Copper transport pathway in *Saccharomyces cerevisiae* 11

Figure 1-4: Model of P-Type ATPase copper transporter ATP7B 21

Figure 1-5: Surface representation model of ATOX1 28

Figure 1-6: Mechanism of copper transfer between ATOX1 and receptor protein 30

Figure 1-7: Structure of yeast Lys7p 33

Figure 2-1: Mouse Ccsd open reading frame (ORF) 68

Figure 2-2: *Ccsd/CCS* amino acid sequence alignment 69

Figure 2-3: Hydrophobicity plots for mouse Ccsd and human CCS 70

Figure 2-4: Chromosomal localization of *Ccsd* 72

Figure 2-5: Chromosomal localization of CCS 73

Figure 2-6: Expression of mouse and human copper chaperones for SOD1. 74

Figure 3-1: Mouse multiple tissues northern blot analysis for Atp7a, Atp7b and Atox1 85

Figure 3-2: RNA probe verification for size and Digoxygenin incorporation 86

Figure 3-3: pGEM-T Easy vector restriction map 87

Figure 3-4: *In situ* hybridization of *Atp7a* in mouse kidney 89

Figure 3-5: *In situ* hybridization of *Atp7b* in mouse kidney 90

Figure 3-6: Western blot analysis of mouse lysates with antibody ATP7B.N60 92

Figure 3-7: Immunohistochemistry in mouse kidney using antibody ATP7B.N60 93

Figure 3-8: Schematic representation of Atp7a and Atp7b in mouse kidney 98

Figure 4-1: Western blot using ATOX1 antibody 107

Figure 4-2: Detection of Atox1 in whole mouse liver 109

Figure 4-3: Fluorescent detection of (hepatic) Atox1 in mouse liver 110

Figure 4-4: Immunohistochemistry in mouse liver using ATOX1 antibody and ATP7B.N60 antibody 111

Figure 4-5: Localization of Atox1 protein in mouse kidney 113

Figure 4-6: Localization of Atox1 protein in mouse placenta 114

Figure 4-7: Northern blot of mouse embryo during prenatal development 115

Figure 5-1: Human BACs containing genomic ATOX1 sequence 126
Figure 5-2: Genomic structure of ATOX1 (human) 127
Figure 6-1: Schematic of glomerular sieve 139
Figure 6-2: Schematic diagram comparing Atp7a, Atp7b, and Atox1 expression in mouse kidney 142
Figure 6-3: Models of renal copper homeostasis 147

LIST OF SYMBOLS, NOMENCLATURE, OR ABBREVIATIONS

Δ	Deletion or disruption
ATP	Adenosine triphosphate
Atp7a	Mouse P-type ATPase copper transport protein
ATP7A	Human P-type ATPase copper transport protein
Atp7a	Mouse gene for P-type ATPase copper transport protein
ATP7A	Human gene for P-type ATPase copper transport protein
bp	Base pair
cM	Centimorgan
CNS	Central nervous system
cR	Centiray
CuMT	Copper bound metallothionein
DHBA	Dihydroxybenzoic acid
DNA	Deoxyribonucleic acid
EST	Expressed sequence tag
FALS	Familial amyotrophic lateral sclerosis
kDa	Kilodalton
kb	Kilobase
LO	Lysyl oxidase
LEC	Long Evans cinnamon
MT	Metallothionein
RNA	Ribonucleic acid
SA	Salicylic acid
SOD1	Superoxide dismutase

CHAPTER 1

INTRODUCTION

1.1) MAMMALIAN COPPER TRANSPORT

1.1.1) Overview of the role of copper

The body of a healthy, 70 kg human adult contains approximately 110 mg of copper (Cu) divided between many organs that utilize its redox cycle between reduced Cu^{1+} and oxidized Cu^{2+} states. The greatest proportion of copper is distributed within five major tissues including the liver (10 mg), brain (8.8 mg), blood (6 mg), skeleton (46 mg), and skeletal muscle (26 mg) (Linder et al., 1998). The majority of copper within the body is associated with active enzymes (Table 1-1).

Copper is easily absorbed and excreted from the body which may explain why, unlike iron, very little copper is stored. Enzymes that utilize the redox potential of copper for cellular function are shown in Table 1-1. These include superoxide dismutase (SOD1), lysyl oxidase, dopamine-ß-monooxygenase, ceruloplasmin, and cytochrome c oxidase. Superoxide dismutase contains zinc and copper that are critical for converting a superoxide anion into hydrogen peroxide for intracellular protection from free radicals (reviewed in Machlin and Bendich, 1987). Ceruloplasmin is a serum copper containing protein that is essential for iron mobilization (iron metabolism reviewed in Walker et al., 2001). Cytochrome c oxidase is localized in the mitochondria and carries out the terminal step in the respiratory chain, which leads to the production of ATP through the transfer of electrons to oxygen (Krab and Wikstrom, 1978). However, the extremely useful redox potential of copper can also be potentially hazardous to cellular structures (Gutteridge, 1984).

Copper catalyzes many oxidation/reduction reactions, one of which is the formation of hydroxyl radicals via the Haber-Weiss reaction (see Figure 1-1). Copper induced production of hydroxyl radicals is potentially hazardous to the intracellular

Table 1-1: Copper-dependent proteins in the human system

Protein	**Activity**	**Effects of deficient activity in humans**
Dopamine-ß-monooxygenase	Neurotransmitter	Temperature instability, hypoglycemia, eyelid ptosis, pupillary constriction
Ceruloplasmin	Iron mobilization	Decreased circulating copper levels
Tyrosinase	Pigment formation	Reduced pigmentation of hair and skin
Peptidylglycine α-amidating monooxygenase (PAM)	Activation of amidated hormones by oxidative cleavage	Reduced bioactivity of many neuroendocrine peptides
Cytochrome c oxidase	Electron transport chain	Impaired myelination, muscle weakness, neurological defects, developmental delay, psychomotor retardation
Amine oxidases - Diamine oxidase - Lysine oxidase	 -Elastin & connective tissue formation	 -Reduced histamine degradation -Decreased strength of collagen and elastin
Superoxide dismutase	Free radical scavenger	
Other copper enzymes Ascorbate oxidase Urate oxidase Galactose oxidase Hexose oxidase		

Haber-Weiss reaction

The Haber-Weiss cycle consists of the following two reactions:

$H_2O_2 + OH^{\cdot} \rightarrow H_2O + O_2^{-} + H^{+}$

$H_2O_2 + O_2^{-} \rightarrow O_2 + OH^{-} + OH^{\cdot}$

Fenton's Reaction

$H_2O_2 + Fe^{2+} \rightarrow Fe^{3+} + HO^{-} + HO^{\cdot}$

Figure 1-1: Haber-Weiss and Fenton's reactions

environment, causing lipid peroxidation, mitochondrial damage, DNA damage (double stranded breaks), and eventually apoptosis (reviewed in Bremner, 1998).

Pathological implications of copper-induced free radical generation were initially suggested in **f**amilial **a**myotrophic **l**ateral **s**clerosis (FALS). FALS is a progressive and fatal neurological disorder that results in damage to the motor neuron system. The first mutation discovered as the cause of FALS was in SOD1 (Aoki et al., 1998). Since then FALS has been associated with over seventy different mutations in SOD1 (reviewed in Gaudette et al., 2000). Initial studies indicated that SOD1 FALS mutations led to proteins that were structurally stable, but showed a significantly altered shape and an impaired ability to bind copper (Carri et al., 1994). These authors noted that the SOD1 FALS mutations enhanced apoptosis. In addition, comparing the crystal structure of SOD1 with known mutation sites, mutations seemed to only affect residues important in subunit dimerization and not residues in the catalytic site of the enzyme (Deng et al., 1993). One study demonstrated that in *sod1*$^{-}$ yeast, characteristic paraquat sensitivity was alleviated by complementing the strain with either a human wild-type SOD1 or a FALS SOD1 mutant protein (Rabizadeh et al., 1995). These data suggest that the change in neuronal survival in FALS patients is independent of their effects on SOD1 free radical scavenging activity. Nevertheless, by examining radical-generating activity of a FALS SOD1 mutant, it was discovered that these mutants have a greater hydroxyl free radical generating activity than wild-type (Yim et al., 1996; Kang and Eum, 2000). The cause of this increased generation has been linked to the inappropriate release of copper from the SOD1 protein (Goto et al., 2000). These data suggest that the increased pathological findings in motor neurons of patients with FALS is the result of oxidative damage

mediated by the activity of free radicals in a Fenton-like reaction (see Figure 1-1) due to the unregulated release of copper ions from SOD1.

Since these reports were published, additional neurological disorders have also been attributed to oxidative damage, with possible involvement of copper, including Alzheimer disease (Markesbery and Carney, 1999), Parkinson disease (Jenner and Olanow, 1996; Jenner, 1998), and Huntington disease (Browne et al., 1999). Under normal conditions, free copper is limited to less than one atom per cell (Rae et al., 1999), thereby limiting the oxidative stress.

1.1.2) Copper transport via the blood

Dietary uptake of copper of a typical adult in Western society is approximately 0.6 to 1.6 mg per day (Linder et al., 1998). Intestinal cells lining the gut, primarily in the duodenum, import copper and transfer approximately half of ingested copper into the serum (Figure 1-2). Experiments with tracer doses of radioactive copper demonstrate two phases of copper absorption from the blood (reviewed in Linder et al., 1998). In the first wave, immediately after intestinal absorption, copper enters the serum and is associated with two high molecular weight copper binding proteins, mainly albumin, and a high molecular weight complex referred to as transcuprein (Weiss and Linder, 1985). Weiss et al. also found that initial absorption did not appear to involve any low molecular weight substances. Once in the serum, radioactive copper is temporarily removed from the serum and appears both in the liver and, to a lesser extent, the kidney. In the second phase, copper re-enters the serum, bound to holoceruloplasmin secreted by the liver (Askwith et al., 1994). Copper from the serum is taken up by peripheral organs, including the heart and brain.

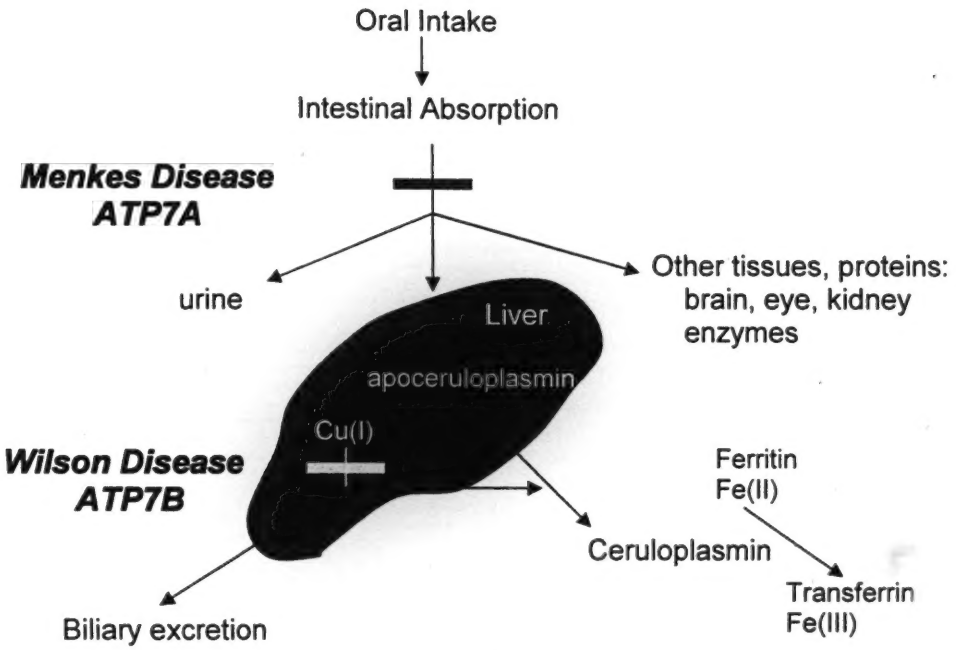

Modified from Cox. (1995)

Figure 1-2: Copper absorption and distribution pathway in humans

Holoceruloplasmin contains approximately 95% of the copper in the serum and is an essential component in iron utilization. Apoceruloplasmin is translated within the liver. After receiving copper, holoceruloplasmin is secreted into the blood. Some evidence suggests, copper-bound holoceruloplasmin is capable of being taken up by many different cell types (reviewed in Harris, 1991), however, transferable copper is thought to be bound to amino acids such as histidine. In addition, ceruloplasmin has a potent ferroxidase activity that catalyzes Fe^{2+} to Fe^{3+} oxidation, essential for the metabolism and tissue distribution of iron (Harris, 1995). Aceruloplasminemia, a rare recessively inherited disorder resulting from a dysfunctional biosynthesis of ceruloplasmin, results in massive iron accumulation in the liver and brain (Harris et al., 1995).

The liver is the major site of copper regulation, with excess copper being excreted into the bile in a form that is not readily reabsorbed (Mistilis and Farrer, 1968). There is a constant balance in copper uptake and excretion that is maintained by the absorption of copper from the intestine and the excretion of copper into the bile. The kidney also has a role in copper excretion, however, urinary copper levels are normally exceedingly low (Table 1-2). Thus the liver and kidney are of particular interest because of their central role in copper homeostasis. The membrane copper transporters, P-type ATPases, are critical for copper transport in these organs (discussed further in sections 1.3.1, 1.3.2, and 3.1).

1.2) YEAST COPPER TRANSPORT

The yeast model system has been important for the discovery of additional proteins in the copper transport pathway. A screen for mutations that affected iron

Table 1-2- Copper levels in Wilson and Menkes disease patients

Feature	Menkes Disease	Wilson disease
Inheritance	X-linked	Autosomal recessive
Copper distribution		
Ceruloplasmin (mg/l)*	< 200 (low)	< 200 (low)
Serum copper (μg/dl)**	<70 (low)	19-64 (low)
Urine copper (μg/day)***	<40 (low)	100-1000 (high)
Liver copper (μg/g dry wt)****	<50 (low)	>250 (high)
Animal model	Mottled mouse	LEC rat Toxic milk mouse

Normal ranges: *200-300 mg/l; **70-152 μg/l; ***<40 μg/day; ****20-50 μg/g dry wt.

Table from Cox (1999)

uptake led to the discovery of a gene (*CTR1*) encoding a protein that contained 11 putative copper binding motifs Met-X_2-Met and was shown to be localized to the plasma membrane, and was localized to the plasma membrane (Dancis et al., 1994). Both exogenous iron and/or copper were required to suppress the mutant phenotype, suggesting that the gene product was either directly or indirectly responsible for both iron and copper uptake. Fet3p is a mediator of high affinity ferrous iron uptake and requires copper's redox potential for its oxidase activity, thus copper uptake is required for iron uptake (Askwith et al., 1994). This was confirmed by demonstrating that ferrous iron uptake was inhibited in *ctr1* mutants (Dancis et al., 1994). Therefore, this copper-binding plasma membrane transporter was required for the uptake of copper into yeast cells; its disruption led to the downstream disruption of high affinity iron uptake.

An additional gene involved in the yeast copper transport pathway was found while screening for genes involved in respiratory defects. Cox17p was found to be necessary for cellular respiration (Glerum et al., 1996a). The translational product, Cox17p, is a small protein (approximately 8.1 kDa) containing the highly conserved CXXC motif involved in copper binding. When yeast were deficient in Cox17p, cytochromes a and a_3 were not properly assembled. The mutant phenotype was rescued by the addition of exogenous copper, suggesting a role in the transport of copper. Later work showed that Cox17p had a labile, binuclear copper thiolate cluster that was stable at high concentrations of thiolates (Srinivasan et al., 1998). Cox17p was one of the first site-specific copper chaperones identified and is speculated to acquire copper from Ctr1p and ultimately deliver the metal ion to the cytochrome c oxidase complex (Figure 1-3).

Cytochrome c oxidase is a membrane protein that is located within the inner membrane of mitochondria. Copper is delivered to cytochrome c oxidase, once the

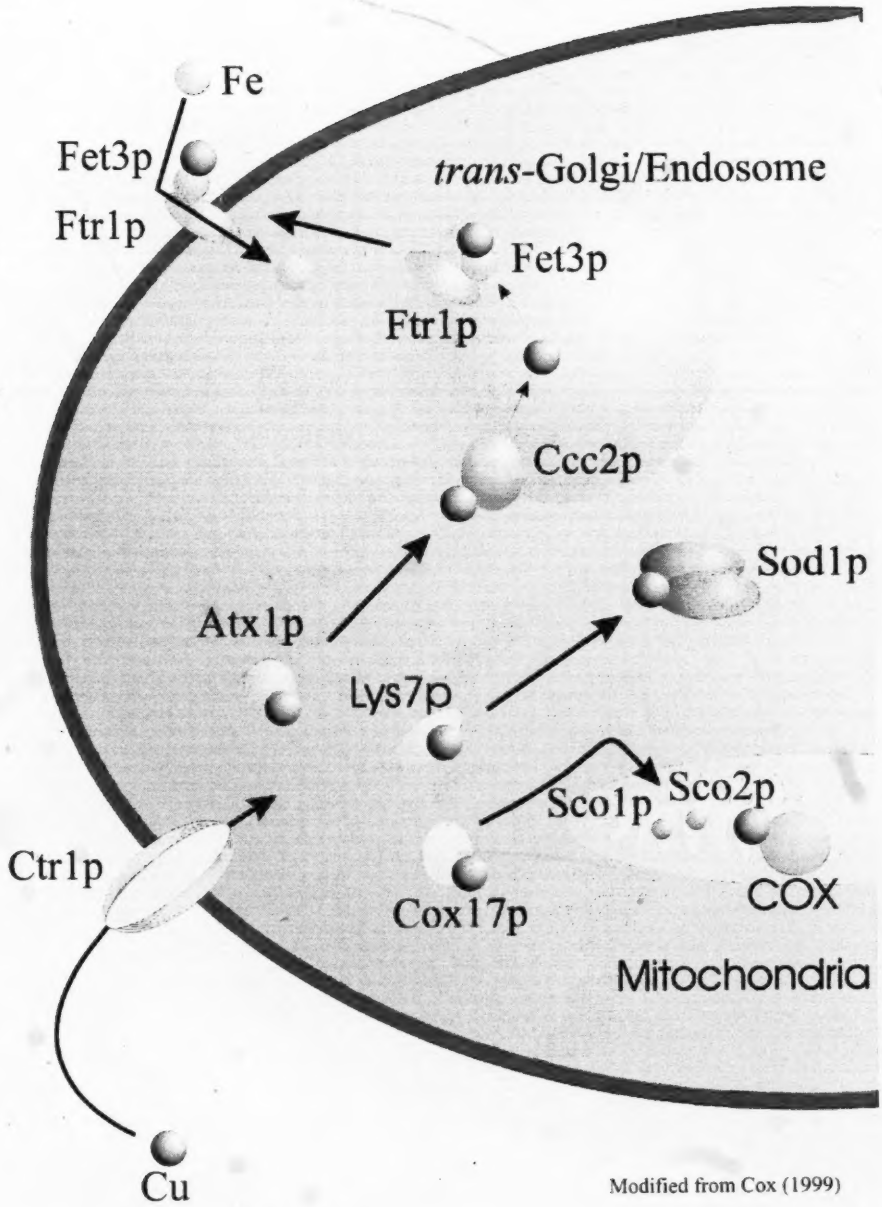

Figure 1-3: Copper transport in yeast. Red circle represents Cu(I) and blue circle represents Fe(III).

polymer is already within the mitochondrial inner membrane, by proteins involved in the assembly of cytochrome c oxidase. Consistent with this suggested mitochondrial involvement, Cox17p is found in the mitochondrial intermembrane space (Beers et al., 1997).

Sco1p and Sco2p are additional proteins involved in the assembly of cytochrome c oxidase (Figure 1-3). Both Sco1p and Sco2p were isolated as multicopy suppressors of a *cox17* mutant yeast strain and are both located in the mitochondrial inner membrane (Glerum et al., 1996b). Since the *cox17* phenotype can be restored by over-expressing Sco1p, Sco1p is likely involved downstream of Cox17p in the transport pathway that delivers copper to cytochrome c oxidase. Sco1p has recently been suggested to provide copper to the Cu_A site on subunit two of cytochrome c oxidase (Dickinson et al., 2000).

A yeast protein, Fet3p, encodes a transmembrane protein with 60% amino acid similarity to regions of ceruloplasmin in humans that is critical for high affinity iron uptake in yeast (Askwith et al., 1994). These data suggested that other human proteins involved in copper transport might have yeast homologues. Two human copper transporting proteins are the human P-type ATPases involved in Menkes and Wilson disease. P-type ATPases are integral membrane proteins that use ATP hydrolysis to generate transmembrane electrochemical ion gradients which involved the phosphorylation of a conserved aspartate amino acid residue (Scarborough, 1999). Both of the human genes for Wilson and Menkes disease had been characterized (Bull et al., 1993; Vulpe et al., 1993; Mercer et al., 1993; Chelly et al., 1993), however no yeast homologue was known. Therefore, using degenerate oligonucleotides for conserved motifs in P-type ATPases, yeast genomic DNA was screened for homologues (Yuan et al., 1995). Yuan et al. showed that a previously identified protein with conserved motifs

of a P-type ATPase transporter, *CCC2* (calcium sensitive cross complementation), originally isolated as a non-allelic complementation of the Ca^{2+} sensitive phenotype conferred by the *csg1* mutation (Fu et al., 1995), was responsible for iron uptake. Mutations in either *CCC2* or *CTR1* resulted in iron deficient phenotypes that could be suppressed by the presence of exogenous copper and/or iron, the latter suggesting an involvement of Fet3p. Because copper delivery into Fet3p was disrupted, even though both extracellular and intracellular levels of copper were normal, it was predicted that Ccc2p was involved in intracellular copper transport. This provided evidence that both Ctr1p and Ccc2p are involved in a copper transport pathway that delivers copper to the multicopper oxidase Fet3p required for ferrous iron uptake (Figure 1-3).

To identify potential new antioxidant factors, multicopy yeast vectors containing the yeast cDNA library were added to SOD deficient (Δ*sod1*Δ*sod2*) yeast in an attempt to rescue the excessive oxidative damage inherent to the double mutant (Lin and Culotta, 1995). One gene, designated *ATX1*, was discovered to increase the resistance to paraquat (superoxide radical generating agent) and atmospheric dioxygen. Atx1p showed significant sequence similarity to proteins previously found in plants and *Caenorhabditis elegans*. Later investigations showed that Atx1p was required for high affinity ferrous iron uptake, suggesting that the protein was involved in the copper transport pathway required for the activation of Fet3p (Lin et al., 1997). Additionally, by studying the incorporation of radioactive copper into Fet3p, both Ccc2p and Atx1p were determined to be necessary for the delivery of copper to the iron transporter. These data predict that the copper transport pathway in yeast necessary for high affinity iron uptake by Fet3p involves the plasma membrane copper transporter Ctr1p, the copper chaperone Atx1p, and the intracellular copper transporter Ccc2p (Figure 1-3).

As work on copper transport progressed, it became apparent that chaperones deliver copper to specific intracellular targets. Therefore a chaperone responsible for the insertion of copper into the copper containing protein, Sod1p, was predicted. Yeast *LYS7* was discovered by screening for genes that had similar phenotypes to *sod1*Δ (Culotta et al., 1997). This cytoplasmic protein is specific for Sod1p since Atx1p could not complement a *LYS7* deficiency. Lys7p is therefore the copper chaperone that specifically delivers copper to Sod1p, enabling the latter's enzymatic function (Figure 1-3).

Increased intracellular levels of copper are sequestered within cells by a small cysteine rich protein, metallothionein. A yeast metallothionein-like gene, *CUP1*, encodes a 53 residue polypeptide with a molecular weight of 5.66 kDa (Winge et al., 1985). CUP1 protein contains twelve cysteines per molecule, which binds eight copper ions, thus conferring resistance to growth media containing increased copper (500 fold) and cadmium concentrations (1000 fold) (Ecker et al., 1986).

Four mammalian metallothionein (MT) isoforms have been identified so far, MT-1, MT-2, MT-3 and MT-4 (reviewed in Miles et al., 2000). MT-1 and 2 are expressed in all tissues, however, MT-3 expression is limited to the brain. MT-4 isoform expression is limited to stratified epithelium. Normally, small amounts of MT are present within the serum (Mulder et al., 1991).

1.3) MAMMALIAN COPPER TRANSPORTERS AND RELATED DISEASES

1.3.1) Menkes disease and animal models

In 1962, Dr. John Menkes first described an X-linked inherited neurodegenerative disease (Menkes et al., 1962), later recognized as consistent with a phenotype resulting

from a deficiency of copper (Danks et al., 1972). Menkes disease affects from 1 in 100,000 to 1 in 250,000 live births, depending upon ethnic origin.

Patients with Menkes disease are unable to transport dietary copper, resulting in a generalized copper deficiency. Dietary copper uptake primarily occurs in the duodenum. In early attempts to determine the cause of copper deficiency, duodenal mucosa samples were obtained and measured for copper content in normal and Menkes disease patients (Danks et al., 1973). These studies suggested that the phenotype was not due to deficient uptake by the intestinal cells, but is due to a defect in the release of copper from these cells. Low amounts of copper, which are acquired by the body, accumulate in various tissues including kidney, spleen, pancreas, skeletal muscle, and placenta. Biochemical studies in patients with Menkes disease indicate low concentrations of holoceruloplasmin levels in the serum. Levels of apoceruloplasmin in the liver are not reduced, suggesting that it is a copper deficiency, and not an impaired protein synthesis, that prevents ceruloplasmin from receiving copper.

Clinical phenotypes of Menkes disease patients include neurodegeneration in infancy, failure to thrive, connective tissue abnormalities, seizures, twisted hair, hypothermia, severe developmental delay, and usually death by three years of age if left untreated (Kaler, 1998). All clinical features can be explained by copper deficiency. For example, connective tissue abnormalities are linked to deficiency of functional lysyl oxidase (LO), a copper dependent protein involved in the first step in collagen cross-link formation (Kosonen et al., 1997) (Table 1-1). In addition, neurological complications in Menkes disease are suggested to be in part from a lower activity of cytochrome c oxidase (Kunz et al., 1999), but could also be related to expression of ATP7A in glial cells, neurons, and the choroid plexus (Iwase et al., 1996). Copper is also known to be a

cofactor for dopamine β-monooxygenase which is essential for the catalytic conversion of dopamine to norepinephrine. Decreased levels of norepinephrine have been shown in epileptic animal models (reviewed in Kanner and Balabanov, 2002). Copper-histidine therapy prevents many of the clinical signs, but does not prevent connective tissue abnormalities (Sherwood et al., 1989).

A less severe form of Menkes disease is a copper transport disorder referred to as occipital horn syndrome, originally called Type IX Ehlers-Danlos syndrome (Kuivaniemi et al., 1982). Occipital horn syndrome results from an allelic mutation of the gene responsible for Menkes disease, which affects the splicing of primary transcripts (Kaler et al., 1994; Das et al., 1995). The consequence of the alternatively spliced transcript is a partially functional product leading to slightly subnormal intelligence or signs of autonomic dysfunction, and typically protrusions of the occiput (reviewed in Kaler, 1998).

The gene for Menkes disease, *ATP7A*, was mapped (Tumer et al., 1992) and finally cloned using a few patients that had balanced translocation breakpoints in Xq13 (Mercer et al., 1993; Vulpe et al., 1993; Chelly et al., 1993).

The mottled gene is the mouse orthologue of the Menkes disease gene (Levinson et al., 1994). Mottled mutants were first identified to have a defect in copper transport which seemed to cause strain phenotypes related to copper deficiency (Hunt, 1974). Cultured cells from human Menkes disease patients (Goka et al., 1976) and allelic mottled (*Mo*) mouse mutants (Camakaris et al., 1980) produced the same impairment in copper efflux.

The mottled locus in mice has several alleles, which produce variable phenotypes. Mutant alleles of the mottled locus include: dappled (Mo^{dp}) due to a lack of *Atp7a*

expression, blotchy (Mo^{blo}) due to a splicing mutation, brindled (Mo^{br}) due to a two amino acid deletion in a highly conserved region (Grimes et al., 1997), macular (Mo^{ma}) due to a missense mutation (Mori and Nishimura, 1997), pewter (Mo^{pew}) and tortoise (Mo^{to}). Severe neurological disease and perinatal lethality are characteristics of brindled and macular mutations, while perinatal lethality is also seen in dappled and tortoise. Of these, the brindled and blotchy mottled mutants are suitable representative animal models for Menkes disease and occipital horn syndrome, respectively.

Brindled mice have been studied extensively, uncovering much important information relevant to human Menkes disease. Duodenal injection of ^{64}Cu revealed a severe deficiency in copper absorption by the intestine. Forty eight hours after injection, a prominent accumulation of copper was found in the liver and kidney (Mann et al., 1979). This deficiency in copper absorption and extrahepatic copper accumulation mimics abnormalities in Menkes disease patients. In addition, brindled mutants and classical Menkes disease patients both have severe copper deficiency in many organs, with profound neurological complications. Neurological irregularities are believed to originate from a decrease in respiratory activity in the brain. Investigations into the activity of cytochrome c oxidase in cortex homogenates indicate that brindled mice have a two fold decrease in cytochrome c oxidase and a 1.4 fold decrease in NADH:cytochrome c reductase activities as compared with normal mice (Kunz et al., 1999). Additional investigations into neurochemical abnormalities showed that there are lower concentrations of norepinephrine and higher levels of dopamine or dopamine metabolites in affected areas of the brain (Martin et al., 1991). Copper neurotoxicity is dependent upon the formation of Cu-dopamine complexes, and brindled mice exhibit a localized increase in dopamine that may partially explain neurological degeneration in

selected regions of the brain. When the alterations of copper homoeostasis in blotchy mice were compared with those of brindled mice, blotchy abnormalities were generally less severe (Mann et al., 1981). The molecular cause for blotchy mouse phenotypes is a splicing mutation within the *Atp7a* gene, resulting in a shorter transcript and a smaller protein, resulting in a reduced level of normal product and the presence of a mutant protein (Das et al., 1995).

Increased levels of intestinal metallothionein in macular mouse mutants are induced by an accumulation of copper in intestinal cells (Shiraishi et al., 1991). This increase in metallothionein, associated with copper accumulation, also occurs in the cells of the proximal convoluted tubules within the kidney (Suzuki-Kurasaki et al., 1997). Metallothionein sequesters excess intracellular metals, thereby providing some protection from excess intracellular copper (reviewed in Dameron and Harrison, 1998). The importance of metallothionein in copper homeostasis was shown in mice by mating mice without MT-I and MT-2 ($Mt^{-/-}$) with Mo^{br} mice (Kelly and Palmiter, 1996). The mating cross resulted in death before embryonic day 11.

1.3.2) Wilson disease and animal models

Wilson disease, or hepatolenticular degeneration, is a rare autosomal recessive disorder that was first clinically described by Kinnear-Wilson in 1912 (Wilson, 1912) and later related to copper accumulation in the liver during the 1940s (Danks, 1995). The accumulation of copper is also seen in other tissues including the brain and eyes (Oldendorf and Kitano, 1965). Wilson disease typically affects approximately 1 in 30,000 individuals, although in Asia and Sardinia, the frequency increases to approximately 1 in 10,000. Patients with Wilson disease can begin to show phenotypic

manifestations as early as five years of age but can also show first symptoms as late as 50.

There appears to be no regulation of copper uptake by intestinal cells, rather the body maintains appropriate copper levels by modifying the amount of copper excreted into the bile (Berge Henegouwen et al., 1977). Results suggest that dietary copper from the intestine enters the circulatory system, is transported to the liver and is excreted into the bile. Wilson disease is caused by an impairment of the excretion of copper into bile, leading to hepatic copper accumulation (reviewed in Cox, 1999). Copper typically accumulates in the liver and increases in the plasma, resulting in accumulation in non-hepatic tissues such as the brain. Hepatic copper accumulation often results in hepatic failure while accumulation in the brain results in neurological complications. Neurological problems can include tremors, seizures, and changes in personality.

In addition to copper accumulation, ceruloplasmin, a protein that contains approximately 95% of serum copper, is typically reduced in Wilson disease patients. The Wilson disease protein is also involved in the delivery of copper to apoceruloplasmin for biosynthesis and secretion of holoceruloplasmin. Therefore, Wilson disease patients typically display both an accumulation of copper and low levels of holoceruloplasmin within the serum (reviewed in Loudianos and Gitlin, 2000).

In 1993, the gene defective in Wilson disease was identified by positional cloning approach (Bull et al., 1993) and as a secondary consequence of a search for amyloid-like proteins (Tanzi et al., 1993). The availability of sequence of the Menkes disease gene was useful for both approaches. Results from the study by Bull et al. identified two Icelandic patients that had a seven base pair deletion in a gene designated *ATP7B*. To date there are over 200 known mutations in *ATP7B*

(www.medgen.med.ualberta.ca/database.html) that are spread out over the entire coding region, making molecular diagnosis very difficult and time consuming.

Both *ATP7A* and *ATP7B* encode P-type ATPase transporters that share sequence similarity with various P-type ATPases in organisms including *Saccharomyces cerevisiae* (Fu et al., 1995), *Enterococcus hirae* (Odermatt et al., 1993) and *Mus musculus* (Levinson et al., 1994). All ion-translocating P-type ATPases share unique and characteristic amino acid domains: aspartate for a phosphorylation site, a SEHPL domain conserved in all copper P-type ATPases, an ATP binding site, and a transmembrane cation channel (see Bull et al., 1993) (Figure 1-4). The phosphorylation site is involved in a molecular mechanism that leads to a transient formation of a high-energy aspartylphosphoryl-enzyme intermediate. These P-type ATPase transporters create ion gradients needed for cellular signaling, nerve impulse transmission, differentiation and growth. ATP7A and ATP7B are specifically responsible for intracellular copper transport and have been extensively studied in humans and in a yeast model system.

Shortly after the discovery of the human P-type ATPase, ATP7B studies began to characterize genes affecting animal models known to be associated with a disruption in copper homeostasis. A mutant rat, Long-Evans Cinnamon (cinnamon coat color) (LEC), was reported from Japan which was phenotypically similar to Wilson disease patients (Li et al., 1991). The LEC rat typically develops acute hepatitis associated with jaundice, and ultimately hepatocellular carcinoma. In an attempt to explain hereditary hepatitis in the rat, copper levels in the liver and serum were obtained, leading to the discovery that copper was elevated in the liver and ceruloplasmin levels in the serum were decreased (Li et al., 1991). Ultimately, it was discovered that the LEC rat has a deletion in the orthologue to *ATP7B* (Wu et al., 1994). The gene deletion was 900 base pairs long

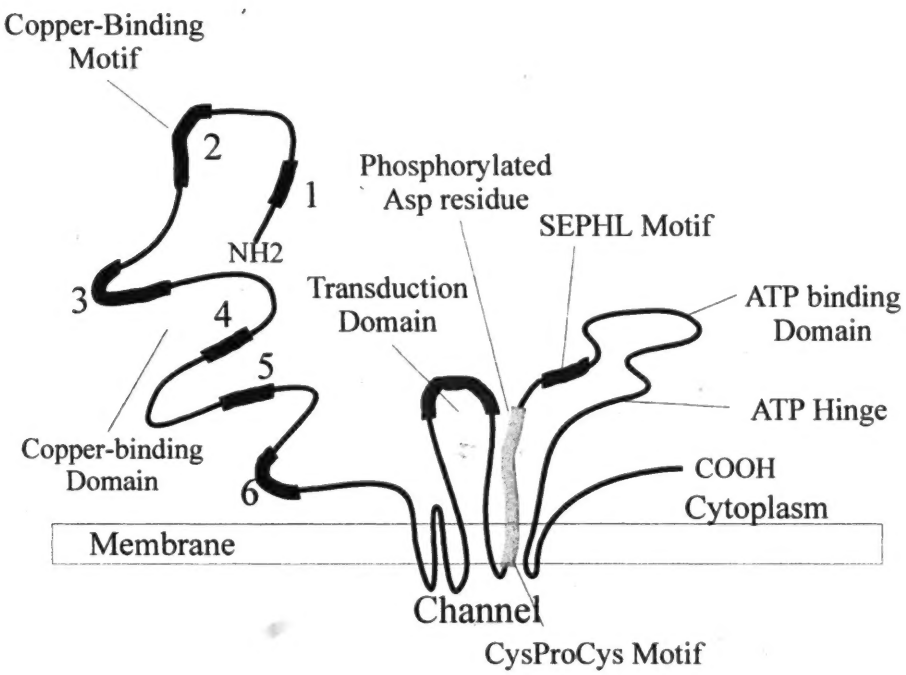

Modified from Bull and Cox (1994)

Figure 1-4: Model of P-type ATPase copper transporter ATP7B. The conserved motifs are indicated and labeled along the protein. The six copper binding motifs are labeled 1 through to 6 on the N-terminal domain.

(including the ATP binding domain), and extended downstream of the rat *Atp7b*. The involvement of *Atp7b* was confirmed in the LEC rat by the addition of a recombinant adenovirus containing the wild-type human gene responsible for Wilson disease, *ATP7B*. The recombinant adenovirus restored holoceruloplasmin in the serum (Terada et al., 1998).

In addition to copper accumulation within the liver of the LEC rat, there is also a marked increase in metallothionein within the liver (Klein et al., 1998). They proposed that copper toxicity in LEC rats proceeds through four steps. The first step involves the accumulation of copper due to the primary genetic defect. Second, the levels of copper-associated metallothionein increase within the hepatocytes. Thirdly, iron mediated polymerization of copper associated metallothionein produces an insoluble complex containing reactive copper. The last step is suggested to be the initiation of lysosomal lipid peroxidation which ultimately leads to necrosis of a hepatocyte (Klein et al., 1998).

The pathogenesis of acute hepatitis in LEC rats is also linked to an increase in hydroxyl radicals. Hydroxyl radicals are a leading factor in hepatic damage resulting from an increase in hepatic copper levels (Yamamoto et al., 2001). By trapping the hydroxyl radical with salicylic acid (SA), salicylic acid is converted to 2,3-dihydroxybenzoic acid (2,3-DHBA). A ratio of 2,3-DHBA/SA allows for quantification of hydroxyl radicals. In serum and liver of LEC rats with hepatitis, the ratio of 2,3-DHBA/SA was significantly higher when compared with wild-type rats and LEC rats yet to develop hepatitis. This increased hydroxyl radical presence is likely associated with an accumulation of copper since Wistar rats that were treated orally with $CuSO_4$ also showed a similar increase in the ratio of 2,3-DHBSA/SA (Yamamoto et al., 2001). This

provides an *in vivo* link between increased copper levels, increased hydroxyl radicals and development of hepatitis in the LEC rat.

Kidney dysfunction also commonly occurs in the LEC rat, usually manifesting as proximal tubular dysfunction, characterized by an increase in alkaline phosphatase, glucose, amino acids and other low molecular weight substances in the urine (Nomiyama et al., 1999). Similar kidney dysfunction is seen in Wilson disease patients. Studies of metallothionein and kidney dysfunction in the LEC rat, indicated that renal dysfunction is temporally linked to an increased metallothionein concentration in the plasma. Metallothionein, produced in the liver, is a low molecular weight protein, suggested to passively enter the glomerular sieve and lead to downstream tubule dysfunction (Nomiyama et al., 1999).

In addition to the LEC rat, there is also a mutant strain of mice with a very similar phenotype to that of Wilson disease. A mouse named toxic milk (*tx*), described in 1983, produced newborn pups with clinical features characteristic of copper deficiency, including poor growth, hypopigmentation, and tremors ultimately leading to death by the second postnatal week (Rauch, 1983). He believed that the neonatal phenotype of *tx* pups was caused by a severe copper deficiency, likely due to the additive effect of being born copper deficient and receiving copper deficient milk from the *tx* mother. These symptoms were consistent with copper deficiency and originally attributed to a failure in normal fetal copper accumulation in the liver. In combination with deficient hepatic copper accumulation, the serum of these pups showed reduced ceruloplasmin activity (Rauch, 1983). Initially, based on the neonatal phenotype, *tx* mice were thought to be a mouse model for Menkes disease since the findings were consistent with copper deficiency. However, as the mice began to mature, hepatic copper levels drastically

increased with age. This hepatic copper accumulation resulted in gross morphologic, histologic, and ultrastructural changes that became progressively more apparent with age (Biempica et al., 1988).

The *tx* mutation was mapped to mouse chromosome 8 (Reed et al., 1995), and to a region of mouse chromosome 8 with synteny to the region of human chromosome 13. Human chromosome 13 contains the human *ATP7B* locus (Harris, 1991; Tanzi et al., 1993). The *tx* gene, designated *Atp7b*, produces a 7.5 kb transcript encoding a 1462 amino acid polypeptide with significant similarity to human and rat genes. The coding sequence of *tx* cDNA has a single nucleotide deviation from wild-type, resulting in a missense mutation M1356V affecting the eighth transmembrane motif of the protein (Theophilos et al., 1996). Another strain from the Jackson Laboratory has a similar phenotype to the *tx* mutant and is designated the tx^J mouse. Recent work in our laboratory has demonstrated that the tx^J phenotype is the result of an allelic missense mutation in the second transmembrane motif of the *Atp7b* gene (Coronado et al., 2001).

Pups born to *tx* mothers die at an early stage unless removed from their mother and nursed by wild-type foster mothers (Rauch, 1983). The milk from the *tx* mothers is deficient in copper, therefore suckling from a *tx* mother compounds the deficiency in newborn pups. Studies analyzing the subcellular localization of Atp7b have found a difference between lactating and non-lactating mammary glands of wild-type mice and the lactating and non-lactating glands of *tx* mice. In wild-type mice, Atp7b was perinuclear in non-lactating mothers and cytoplasmic in lactating mothers (Michalczyk et al., 2000). In contrast, subcellular localization of Atp7b in *tx* mice demonstrated a perinuclear distribution in both the non-lactating and lactating mothers. It was therefore concluded that copper deficient milk from *tx* mothers correlates with an inability of

Atp7b to traffic to the cytoplasm. Presumably, trafficking is necessary for incorporating copper into proteins found in milk.

In *tx* mice, hepatic copper accumulation is associated with an increase in hepatic metallothionein (Deng et al., 1998; Mercer et al., 1992). Studies revealed MT-1 mRNA levels were not increased in *tx* mouse livers compared with normal mouse hepatocytes (Koropatnick and Cherian, 1993), however, the half life of the protein is approximately 77-79% greater in adult *tx* mice suggesting the increased hepatic accumulation is the result of decreased protein degradation. *In vitro*, an increase in copper-associated metallothionein leads to an increase in lipid peroxidation suggesting that copper-associated metallothionein results in a predisposition to oxidative stress within the cell (Stephenson et al., 1994).

1.3.3) Canine copper toxicosis

Wilson disease results from the accumulation of copper that leads to either hepatic and/or neurological manifestations. In 1975, Ludwig et al. reported hereditary hepatic cirrhosis in Bedlington terriers (Ludwig et al., 1980). Like Wilson disease, Bedlington toxicosis has an autosomal recessive inheritance and leads to hepatic accumulation of copper (reviewed in Owen, Jr. and Ludwig, 1982). However, investigations excluded the canine orthologue of ATP7B (van De et al., 1999). Finally, positional cloning experiments identified a candidate gene that was found to contain a homozygous deletion in all affected Bedlington terriers (van De et al., 2002, Coronado et al., personal communication). This gene, *MURR1*, is ubiquitously expressed but has relatively high levels in the liver. The function of the protein is unknown. This work demonstrates that the complete mammalian copper transport pathway is not yet fully understood.

1.3.4) Ctr1$^{-/-}$ animal model

Since the discovery of the original high affinity copper uptake protein *CTR1* in yeast, studies have begun to elucidate cellular copper uptake in mammals. The human *CTR1* orthologue was isolated by functional complementation in yeast (Zhou and Gitschier, 1997). Using SOD1 activity as an assay of intracellular copper levels, they demonstrated that in yeast, human *CTR1* rescued SOD1 activity. In addition, the human *CTR1* construct increased copper sensitivity and rescued high-affinity iron transport. Expression of human *CTR1* was shown in every tissue examined, with higher levels seen in the liver and kidney and lower levels in the spleen and brain (Lee et al., 2000). The *CTR1* locus was mapped to 9q34, but no human disease has yet been mapped to the region that would be consistent with a *CTR1* defect. Therefore, in order to study the phenotypic consequences of a dysfunctional *CTR1* transporter, mouse mutants were created.

When *Ctr1* was disrupted in mice, the resulting mutants demonstrated a severe deficiency in copper absorption (Lee et al., 2001; Kuo et al., 2001). *Ctr1*$^{-/-}$ embryos terminate at developmental stage E8.5 and typically show growth retardation and increased cell death with impaired brain development. Heterozygotes (Ctr1$^{+/-}$) survive after birth and are phenotypically normal; however copper levels in the brain are approximately half of those in the wild-type mouse (Kuo et al., 2001). These results indicate the essential nature of *Ctr1* is in normal development. Based on the phenotypic consequences in mutant *Ctr1* mice, a complete absence of CTR1 in humans would be predicted to result in a lethal phenotype. In contrast, a less severe mutation or heterozygotes of *CTR1* may have a general copper deficiency, and therefore, copper

deficient phenotypes. Human *Ctr1* is mapped to 9q31-32, however, no apparent copper associated disorders are mapped to this region.

1.4) COPPER CHAPERONES AND THEIR POTENTIAL ROLES

1.4.1) ATOX1, putative chaperone for ATP7A and ATP7B

Atox1 is predicted to have two functional domains, based on conserved residues (Hung et al., 1998). The first domain is in the N-terminus and consists of conserved cysteine residues characteristic of copper binding domains. The second domain is in the carboxy terminus and contains lysine residues that are conserved between all the chaperone orthologues. In yeast (Portnoy et al., 1999) and human studies (Hung et al., 1998), analysis of mutations affecting both the conserved cysteine and lysine residues showed that the two domains have independent functions. The cysteine residues acted as copper chelators and when mutated disrupt the copper transport pathway, as detected by a lack of Fet3p activity. In contrast, when the lysine residues were mutated, copper transport was not affected, but oxidative protection was eliminated. However, alterations of the cysteine residues did not alter oxidative protection.

The role Atx1 plays in copper binding and transport can be supported by crystallographic studies. In the presence of copper, two Atx1p molecules form a homodimer, with the copper ion associating with cysteine residues Cys15 and Cys18 (Figure 1-5). These two cysteine residues occur in the CXXC domain, located at the junction of the first β strand and the first α helix in the *βαββαβ* fold (Rosenzweig et al., 1999). In the human orthologue, ATOX1, the crystal structure supports the importance of these two cysteine residues in copper ligation and also shows that the metal binding

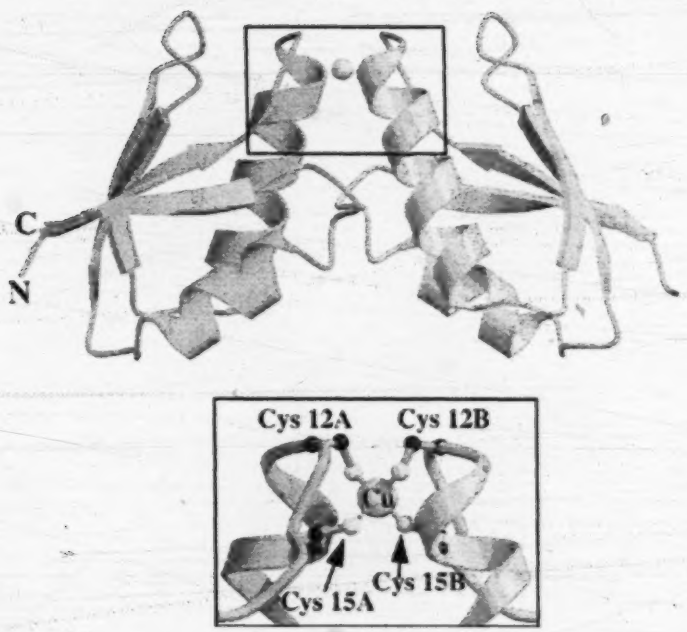

Figures from Rosenzweig (2001)

Figure 1-5: Structure of ATOX1. The metal ion is coordinated by the conserved cysteine residues from two ATOX1 molecules, shown in blue and yellow. The enlargement shows detailed cysteine interactions responsible for Cu(I) binding. Structural model was based on crystal structure.

site is stabilized by a number of hydrogen bonds from residues in the MT/HCXXC motif (Wernimont et al., 2000).

Based on yeast two hybrid experiments (Pufahl et al., 1997), structures, and metal transfer studies (Rosenzweig et al., 1999) it is suggested that Atx1p can transfer copper to the transporter Ccc2p. The copper binding sites in Ccc2p contain negatively charged amino acids that are proposed to interact with a conserved positively charged amino acids on the face of Atx1p (Rosenzweig et al., 1999). In metal transfer studies using mercury (Hg) in place of copper (due to its higher success rate), Atx1 already associated with Hg was combined with Ccc2a (copper binding domain of Ccc2p), and Hg was successfully transferred from Atx1 to Ccc2a. Additional studies involving copper also demonstrated this metal transfer (Huffman and O'Halloran, 2000).

Spectroscopic studies predict that the copper ion is transferred by the formation of two- and three-coordinate intermediates utilizing the cysteine residues from both proteins (Figure 1-6) (Pufahl et al., 1997). This proposal is supported by structural features: the exposure of the metal binding site at the surface of the protein, the flexible metal binding loop able to accommodate changes in coordinate geometry, and the ability of two CXXC motifs to transfer metal between cysteine residues (Rosenzweig et al., 1999; Wernimont et al., 2000). Human protein interactions were studied by mammalian two-hybrid analysis using ATOX1 and ATP7B metal binding domains (Larin et al., 1999), as well as co-immunoprecipitation of ATOX1 and ATP7A and ATP7B, in HeLa and HepG2 cells respectively (Hamza et al., 1999).

Mammalian ATOX1 may also, like its yeast orthologue, have a potential role in antioxidation. *Atox1* is expressed in several regions of the mouse brain, particularly in the choroid plexus (Nishihara et al., 1998; Naeve et al., 1999). To explore a possible

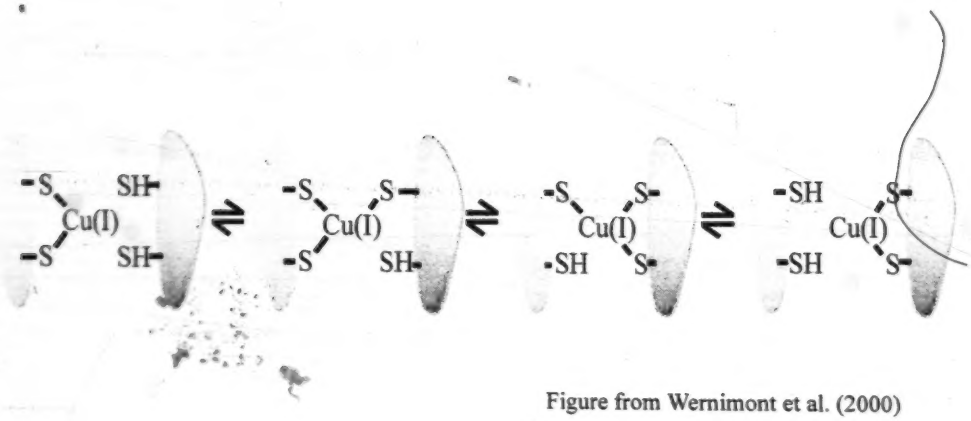

Figure from Wernimont et al. (2000)

Figure 1-6: Proposed mechanism of copper transfer between ATOX1 and a domain of a receptor protein. Prior to docking, the copper ion is likely bound in a two-coordinate geometry. Upon docking, the copper ion forms a tertiary-coordinate geometry which eventually leads to the re-establishment of a two-coordinate geometry with the receptor protein. ATOX1 is shown in on the left and the target domain is shown on the right.

antioxidant role for Atox1 in neuronal tissue, various neuronal cell lines were transiently transfected with *Atox1* cDNA and exposed to oxidative agents to artificially induce oxidative injury (Kelner et al., 2000). Resulting increases in viability in the presence of Atox1 provided evidence that Atox1 protects cells from oxidative damage. The brain is the organ most sensitive to oxidative damage and requires a strict control of antioxidants to avoid neurological complications. There was a linear correlation between the amount of oxidative tolerance and the copy number of *ATOX1* within the cells (Portnoy et al., 1999). This linear correlation suggests that ATOX1 does not have an enzymatic activity, but simply sequesters potentially damaging agents, particularly copper, from the cellular environment.

In order to study the systematic function of the copper chaperone Atox1, a null mutation was generated in mice (Hamza et al., 2001). This mutation had multiple effects. After birth, 45% of pups died before weaning. However the surviving pups exhibited growth failure, skin laxity, hypopigmentation and seizures attributed to perinatal copper deficiency. In addition, Atox1-deficient cells accumulated high levels of intracellular copper, suggesting impairment in copper efflux. Neurological problems in the *Atox1*$^{-/-}$ mouse may result from a lack of copper enzymes, as well as a lack of antioxidant protection.

Placental transfer of nutrients is dependent upon both maternal and fetal components. When a homozygous deficient parent (*Atox1*$^{-/-}$) was crossed with a heterozygous parent (*Atox1*$^{-/+}$), it was found that the phenotypes of *Atox1*$^{-/-}$ progeny were more severe when the homozygous parent was a female. In addition, when the homozygous parent was a mother, there was a greater retention of copper within the placenta and embryo (Hamza et al., 2001). If Atox1 deficiency only affected the

placental transfer of nutrients, it would suggest copper would only accumulate in the placenta and the embryo would be copper deficient, this however is not the case.

1.4.2) Ccsd and delivery to superoxide dismutase

Superoxide dismutase (SOD1) is a cytoplasmic homodimer that facilitates the conversion of hydroxyl ions into water. SOD1, therefore, eliminates free radicals which potentially damage phospholipids and DNA molecules. As previously discussed, mutations SOD1 have been found to be associated with FALS (Deng et al., 1993). This study also demonstrated that FALS mutations did not affect the catalytic activity of SOD1, rather, the mutations altered residues important for protein-protein interaction.

SOD1 is a copper requiring enzyme that accepts its copper cofactor by protein-protein interactions involving a cytoplasmic copper chaperone, called CCS (Culotta et al., 1997). Proteolysis protection studies of CCS indicate three conserved domains, designated domain I (Atx1 like), domain II (SOD1 like), and domain III (unique CCS sequence) (Figure 1-7) (Schmidt et al., 1999). Domain I contains the highly conserved CXXC sequence predicted to acquire copper from a cellular source. Domain II contains a β-barrel conformation similar to its target, SOD1, and is likely the site of protein-protein interaction between the chaperone and its acceptor. Domain III contains a CXC motif that also binds copper and may facilitate copper insertion into apo-SOD1. The coordination of these three domains enables the catalytic metal cofactor to be acquired by, and inserted into, SOD1 (Schmidt et al., 1999).

The transfer of copper from CCS to SOD1 occurs by the formation of a heterodimeric protein containing one subunit from SOD1 and a second subunit from CCS (Lamb et al., 2001; Lamb et al., 2000). In addition, the transfer of copper from CCS to

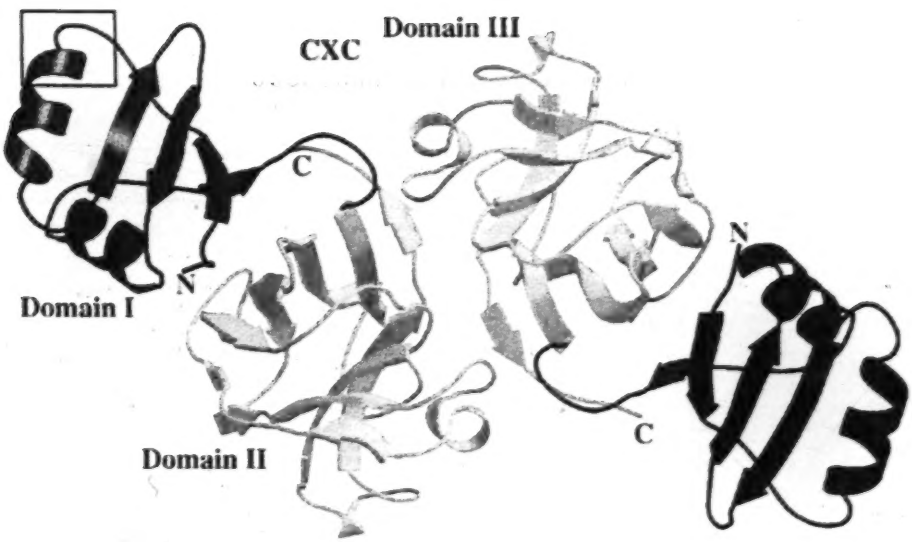

Figure from Rosenzweig (2001)

Figure 1-7: Structure of yeast Lys7p. The CXXC motif is denoted by a black box. Domain III is represented by the blue oval. The dimer interface is formed exclusively by residues from domain II.

SOD1 has been shown to involve a dinuclear copper-bridged cluster (Eisses et al., 2000), as first proposed as a mechanism of copper transfer involving Atx1p (Pufahl et al., 1997; Rosenzweig et al., 1999). The transfer of copper from CCS to SOD1 is proposed to involve three ligand-exchange steps that prevent the release of copper from the protein complex (Rae et al., 2001). The first step, "copper acquisition", relies upon the first domain only in copper limited conditions. In CCS, domain I is believed to interact with a yet unidentified donor protein and acquires copper utilizing its cysteine motifs. The second step, a "transiting state", likely involves domains I and III, utilizing an interaction via a cysteine-bridged dicopper(I) cluster. Copper is predicted to be bound to both the Cu-cysteine binding sites of domains I and III in CCS, and possibly to the histidine-like metal binding sites of domain II (Eisses et al., 2000). The "copper insertion state" refers to the transfer of copper to domain III in combination with interactions with SOD1, followed by a ligand-exchange transfer of the copper ion from domain III to SOD1. The direct transfer of copper involves conformational changes and utilization of the various domains in the chaperone in a coordinated effort.

The pathophysiological effects of defects or deficiencies of superoxide dismutase and its copper chaperone have been discovered by studying transgenic mice. A transgenic mouse model, carrying an FALS mutation that affects protein-protein interactions, developed paralysis due to motor neuron loss and died before 6 months of age (Gurney et al., 1994). This and other mutations in human FALS patients have very little effect on the enzymatic activity of the protein but are proposed to cause dominant, gain-of-function mutations resulting in an increase in free radicals which ultimately increase neuronal damage. Recent investigations showed, that mice with a targeted disruption of the mouse chaperone for superoxide dismutase, *Ccsd*, (Wong et al., 2000)

displayed similar phenotypes to SOD1 mouse knock-outs, both knock-outs show an increase in the death of motor neurons and a decrease in neuronal size by six months of age (Shefner et al., 1999).

1.4.3) Cox17 and delivery of copper to cytochrome c oxidase

Structural characterization of Cox17p supports the hypothesis that this small cytoplasmic protein is involved in copper shuttling. Cox17p is observed to bind copper as a binuclear cuprous-thiolate cluster. Various detection methods, including X-ray absorption spectroscopy, UV-visible absorption and emission spectroscopy, demonstrate the presence of bound cuprous ions in a trigonal coordination by thiolate ligands (Srinivasan et al., 1998). Recent investigations with purified recombinant Cox17p indicate that in the presence of copper, this protein exists in dimer/tetramer equilibrium. Cox17p is predominantly tetrameric within the intermembrane space of the mitochondrion, but is principally a dimer in the cytoplasm. Mutations within the three cysteines (Cys23, Cys24, or Cys26) abolish function and disrupt tetramerization, suggesting that oligomerization may have a significant role in function (Heaton et al., 2001).

Based on structural data and studies in yeast, Cox17 is also speculated to be a mammalian copper chaperone. However, its exact physiological involvement in the mammalian system is still unresolved. Human *Cox17* has been identified including its structure, expression and chromosomal localization (Punter et al., 2000). The mouse *Cox17* gene has been found to consist of three exons spanning a genomic region of 6 kb and is mapped to the center of chromosome 16 (Takahashi et al., 2001). The promoter region has been characterized using sequential deletions of upstream genomic sequence

(Takahashi et al., 2002). The expression pattern of Cox17, by northern blot analysis, indicates expression in a wide range of tissues examined, but is most intense in the kidney, heart and brain (Kako et al., 2000; Punter et al., 2000). Relatively intense expression in the pituitary and pituitary cell lines suggests that Cox17 may have additional roles beyond its involvement with the respiratory chain, and may be involved in neuoendocrine function as well.

1.5) TISSUE EXPRESSION OF GENES INVOLVED IN COPPER TRANSPORT

Copper transporters are expressed in many organs that there are specialized structural regions dedicated to copper homeostasis. By investigating localized tissue expression of copper regulatory proteins, a more detailed molecular explanation can be elucidated for disease phenotypes in animal models and in patients affected by disrupted copper homeostasis.

1.5.1) Distribution of Atp7a

Studies using northern blot analysis showed that *ATP7A* is expressed in many tissues, including the placenta, lung, heart, brain, kidney, testis, and gut mucosa (Vulpe et al., 1993). Interestingly, there is very little expression in spleen or adult liver (Vulpe et al., 1993; Paynter et al., 1994).

During normal prenatal embryonic development, copper levels in both human and mouse liver exceed levels typically measured in adults. This elevated hepatic copper mimics levels found in Wilson disease patients (Klein et al., 1991). During development, as levels of copper increase, *Atp7a* is expressed in the spleen and liver (Paynter et al., 1994; Kuo et al., 1999). Just before birth in mice, at gestation day 19, there is a shift in

expression of *Atp7a* in the liver (Paynter et al., 1994). *Atp7a* begins to undergo some type of repression, resulting in a decreased level of transcription. The expression levels of Atp7a in the adult spleen and liver are very limited.

Detailed localization studies of *Atp7a* within the mouse kidney demonstrate a structure-specific expression pattern. Polyclonal antibodies, derived from the N-terminal metal binding domains, were used for immunohistochemistry and localized protein within the proximal and distal tubules of the mouse kidney (Grimes et al., 1997). In patients lacking functional ATP7A, copper accumulates within the proximal tubules of the kidney. Grimes et al. believed that copper accumulation occurs as the result of a disruption in localized copper efflux from cells of the proximal tubules.

The expression pattern of *Atp7a* in the central nervous system (CNS) has suggested that localized neuronal necrosis in Menkes disease patients is associated with expression of the transporter in the affected regions. *In situ* hybridization revealed *Atp7a* expression primarily in the hippocampus and dentate gyrus, olfactory bulb nuclei, cerebellar granular cell layer, choroid plexus and the ependyma (Iwase et al., 1996). A region with less signal intensity was noted in the cerebellar Purkinje cells. Although expressed in other regions, *Atp7a* expression partially overlapped with regions known to be involved in neuronal necrosis in macular mice including the hippocampus and the cerebellar Purkinje cells.

1.5.2) Distribution of Atp7b

Since the discovery of *ATP7B*, the expression pattern of this transporter has been shown by northern blot analysis, *in situ* hybridization, and immunohistochemistry. Northern blot analysis reveals that expression is highest in adult liver, kidney, and slight

in brain, placenta, heart and lungs (Bull et al., 1993; Muramatsu et al., 1998; Tanzi et al., 1993).

Developmental studies in mouse revealed that expression was induced near birth (Kuo et al., 1999). In the adult liver, Atp7b acts to export copper via the bile, balancing the body's copper levels. Bile, the primary route for copper excretion, is not produced during gestation. The lack of fetal biliary excretion is suggested to be responsible for the hepatic accumulation of copper during development (Buiakova et al., 1999). In human newborns, copper levels are from 93 -335 mg/kg dry weight (Diaz et al., 1990), which corresponds to levels seen in Wilson disease patients unable to export hepatic copper stores (Table 1-2). After birth, infants excrete bile leading to a decrease in the embryonic hepatic copper levels. Hepatic copper levels eventually stabilize to adult-like levels ranging from 49-123 mg/kg (Diaz et al., 1990). *Atp7b*, which is believed to export copper into the bile, is up-regulated just prior to birth and continues its upward trend until it stabilizes shortly after birth to adult-like transcription levels (Kuo et al., 1999). This up-regulation coincides with the rapid decrease in hepatic copper levels after birth.

Nutrients for the developing fetus are derived from the mother and transferred to the fetus via the placenta. In the placenta of the LEC rat, *Atp7b* is expressed in the maternal portion, indicating that the transporter has a role in copper delivery to the developing fetus. The importance of *Atp7b* in placental copper transfer was supported by finding placental copper accumulation in the null mutant knockout of the murine *Atp7b* gene in pregnant mothers (Buiakova et al., 1999). In addition, copper also accumulated in the lactating mammary gland, liver, kidney, brain, and eye.

After birth, an important source of copper is from the milk of the lactating mother (Casey et al., 1989). Atp7b is presumed to be the major copper transporter in the

mammary gland, responsible for delivering copper into the secreted milk. The intracellular redistribution in lactating mice does not occur in the *tx* mouse, as discussed above, explaining why *tx* pups nursed from *tx* mothers die from copper deficiency (Rauch, 1983).

Within human and rat, *ATP7B/Atp7b* studies have been undertaken on the copper induced trafficking in hepatocytes (Schaefer et al., 1999a). In rat hepatocytes, increased copper in the media resulted in a redistribution of ATP7B from a perinuclear region to a more diffuse cytoplasmic location (Schaefer et al., 1999a). Trafficking of ATP7B in hepatocytes during the presence of elevated copper is also supported by later studies in cultured polarized HepG2 hepatoma cells that demonstrated a redistribution of ATP7B to vesicles that have a tendency to cluster at the apical pole of the cell during exposure to elevated copper (Roelofsen et al., 2000).

Cell culture data were supported by immunohistochemical localization in the human and rat liver. Tissue localization in rat liver indicates that ATP7B has an intracellular punctate pattern oriented toward the canalicular pole (Schaefer et al., 1999a). In an additional study involving human liver, ATP7B was localized to two regions (Schaefer et al., 1999b). In the first region, which is unidentified, immunostaining is in an intracellular punctate pattern within specific hepatocytes. The second region, only found with elevated copper, describes a localization pattern to the pericanalicular area, confirming copper induced trafficking seen in cell culture.

Atp7b/ATP7B distribution studies demonstrate the usefulness of expression and tissue localization studies to predict functional characteristics of protein products. The hepatic localization of *Atp7b* is not completely resolved, since regions showing expression are not yet characterized. In addition, the kidney is known to be involved

both in copper excretion and absorption as well as having a role in the pathogenesis of Wilson disease. Investigation into the kidney localization pattern for *Atp7b* would provide meaningful information about a functional role in renal copper homeostasis.

1.5.3) Distribution of Atox1

Atox1 is a mammalian copper chaperone for the copper transporters Atp7a and Atp7b. Tissue expression patterns of the chaperone should therefore overlap with the expression pattern of both copper transporters. Based on northern blot analysis, discrepancies have already been found between Atox1 expression and Atp7a expression. Northern blot analysis indicates that *Atox1* is widely expressed in tissues including liver, heart, lung, kidney, spleen, thymus, prostate, testes, ovary, small intestine, colon, and central nervous system (Hamza et al., 2000; Naeve et al., 1999). In the central nervous system *Atox1* is expressed in the amygdala, caudate nucleus, corpus callosum, hippocampus, hypothalamus, substantia nigra, subthalamic nucleus and thalamus (Naeve et al., 1999). Interestingly, it was also discovered that skeletal muscle does not express *Atox1*. Atp7a was previously demonstrated to be expressed in the skeletal muscle (Vulpe et al., 1993) indicating a difference between expression of the putative chaperone Atox1, and Atp7a.

In situ hybridization studies of *Atox1* have provided detailed information concerning specific expression in rat brain (Naeve et al., 1999). There was a low level basal expression throughout neuronal tissue. However, the highest level of expression was in the pyramidal neurons of the cerebral cortex and hippocampus, as well as the neurons of the locus coeruleus. These localized structures with high levels of *Atox1* expression also correspond to the same regions that normally contain high levels of

copper, iron, and zinc. These data suggest that Atox1 has a particular role in the central nervous system and is involved in metal ion transport in specific regions.

Atox1 sequence similarity extends throughout many organisms including the round worm, *Caenorhabditis elegans*. By fusing the *CUC-1* (*C. elegans* orthologue of *Atox1*) promoter and N-terminal region into a promoter-less GFP reporter plasmid, localized expression of this chaperone was assayed both in larval and adult stages (Wakabayashi et al., 1998). The *cuc-1::GFP* fusion gene was strongly expressed in the intestine of the adult and the hypodermal cells of the head and body regions in the L1 larval stage. The only membrane copper transporter in *C. elegans*, *CAU-1*, has sequence identity with both *Atp7b* and *Atp7a*. Using a *cau1*::GFP promoter fusion protein, *CAU-1* was shown to be expressed both in the intestinal cells and the pharyngeal muscle of the adult and in the hypodermal cells in the larva (Wakabayashi et al., 1998). Therefore in *C. elegans CAU-1* is expressed in the pharynx and *CUC-1* is not. These data provide additional evidence that the putative copper chaperone for copper transporters Atp7a and Atp7b may not completely co-localize in cells within the same mammalian tissue.

The copper chaperone Atox1 is expressed in every mouse tissue examined except for skeletal muscle. As a copper chaperone for the copper transporters Atp7a and Atp7b, expression should completely overlap with both of these transporters. If the expression pattern does not overlap, it is possible that the protein either has functions beyond those involved in transferring copper to Atp7a and Atp7b or there are additional chaperones that deliver copper to these transporters. Northern blot analysis for both copper transporters Atp7a and Atp7b has been the primary source for tissue expression patterns. By identifying and comparing the tissue expression pattern in specific cells within an

organ expressing the Atox1 with that of the transporters, the functional significance of this chaperone may be better understood.

1.6) HYPOTHESES AND AIMS OF THESIS

HYPOTHESES:

Numerous tissues have been found to express genes *Atp7a* and *Atp7b*, however, very little cell specific expression profiles within these tissues have been investigated in the adult mammalian system. Given the complexity of organs and the cell specific functions within the regions of each organ, copper transport proteins are expected to show localized expression within specific organs. Studying the expression pattern of copper transporters and chaperones within tissues involved in copper transport will aid in defining *in vivo* roles for these proteins, not only on an intracellular level, but on an organismal level as well.

Investigations in yeast copper transport have revealed a pathway for copper movement within the cell. Ccc2p, homologous to Atp7a and Atp7b, receives copper from the chaperone Atx1p, homologous to Atox1. This copper pathway appears to be generally conserved in the mammalian system. However, details are yet to be clarified. For example, it is possible there are additional chaperones in the mammalian system for the aforementioned transporters. If Atox1 is a chaperone for both of these transporters, I hypothesize that Atox1 will co-express with both Atp7a and Atp7b. If discrepancies are found in the expression patterns between Atox1 and the transporters it would suggest that additional chaperones may exist, or that chaperones carry out functions in addition to direct transport.

In both Menkes and Wilson disease patients, copper accumulates to the same extent in the proximal convoluted tubules of the kidney. Since Wilson disease patients have elevated levels of copper in the serum and urine, it is generally felt that these elevated levels somehow contribute to the copper retention in the proximal tubules. However, Menkes disease patients are generally copper deficient but also show the same accumulations of copper in the proximal tubules. Investigating the renal expression pattern of genes involved in copper transport may help to explain the pattern of copper accumulation. If renal expression of Atp7a, Atp7b and Atox1 are limited to the proximal convoluted tubules, this would suggest that copper accumulates in the proximal tubules because of a localized disruption of copper efflux.

AIMS:

The general aim of this thesis was to study the tissue specific expression of genes involved in the copper transport pathway in an attempt to elucidate possible functions and pathway interactions within specific organs. Specific goals were as follows:

1) To define uncharacterized mouse genes (*Ccsd*), involved in copper transport in order to study tissue expression pattern or to determine possible functional interactions with co-expressed copper transporting genes.

2) To study the expression pattern of proteins involved in copper homeostasis within the liver, kidney and placenta, using the mouse as a mammalian model.

1.7) REFERENCES

Aoki,M., Abe,K., and Itoyama,Y. (1998). Molecular analyses of the Cu/Zn superoxide dismutase gene in patients with familial amyotrophic lateral sclerosis (ALS) in Japan. Cell Mol. Neurobiol. *18*, 639-647.

Askwith,C., Eide,D., Van Ho,A., Bernard,P.S., Li,L., Davis-Kaplan,S., Sipe,D.M., and Kaplan,J. (1994). The FET3 gene of S. cerevisiae encodes a multicopper oxidase required for ferrous iron uptake. Cell *76*, 403-410.

Beers,J., Glerum,D.M., and Tzagoloff,A. (1997). Purification, characterization, and localization of yeast Cox17p, a mitochondrial copper shuttle. J. Biol. Chem. *272*, 33191-33196.

Berge Henegouwen,G.P., Tangedahl,T.N., Hofmann,A.F., Northfield,T.C., LaRusso,N.F., and McCall,J.T. (1977). Biliary secretion of copper in healthy man. Quantitation by an intestinal perfusion technique. Gastroenterology *72*, 1228-1231.

Biempica,L., Rauch,H., Quintana,N., and Sternlieb,I. (1988). Morphologic and chemical studies on a murine mutation (toxic milk mice) resulting in hepatic copper toxicosis. Lab Invest *59*, 500-8.

Bremner,I. (1998). Manifestations of copper excess. Am. J. Clin. Nutr. *67*, 1069S-1073S.

Browne,S.E., Ferrante,R.J., and Beal,M.F. (1999). Oxidative stress in Huntington's disease. Brain Pathol *9*, 147-63.

Buiakova,O.I., Xu,J., Lutsenko,S., Zeitlin,S., Das,K., Das,S., Ross,B.M., Mekios,C., Scheinberg,I.H., and Gilliam,T.C. (1999). Null mutation of the murine ATP7B (Wilson disease) gene results in intracellular copper accumulation and late-onset hepatic nodular transformation. Hum Mol Genet *8*, 1665-71.

Bull,P.C. and Cox,D.W. (1994). Wilson disease and Menkes disease: new handles on heavy-metal transport. Trends Genet *10*, 246-52.

Bull,P.C., Thomas,G.R., Rommens,J.M., Forbes,J.R., and Cox,D.W. (1993). The Wilson disease gene is a putative copper transporting P-type ATPase similar to the Menkes gene. Nat. Genet. *5*, 327-337.

Camakaris,J., Danks,D.M., Ackland,L., Cartwright,E., Borger,P., and Cotton,R.G. (1980). Altered copper metabolism in cultured cells from human Menkes' syndrome and mottled mouse mutants. Biochem. Genet. *18*, 117-131.

Carri,M.T., Battistoni,A., Polizio,F., Desideri,A., and Rotilio,G. (1994). Impaired copper binding by the H46R mutant of human Cu,Zn superoxide dismutase, involved in amyotrophic lateral sclerosis. FEBS Lett. *356*, 314-316.

Casey,C.E., Neville,M.C., and Hambidge,K.M. (1989). Studies in human lactation: secretion of zinc, copper, and manganese in human milk. Am. J. Clin. Nutr. *49*, 773-785.

Chelly,J., Tumer,Z., Tonnesen,T., Petterson,A., Ishikawa-Brush,Y., Tommerup,N., Horn,N., and Monaco,A.P. (1993). Isolation of a candidate gene for Menkes disease that encodes a potential heavy metal binding protein. Nat. Genet. *3*, 14-19.

Coronado,V., Nanji,M., and Cox,D.W. (2001). The Jackson toxic milk mouse as a model for copper loading. Mamm. Genome *12*, 793-795.

Cox,D.W. (1999). Disorders of copper transport. Br. Med. Bull. *55*, 544-555.

Culotta,V.C., Klomp,L.W., Strain,J., Casareno,R.L., Krems,B., and Gitlin,J.D. (1997). The copper chaperone for superoxide dismutase. J Biol Chem *272*, 23469-72.

Dameron,C.T. and Harrison,M.D. (1998). Mechanisms for protection against copper toxicity. Am. J. Clin. Nutr. *67*, 1091S-1097S.

Dancis,A., Yuan,D.S., Haile,D., Askwith,C., Eide,D., Moehle,C., Kaplan,J., and Klausner,R.D. (1994). Molecular characterization of a copper transport protein in S. cerevisiae: an unexpected role for copper in iron transport. Cell *76*, 393-402.

Danks,D.M. (1995). Disorders of Copper Transport. In The Metabolic and Molecular Bases of Inherited Disease, C.R.Scriver, A.L.Beaudet, W.S.Sly, and D.Valle, eds. McGraw-Hill, Inc.), pp. 2211-2235.

Danks,D.M., Campbell,P.E., Walker-Smith,J., Stevens,B.J., Gillespie,J.M., Blomfield,J., and Turner,B. (1972). Menkes' kinky-hair syndrome. Lancet *1*, 1100-1102.

Danks,D.M., Cartwright,E., Stevens,B.J., and Townley,R.R. (1973). Menkes' kinky hair disease: further definition of the defect in copper transport. Science *179*, 1140-1142.

Das,S., Levinson,B., Vulpe,C., Whitney,S., Gitschier,J., and Packman,S. (1995). Similar splicing mutations of the Menkes/mottled copper-transporting ATPase gene in occipital horn syndrome and the blotchy mouse. Am. J. Hum. Genet. *56*, 570-576.

Deng,D.X., Ono,S., Koropatnick,J., and Cherian,M.G. (1998). Metallothionein and apoptosis in the toxic milk mutant mouse. Lab Invest *78*, 175-183.

Deng,H.X., Hentati,A., Tainer,J.A., Iqbal,Z., Cayabyab,A., Hung,W.Y., Getzoff,E.D., Hu,P., Herzfeldt,B., Roos,R.P., and et al. (1993). Amyotrophic lateral sclerosis and structural defects in Cu,Zn superoxide dismutase . Science *261*, 1047-51.

Diaz,G., Faa,G., Farci,A.M., Balestrieri,A., Liguori,C., and Costa,V. (1990). Copper distribution within and between newborn livers. J. Trace Elem. Electrolytes Health Dis. *4*, 61-64.

Dickinson,E.K., Adams,D.L., Schon,E.A., and Glerum,D.M. (2000). A human SCO2 mutation helps define the role of Sco1p in the cytochrome oxidase assembly pathway. J. Biol. Chem. *275*, 26780-26785.

Ecker,D.J., Butt,T.R., Sternberg,E.J., Neeper,M.P., Debouck,C., Gorman,J.A., and Crooke,S.T. (1986). Yeast metallothionein function in metal ion detoxification. J. Biol. Chem. *261*, 16895-16900.

Eisses,J.F., Stasser,J.P., Ralle,M., Kaplan,J.H., and Blackburn,N.J. (2000). Domains I and III of the human copper chaperone for superoxide dismutase interact via a cysteine-bridged Dicopper(I) cluster. Biochemistry *39*, 7337-7342.

Fu,D., Beeler,T.J., and Dunn,T.M. (1995). Sequence, mapping and disruption of CCC2, a gene that cross-complements the Ca(2+)-sensitive phenotype of csg1 mutants and encodes a P-type ATPase belonging to the Cu(2+)-ATPase subfamily. Yeast *11*, 283-292.

Gaudette,M., Hirano,M., and Siddique,T. (2000). Current status of SOD1 mutations in familial amyotrophic lateral sclerosis. Amyotroph. Lateral. Scler. Other Motor Neuron Disord. *1*, 83-89.

Glerum,D.M., Shtanko,A., and Tzagoloff,A. (1996a). Characterization of COX17, a yeast gene involved in copper metabolism and assembly of cytochrome oxidase. J Biol Chem *271*, 14504-9.

Glerum,D.M., Shtanko,A., and Tzagoloff,A. (1996b). SCO1 and SCO2 act as high copy suppressors of a mitochondrial copper recruitment defect in *Saccharomyces cerevisiae*. J. Biol. Chem. *271*, 20531-20535.

Goka,T.J., Stevenson,R.E., Hefferan,P.M., and Howell,R.R. (1976). Menkes disease: a biochemical abnormality in cultured human fibroblasts. Proc. Natl. Acad. Sci. U. S. A *73*, 604-606.

Goto,J.J., Zhu,H., Sanchez,R.J., Nersissian,A., Gralla,E.B., Valentine,J.S., and Cabelli,D.E. (2000). Loss of in vitro metal ion binding specificity in mutant copper-zinc superoxide dismutases associated with familial amyotrophic lateral sclerosis. J. Biol. Chem. *275*, 1007-1014.

Grimes,A., Hearn,C.J., Lockhart,P., Newgreen,D.F., and Mercer,J.F. (1997). Molecular basis of the brindled mouse mutant (Mo(br)): a murine model of Menkes disease. Hum. Mol. Genet. *6*, 1037-1042.

Gurney,M.E., Pu,H., Chiu,A.Y., Dal Canto,M.C., Polchow,C.Y., Alexander,D.D., Caliendo,J., Hentati,A., Kwon,Y.W., Deng,H.X., and et al. (1994). Motor neuron degeneration in mice that express a human Cu,Zn superoxide dismutase mutation [published erratum appears in Science (1995) *269*(5221):149]. Science *264*, 1772-5.

Gutteridge,J.M. (1984). Tissue damage by oxy-radicals: the possible involvement of iron and copper complexes. Med. Biol. *62*, 101-104.

Hamza,I., Faisst,A., Prohaska,J., Chen,J., Gruss,P., and Gitlin,J.D. (2001). The metallochaperone Atox1 plays a critical role in perinatal copper homeostasis. Proc. Natl. Acad. Sci. U. S. A *98*, 6848-6852.

Hamza,I., Klomp,L.W., Gaedigk,R., White,R.A., and Gitlin,J.D. (2000). Structure, expression, and chromosomal localization of the mouse Atox1 gene. Genomics *63*, 294-7.

Hamza,I., Schaefer,M., Klomp,L.W., and Gitlin,J.D. (1999). Interaction of the copper chaperone HAH1 with the Wilson disease protein is essential for copper homeostasis. Proc Natl Acad Sci U S A *96*, 13363-8.

Harris,E.D. (1991). Copper transport: an overview. Proc. Soc. Exp. Biol. Med. *196*, 130-140.

Harris,E.D. (1995). The iron-copper connection: the link to ceruloplasmin grows stronger. Nutr Rev *53*, 170-3.

Harris,Z.L., Takahashi,Y., Miyajima,H., Serizawa,M., MacGillivray,R.T., and Gitlin,J.D. (1995). Aceruloplasminemia: molecular characterization of this disorder of iron metabolism. Proc Natl Acad Sci U S A *92*, 2539-43.

Heaton,D.N., George,G.N., Garrison,G., and Winge,D.R. (2001). The mitochondrial copper metallochaperone Cox17 exists as an oligomeric, polycopper complex. Biochemistry *40*, 743-751.

Huffman,D.L. and O'Halloran,T.V. (2000). Energetics of copper trafficking between the Atx1 metallochaperone and the intracellular copper transporter, Ccc2. J. Biol. Chem. *275*, 18611-18614.

Hung,I.H., Casareno,R.L., Labesse,G., Mathews,F.S., and Gitlin,J.D. (1998). HAH1 is a copper-binding protein with distinct amino acid residues mediating copper homeostasis and antioxidant defense. J Biol Chem *273*, 1749-54.

Hunt,D.M. (1974). Primary defect in copper transport underlies mottled mutants in the mouse. Nature *249*, 852-854.

Iwase,T., Nishimura,M., Sugimura,H., Igarashi,H., Ozawa,F., Shinmura,K., Suzuki,M., Tanaka,M., and Kino,I. (1996). Localization of Menkes gene expression in the mouse

brain; its association with neurological manifestations in Menkes model mice. Acta Neuropathol *91*, 482-8.

Jenner,P. (1998). Oxidative mechanisms in nigral cell death in Parkinson's disease. Mov Disord *13*, 24-34.

Jenner,P. and Olanow,C.W. (1996). Oxidative stress and the pathogenesis of Parkinson's disease. Neurology *47*, 161-70.

Kako,K., Tsumori,K., Ohmasa,Y., Takahashi,Y., and Munekata,E. (2000). The expression of Cox17p in rodent tissues and cells. Eur. J. Biochem. *267*, 6699-6707.

Kaler,S.G. (1998). Metabolic and molecular bases of Menkes disease and occipital horn syndrome. Pediatr. Dev. Pathol. *1*, 85-98.

Kaler,S.G., Gallo,L.K., Proud,V.K., Percy,A.K., Mark,Y., Segal,N.A., Goldstein,D.S., Holmes,C.S., and Gahl,W.A. (1994). Occipital horn syndrome and a mild Menkes phenotype associated with splice site mutations at the MNK locus. Nat. Genet. *8*, 195-202.

Kang,J.H. and Eum,W.S. (2000). Enhanced oxidative damage by the familial amyotrophic lateral sclerosis- associated Cu,Zn-superoxide dismutase mutants. Biochim. Biophys. Acta *1524*, 162-170.

Kanner,A.M. and Balabanov,A. (2002). Depression and epilepsy: how closely related are they? Neurology *58*, S27-S39.

Kelly,E.J. and Palmiter,R.D. (1996). A murine model of Menkes disease reveals a physiological function of metallothionein. Nat. Genet. *13*, 219-222.

Kelner,G.S., Lee,M., Clark,M.E., Maciejewski,D., McGrath,D., Rabizadeh,S., Lyons,T., Bredesen,D., Jenner,P., and Maki,R.A. (2000). The copper transport protein Atox1 promotes neuronal survival. J Biol Chem *275*, 580-4.

Klein,D., Lichtmannegger,J., Heinzmann,U., Muller-Hocker,J., Michaelsen,S., and Summer,K.H. (1998). Association of copper to metallothionein in hepatic lysosomes of Long- Evans cinnamon (LEC) rats during the development of hepatitis [se e comments]. Eur. J. Clin. Invest *28*, 302-310.

Klein,D., Scholz,P., Drasch,G.A., Muller-Hocker,J., and Summer,K.H. (1991). Metallothionein, copper and zinc in fetal and neonatal human liver: changes during development. Toxicol. Lett. *56*, 61-67.

Koropatnick,J. and Cherian,M.G. (1993). A mutant mouse (tx) with increased hepatic metallothionein stability and accumulation. Biochem. J. *296 (Pt 2)*, 443-449.

Kosonen,T., Uriu-Hare,J.Y., Clegg,M.S., Keen,C.L., and Rucker,R.B. (1997). Incorporation of copper into lysyl oxidase. Biochem J *327*, 283-9.

Krab,K. and Wikstrom,M. (1978). Proton-translocating cytochrome c oxidase in artificial phospholipid vesicles. Biochim. Biophys. Acta *504*, 200-214.

Kuivaniemi,H., Peltonen,L., Palotie,A., Kaitila,I., and Kivirikko,K.I. (1982). Abnormal copper metabolism and deficient lysyl oxidase activity in a heritable connective tissue disorder. J. Clin. Invest *69* , 730-733.

Kunz,W.S., Kuznetsov,A.V., Clark,J.F., Tracey,I., and Elger,C.E. (1999). Metabolic consequences of the cytochrome c oxidase deficiency in brain of copper-deficient Mo(vbr) mice. J. Neurochem. *72*, 1580-1585.

Kuo,Y.M., Gitschier,J., and Packman,S. (1999). Developmental expression of the mouse mottled and toxic milk genes. Adv Exp Med Biol *448*, 109-14.

Kuo,Y.M., Zhou,B., Cosco,D., and Gitschier,J. (2001). The copper transporter CTR1 provides an essential function in mammalian embryonic development. Proc. Natl. Acad. Sci. U. S. A *98*, 6836-6841.

Lamb,A.L., Torres,A.S., O'Halloran,T.V., and Rosenzweig,A.C. (2000). Heterodimer formation between superoxide dismutase and its copper chaperone. Biochemistry *39*, 14720-14727.

Lamb,A.L., Torres,A.S., O'Halloran,T.V., and Rosenzweig,A.C. (2001). Heterodimeric structure of superoxide dismutase in complex with its metallochaperone. Nat. Struct. Biol. *8*, 751-755.

Larin,D., Mekios,C., Das,K., Ross,B., Yang,A.S., and Gilliam,T.C. (1999). Characterization of the interaction between the Wilson and Menkes disease proteins and the cytoplasmic copper chaperone, HAH1p. J Biol Chem *274*, 28497-504.

Lee,J., Prohaska,J.R., Dagenais,S.L., Glover,T.W., and Thiele,D.J. (2000). Isolation of a murine copper transporter gene, tissue specific expression and functional complementation of a yeast copper transport mutant. Gene *254*, 87-96.

Lee,J., Prohaska,J.R., and Thiele,D.J. (2001). Essential role for mammalian copper transporter Ctr1 in copper homeostasis and embryonic development. Proc. Natl. Acad. Sci. U. S. A *98*, 6842-6847.

Levinson,B., Vulpe,C., Elder,B., Martin,C., Verley,F., Packman,S., and Gitschier,J. (1994). The mottled gene is the mouse homologue of the Menkes disease gene . Nat Genet *6*, 369-73.

Li,Y., Togashi,Y., Sato,S., Emoto,T., Kang,J.H., Takeichi,N., Kobayashi,H., Kojima,Y., Une,Y., and Uchino,J. (1991). Spontaneous hepatic copper accumulation in Long-Evans Cinnamon rats with hereditary hepatitis. A model of Wilson's disease. J. Clin. Invest *87*, 1858-1861.

Lin,S.J. and Culotta,V.C. (1995). The ATX1 gene of Saccharomyces cerevisiae encodes a small metal homeostasis factor that protects cells against reactive oxygen toxicity. Proc Natl Acad Sci U S A *92*, 3784-8.

Lin,S.J., Pufahl,R.A., Dancis,A., O'Halloran,T.V., and Culotta,V.C. (1997). A role for the Saccharomyces cerevisiae ATX1 gene in copper trafficking and iron transport. J Biol Chem *272*, 9215-20.

Linder,M.C., Wooten,L., Cerveza,P., Cotton,S., Shulze,R., and Lomeli,N. (1998). Copper transport. Am. J. Clin. Nutr. *67*, 965S-971S.

Loudianos,G. and Gitlin,J.D. (2000). Wilson's disease. Semin. Liver Dis. *20*, 353-364.

Ludwig,J., Owen,C.A., Jr., Barham,S.S., McCall,J.T., and Hardy,R.M. (1980). The liver in the inherited copper disease of Bedlington terriers. Lab Invest *43*, 82-87.

Machlin,L.J. and Bendich,A. (1987). Free radical tissue damage: protective role of antioxidant nutrients. FASEB J. *1*, 441-445.

Mann,J.R., Camakaris,J., and Danks,D.M. (1979). Copper metabolism in mottled mouse mutants: distribution of 64Cu in brindled (Mobr) mice. Biochem J *180*, 613-9.

Mann,J.R., Camakaris,J., Francis,N., and Danks,D.M. (1981). Copper metabolism in mottled mouse (Mus musculus) mutants. Studies of blotchy (Moblo) mice and a comparison with brindled (Mobr) mice. Biochem. J. *196*, 81-88.

Markesbery,W.R. and Carney,J.M. (1999). Oxidative alterations in Alzheimer's disease. Brain Pathol *9*, 133-46.

Martin,P.M., Irino,M., Suzuki,K., Lewis,M.H., and Mailman,R.B. (1991). The female brindled mouse as a model of Menkes' disease: the relationship of fur pattern to behavioral and neurochemical abnormalities. Dev. Neurosci. *13*, 121-129.

Menkes,J.H., Alter,M., Steigleder,D.R., Weakley,D.R., and Sung,J.H. (1962). A sex-linked recessive disorder with retardation of growth, peculiar hair, and focal cerebral and cerebellar degeneration. Pediatrics *29*, 764-7.

Mercer,J.F., Grimes,A., and Rauch,H. (1992). Hepatic metallothionein gene expression in toxic milk mice. J Nutr *122*, 1254-9.

Mercer,J.F., Livingston,J., Hall,B., Paynter,J.A., Begy,C., Chandrasekharappa,S., Lockhart,P., Grimes,A., Bhave,M., Siemieniak,D., and . (1993). Isolation of a partial candidate gene for Menkes disease by positional cloning. Nat. Genet. *3*, 20-25.

Michalczyk,A.A., Rieger,J., Allen,K.J., Mercer,J.F., and Ackland,M.L. (2000). Defective localization of the Wilson disease protein (ATP7B) in the mammary gland of the toxic milk mouse and the effects of copper supplementation. Biochem. J. *352 Pt 2*, 565-571.

Miles,A.T., Hawksworth,G.M., Beattie,J.H., Rodilla,V. (2000). Induction, regulation, degradation, and biological significance of mammalian metallothioneins. Crit. Rev. Biochem. Mol. Biol. *35*(1):35-70.

Mistilis,S.P. and Farrer,P.A. (1968). The absorption of biliary and non-biliary radiocopper in the rat. Scand. J. Gastroenterol. *3*, 586-592.

Mori,M. and Nishimura,M. (1997). A serine-to-proline mutation in the copper-transporting P-type ATPase gene of the macular mouse. Mamm. Genome *8*, 407-410.

Mulder,T.P., Janssens,A.R., Verspaget,H.W., and Lamers,C.B. (1991). Plasma metallothionein concentration in patients with liver disorders: special emphasis on the relation with primary biliary cirrhosis. Hepatology *14*, 1008-1012.

Muramatsu,Y., Yamada,T., Moralejo,D.H., Suzuki,Y., and Matsumoto,K. (1998). Fetal copper uptake and a homolog (Atp7b) of the Wilson's disease gene in rats. Res. Commun. Mol. Pathol. Pharmacol. *101*, 225-231.

Naeve,G.S., Vana,A.M., Eggold,J.R., Kelner,G.S., Maki,R., Desouza,E.B., and Foster,A.C. (1999). Expression profile of the copper homeostasis gene, rAtox1, in the rat brain. Neuroscience *93*, 1179-87.

Nishihara,E., Furuyama,T., Yamashita,S., and Mori,N. (1998). Expression of copper trafficking genes in the mouse brain. Neuroreport *9*, 3259-63.

Nomiyama,K., Nomiyama,H., Kameda,N., Tsuji,A., and Sakurai,H. (1999). Mechanism of hepatorenal syndrome in rats of Long-Evans Cinnamon strain, an animal model of fulminant Wilson's disease. Toxicology *132* , 201-214.

Odermatt,A., Suter,H., Krapf,R., and Solioz,M. (1993). Primary structure of two P-type ATPases involved in copper homeostasis in Enterococcus hirae. J. Biol. Chem. *268*, 12775-12779.

Oldendorf,W.H. and Kitano,M. (1965). Increased brain radiocopper uptake in Wilson's disease. Arch. Neurol. *13*, 533-540.

Owen,C.A., Jr. and Ludwig,J. (1982). Inherited copper toxicosis in Bedlington terriers: Wilson's disease (hepatolenticular degeneration). Am. J. Pathol. *106*, 432-434.

Paynter,J.A., Grimes,A., Lockhart,P., and Mercer,J.F. (1994). Expression of the Menkes gene homologue in mouse tissues lack of effect of copper on the mRNA levels. FEBS Lett *351*, 186-90.

Portnoy,M.E., Rosenzweig,A.C., Rae,T., Huffman,D.L., O'Halloran,T.V., and Culotta,V.C. (1999). Structure-function analyses of the ATX1 metallochaperone. J Biol Chem *274*, 15041-5.

Pufahl,R.A., Singer,C.P., Peariso,K.L., Lin,S.J., Schmidt,P.J., Fahrni,C.J., Culotta,V.C., Penner-Hahn,J.E., and O'Halloran,T.V. (1997). Metal ion chaperone function of the soluble Cu(I) receptor Atx1 . Science *278*, 853-6.

Punter,F.A., Adams,D.L., and Glerum,D.M. (2000). Characterization and localization of human COX17, a gene involved in mitochondrial copper transport. Hum. Genet. *107*, 69-74.

Rabizadeh,S., Gralla,E.B., Borchelt,D.R., Gwinn,R., Valentine,J.S., Sisodia,S., Wong,P., Lee,M., Hahn,H., and Bredesen,D.E. (1995). Mutations associated with amyotrophic lateral sclerosis convert superoxide dismutase from an antiapoptotic gene to a proapoptotic gene: studies in yeast and neural cells. Proc. Natl. Acad. Sci. U. S. A *92*, 3024-3028.

Rae,T.D., Schmidt,P.J., Pufahl,R.A., Culotta,V.C., and O'Halloran,T.V. (1999). Undetectable intracellular free copper: the requirement of a copper chaperone for superoxide dismutase . Science *284*, 805-8.

Rae,T.D., Torres,A.S., Pufahl,R.A., and O'Halloran,T.V. (2001). Mechanism of Cu,Zn-superoxide dismutase activation by the human metallochaperone hCCS. J. Biol. Chem. *276*, 5166-5176.

Rauch,H. (1983). Toxic milk, a new mutation affecting cooper metabolism in the mouse. J Hered *74*, 141-4.

Reed,V., Williamson,P., Bull,P.C., Cox,D.W., and Boyd,Y. (1995). Mapping of the mouse homologue of the Wilson disease gene to mouse chromosome 8. Genomics *28*, 573-5.

Roelofsen,H., Wolters,H., Van Luyn,M.J., Miura,N., Kuipers,F., and Vonk,R.J. (2000). Copper-induced apical trafficking of ATP7B in polarized hepatoma cells provides a mechanism for biliary copper excretion. Gastroenterology *119*, 782-93.

Rosenzweig,A.C. (2001). Copper delivery by metallochaperone proteins. Acc. Chem. Res. *34*, 119-128.

Rosenzweig,A.C., Huffman,D.L., Hou,M.Y., Wernimont,A.K., Pufahl,R.A., and O'Halloran,T.V. (1999). Crystal structure of the Atx1 metallochaperone protein at 1.02 A resolution. Structure Fold Des *7*, 605-17.

Scarborough,G.A. (1999). Structure and function of the P-type ATPases. Curr. Opin. Cell Biol. *11*, 517-522.

Schaefer,M., Hopkins,R.G., Failla,M.L., and Gitlin,J.D. (1999a). Hepatocyte-specific localization and copper-dependent trafficking of the Wilson's disease protein in the liver. Am J Physiol *276*, 639-46.

Schaefer,M., Roelofsen,H., Wolters,H., Hofmann,W.J., Muller,M., Kuipers,F., Stremmel,W., and Vonk,R.J. (1999b). Localization of the Wilson's disease protein in human liver. Gastroenterology *117*, 1380-1385.

Schmidt,P.J., Rae,T.D., Pufahl,R.A., Hamma,T., Strain,J., O'Halloran,T.V., and Culotta,V.C. (1999). Multiple protein domains contribute to the action of the copper chaperone for superoxide dismutase. J. Biol. Chem. *274*, 23719-23725.

Shefner,J.M., Reaume,A.G., Flood,D.G., Scott,R.W., Kowall,N.W., Ferrante,R.J., Siwek,D.F., Upton-Rice,M., and Brown,R.H., Jr. (1999). Mice lacking cytosolic copper/zinc superoxide dismutase display a distinctive motor axonopathy. Neurology *53*, 1239-1246.

Sherwood,G., Sarkar,B., and Kortsak,A.S. (1989). Copper histidinate therapy in Menkes' disease: prevention of progressive neurodegeneration. J. Inherit. Metab Dis. *12 Suppl 2*, 393-396.

Shiraishi,N., Taguchi,T., and Kinebuchi,H. (1991). Metallothionein messenger RNA levels in the macular mutant mouse: an animal model of Menkes' kinky-hair disease. Biol. Neonate *60*, 52-61.

Srinivasan,C., Posewitz,M.C., George,G.N., and Winge,D.R. (1998). Characterization of the copper chaperone Cox17 of Saccharomyces cerevisiae. Biochemistry *37*, 7572-7577.

Stephenson,G.F., Chan,H.M., and Cherian,M.G. (1994). Copper-metallothionein from the toxic milk mutant mouse enhances lipid peroxidation initiated by an organic hydroperoxide. Toxicol. Appl. Pharmacol. *125*, 90-96.

Suzuki-Kurasaki,M., Okabe,M., and Kurasaki,M. (1997). Copper-metallothionein in the kidney of macular mice: a model for Menkes disease. J Histochem Cytochem *45*, 1493-501.

Takahashi,Y., Kako,K., Arai,H., Ohishi,T., Inada,Y., Takehara,A., Fukamizu,A., and Munekata,E. (2002). Characterization and identification of promoter elements in the mouse COX17 gene. Biochim. Biophys. Acta *1574*, 359-364.

Takahashi,Y., Kako,K., Ohmura,K., Tsumori,K., Ohmasa,Y., Kashiwabara,S., Baba,T., and Munekatat,E. (2001). Genomic structure of mouse copper chaperone, COX17. DNA Seq. *12*, 305-318.

Tanzi,R.E., Petrukhin,K., Chernov,I., Pellequer,J.L., Wasco,W., Ross,B., Romano,D.M., Parano,E., Pavone,L., Brzustowicz,L.M., and . (1993). The Wilson disease gene is a copper transporting ATPase with homology to the Menkes disease gene. Nat. Genet. *5*, 344-350.

Terada,K., Nakako,T., Yang,X.L., Iida,M., Aiba,N., Minamiya,Y., Nakai,M., Sakaki,T., Miura,N., and Sugiyama,T. (1998). Restoration of holoceruloplasmin synthesis in LEC rat after infusion of recombinant adenovirus bearing WND cDNA. J. Biol. Chem. *273*, 1815-1820.

Theophilos,M.B., Cox,D.W., and Mercer,J.F. (1996). The toxic milk mouse is a murine model of Wilson disease. Hum Mol Genet *5* , 1619-24.

van De,S.B, Breen,M., Nanji,M., van Wolferen,M., de Jong,P., Binns,M.M., Pearson,P.L., Kuipers,J., Rothuizen,J., Cox,D.W., Wijmenga,C., and van Oost,B.A. (1999). Genetic mapping of the copper toxicosis locus in Bedlington terriers to dog chromosome 10, in a region syntenic to human chromosome region 2p13- p16. Hum. Mol. Genet. *8*, 501-507.

Tumer,Z., Tommerup,N., Tonnesen,T., Kreuder,J., Craig,I.W., and Horn,N. (1992). Mapping of the Menkes locus to Xq13.3 distal to the X-inactivation center by an

intrachromosomal insertion of the segment Xp13.3-q21.2. Hum. Mol. Genet. *88*, 668-672.

van De,S.B., Rothuizen,J., Pearson,P.L., van Oost,B.A., and Wijmenga,C. (2002). Identification of a new copper metabolism gene by positional cloning in a purebred dog population. Hum. Mol. Genet. *11*, 165-173.

Vulpe,C., Levinson,B., Whitney,S., Packman,S., and Gitschier,J. (1993). Isolation of a candidate gene for Menkes disease and evidence that it encodes a copper-transporting ATPase [published erratum appears in Nat Genet (1993) *3*(3):273]. Nat Genet *3*, 7-13.

Wakabayashi,T., Nakamura,N., Sambongi,Y., Wada,Y., Oka,T., and Futai,M. (1998). Identification of the copper chaperone, CUC-1, in *Caenorhabditis elegans*: tissue specific co-expression with the copper transporting ATPase, CUA-1. FEBS Lett. *440*, 141-146.

Walker,B.L., Tiong,J.W., and Jefferies,W.A. (2001). Iron metabolism in mammalian cells. Int. Rev. Cytol. *211*, 241-278.

Weiss,K.C. and Linder,M.C. (1985). Copper transport in rats involving a new plasma protein. Am. J. Physiol *249*, E77-E88.

Wernimont,A.K., Huffman,D.L., Lamb,A.L., O'Halloran,T.V., and Rosenzweig,A.C. (2000). Structural basis for copper transfer by the metallochaperone for the Menkes/Wilson disease proteins. Nat. Struct. Biol. *7*, 766-771.

Wilson,S.A.K. (1912). Progressive lenticular degeneration: A familial nervous disease associated with cirrhosis of the liver. Brain *34*, 295-507.

Winge,D.R., Nielson,K.B., Gray,W.R., and Hamer,D.H. (1985). Yeast metallothionein. Sequence and metal-binding properties. J. Biol. Chem. *260*, 14464-14470.

Wong,P.C., Waggoner,D., Subramaniam,J.R., Tessarollo,L., Bartnikas,T.B., Culotta,V.C., Price,D.L., Rothstein,J., and Gitlin,J.D. (2000). Copper chaperone for superoxide dismutase is essential to activate mammalian Cu/Zn superoxide dismutase. Proc Natl Acad Sci U S A *97*, 2886-91.

Wu,J., Forbes,J.R., Chen,H.S., and Cox,D.W. (1994). The LEC rat has a deletion in the copper transporting ATPase gene homologous to the Wilson disease gene. Nat. Genet. *7*, 541-545.

Yamamoto,H., Watanabe,T., Mizuno,H., Endo,K., Hosokawa,T., Kazusaka,A., Gooneratne,R., and Fujita,S. (2001). In vivo evidence for accelerated generation of hydroxyl radicals in liver of Long-Evans Cinnamon (LEC) rats with acute hepatitis. Free Radic. Biol. Med. *30*, 547-554.

Yim,M.B., Kang,J.H., Yim,H.S., Kwak,H.S., Chock,P.B., and Stadtman,E.R. (1996). A gain-of-function of an amyotrophic lateral sclerosis-associated Cu,Zn- superoxide dismutase mutant: An enhancement of free radical formation due to a decrease in Km for hydrogen peroxide. Proc. Natl. Acad. Sci. U. S. A *93*, 5709-5714.

Yuan,D.S., Stearman,R., Dancis,A., Dunn,T., Beeler,T., and Klausner,R.D. (1995). The Menkes/Wilson disease gene homologue in yeast provides copper to a ceruloplasmin-like oxidase required for iron uptake. Proc Natl Acad Sci U S A *92*, 2632-6.

Zhou,B. and Gitschier,J. (1997). hCTR1: a human gene for copper uptake identified by complementation in yeast. Proc Natl Acad Sci U S A *94*, 7481-6.

CHAPTER 2

COPPER CHAPERONE FOR SUPEROXIDE DISMUTASE

Methods and data discussed in this chapter have been published in part in the following publication:

Moore S.D.P., Chen M.M., Cox D.W. (2000) Cloning and mapping of murine superoxide dismutase copper chaperone (*Ccsd*) and mapping of the human ortholog. *Cyto and Cell Genet.* **88**(1-2): 35-37.

Matthew Chen, undergraduate student, isolated the cDNA clone for *Ccsd* from a mouse fetal phage library.

2.1) INTRODUCTION

Copper is an essential cofactor for many different cellular metalloproteins. Free heavy metals within the cell can potentially damage cellular components, such as lipids, nucleic acids, and proteins, because of their endogenous oxidative potential. The cell contains little or no damaging free intracellular copper (Rae et al., 1999); instead, the copper is bound to many different proteins that sequester the metal and prevent damage to cellular components. Human metallochaperones, such as ATOX1 (previously named HAH1) (Klomp et al., 1997), CCS (Culotta et al., 1997), and COX17 (Amaravadi et al., 1997) help deliver copper to metalloproteins that either use copper as an enzymatic cofactor or transport copper to another compartment within the cell. Lys7p (the yeast homolog of CCS) has been demonstrated to activate cytoplasmic SOD1 (superoxide dismutase) in the presence of low intracellular copper concentrations by direct insertion of its copper cofactor (Corson et al., 1998; Rae et al., 1999). In addition, the copper chaperone CCS specifically delivers copper to both wild-type and familial amyotrophic lateral sclerosis SOD1 mutant proteins (Casareno et al., 1998).

The yeast metallochaperone *Lys7* and the human orthologue *CCS* cDNA sequence have been elucidated. However, the murine orthologue for this chaperone had yet to be characterized at the beginning of my studies. The purpose of my study was to identify the mouse orthologue of human *CCS*. When cDNA sequence was determined, it would be possible to compare the expression profiles between human and mice and to map both genes.

I report cloning of the complete cDNA for mouse *Ccsd* (including the 3' and 5' UTRs) and mapping of the locus to the proximal region of chromosome 19, in a region homologous to a cluster of syntenic genes on human 11q13. Additionally, we mapped

human CCS to chromosome 11q13. The expression pattern of CCS in mouse was studied using multiple tissue northern blots.

2.2) MATERIALS AND METHODS

2.2.1) Human CCS probe

To identify the mouse ortholog of CCS, we screened an adult mouse brain cDNA library with a partial human *CCS* cDNA probe (553-898). The human clone was obtained using the reverse transcription polymerase chain reaction (RT-PCR) with total brain RNA as a template. The first strand was synthesized using an oligo-dT primer followed by PCR using two constructed human CCS primers: CCS.L1 553 (5′-TGT CCG TGC TGA TGC TGA CG-3′) and CCS.R1 898 (5′- GAA AGT GCT CGC CCT GGA GG -3′). PCR conditions included 1 cycle of 94°C for 2 min, followed by 35 cycles of 94°C for 30 s, 55°C for 35 s, and 72°C for 30 s. The resulting 346 base pair fragment was cloned using the pGEM-T Easy Vector System (Promega), transformed into JM109 High Efficiency Competent Cells, and selected for by carbenicillin resistance and LacZ expression. The cloned fragment was then manually sequenced and confirmed to be a 346 base pair fragment of human *CCS* (GenBank Accession number AF002210).

A mouse multiple tissue northern blot was prepared to determine if the human *CCS* probe would successfully recognize the murine orthologue, thereby supporting its use to screen the mouse cDNA library. RNA samples from various tissues (kidney, placenta, liver, brain, and spleen) were quantified and electrophoresed on a 0.8% denaturing gel (6% formaldehyde, 1 X MOPS, 0.8% agarose). RNA was transfered to a Hybond-N^+ nylon membrane (Amersham) and analyzed with ^{32}P radiolabelled *CCS* (553-898).

2.2.2) Screening a cDNA library

A mouse adult brain cDNA library, generated by poly-T priming and cloned into λZAP (with *Eco*RI and *Xho*I flanking restriction sites) (provided by Dr. Heather McDermid), was used. Library titer was 8.5×10^6 pfu/ml (pfu: plaque forming units) and was plated on eighteen 150 x 15 mm plates, with approximately 20,000 plaques on each plate allowing roughly 360,000 recombinant phage to be screened. The library was plated using *E. coli* XL1-Blue cells mixed in with phage and 0.7% top agar. Nylon-N^+ membranes used for plaque lifting were soaked in denaturation solution followed by neutralization treatment and fixation by UV cross-linking. Treated membranes were probed with radiolabeled *CCS* (553-898) and the resulting hybridized products were detected by exposing to autoradiograph film. Positive plaques were plugged and plated for a secondary and subsequent tertiary screen to ensure the isolation of single positive clones.

2.2.3) Subcloning and Sequencing

Positive phage were isolated and subcloned into a vector for characterizing the λZAP insert. Subcloning into a vector was performed by *in vivo* excision of the pBLUESCRIPT phagemid from the λZAP vector (protocol from Stratagene). This was accomplished by co-infecting *E. coli* (strain BB4) with positive λZAP clones and R408 helper phage. Helper phage provided the necessary proteins needed for the conversion of the λZAP into pBLUESCRIPT. The resulting plasmids derived from the positive phage particles were analyzed by restriction digest cleavage at the cloning sites derived from *Eco*RI and *Xho*I sites. Clones suspected to contain *Ccsd* were selected and sequenced by LICOR-4200 automated sequencing.

2.2.4) Mapping mouse Ccsd

For mapping mouse *Ccsd,* genomic primers were designed using BCM launcher (http://www.hgsc.bcm.tmc.edu/SearchLauncher/) to predict intron/exon boundaries within the cDNA. The resulting primers designated CCS.UP (5′-TCA GTT GGA GAA CCA GAT GG-3′) and CCS.LP (5′-TTC TGT AAT TGG CTA CTG CCC-3′) provided a band of 120 base pairs from mouse and not hamster genomic DNA. These primers were then used on the T31 mouse × hamster radiation hybrid panel and results were submitted to the Jackson Laboratory (The Jackson Laboratory, Bar Harbor, ME, USA; (http://www.jax.org/resources/documents/cmdata/rhmap/rhsubmit.html).

2.2.5) Mapping human CCS

For mapping of human *CCS*, human genomic primers for *CCS* (CCS.L1 and CCS.R1) were used for the amplification of a genomic fragment from the human × hamster radiation hybrid panel (GENEBRIDGE 4 human × hamster RH panel purchased from Research Genetics). The primers span an intron, since amplification of a cDNA template produced a fragment of ~ 350 bp, but amplification from a genomic template produced a fragment of ~ 550 bp which was confirmed by sequencing to contain intronic sequence.

2.2.6) Northern blot analysis

The expression patterns of mouse and human *CCS* were determined by using species-specific probes on species-specific multiple tissue northern blots. A mouse multiple tissue northern blot (ClonTech) was probed with a portion of mouse *Ccsd.* In

addition, a human multiple tissue northern blot (Origene) was probed with the human CCS clone (ClonTech Express Hybridization protocol).

2.3) RESULTS

2.3.1) Screening a mouse cDNA Library

The adult mouse brain cDNA library was screened using the human *CCS* cDNA clone. After the secondary screen, 12 positive clones were selected. Following tertiary screening, clones with the longest insert were sequenced using a LONG READIR 4200 automated sequencer (LI-COR) with M13 forward and reverse primers (as described by the manufacturer).

The murine cDNA sequence (Genbank accession # AF173379) was 80.6% identical to the human orthologue. An 825 bp open reading frame (ORF), flanked by a 60 bp 5′ UTR and a 167 bp 3′ UTR, was identified within the cDNA sequence. The ORF was predicted to encode 274 amino acids with a molecular weight of ~ 29 kDa (Figure 2-1). A comparison between the predicted amino acid sequences for human and mouse showed 86.9% identity, including complete conservation of the copper-binding motif MXCXXC at amino acid residues 20–25 (Figure 2-2). A 572-bp mouse EST (GenBank accession number AA123360) and a partial cDNA (coding segment only, GenBank accession number AF121906) were identical to relevant portions of our clone. When compared with the yeast ortholog Lys7p, the mouse sequence revealed 25.5% amino acid conservation, including a complete identity of the copper-binding domain (MXCXXC). A hydrophobicity plot of the yeast, mouse, and human amino acid sequences was generated, revealing no potential transmembrane domains, consistent with what would be expected of a cytoplasmic protein (Figure 2-3).

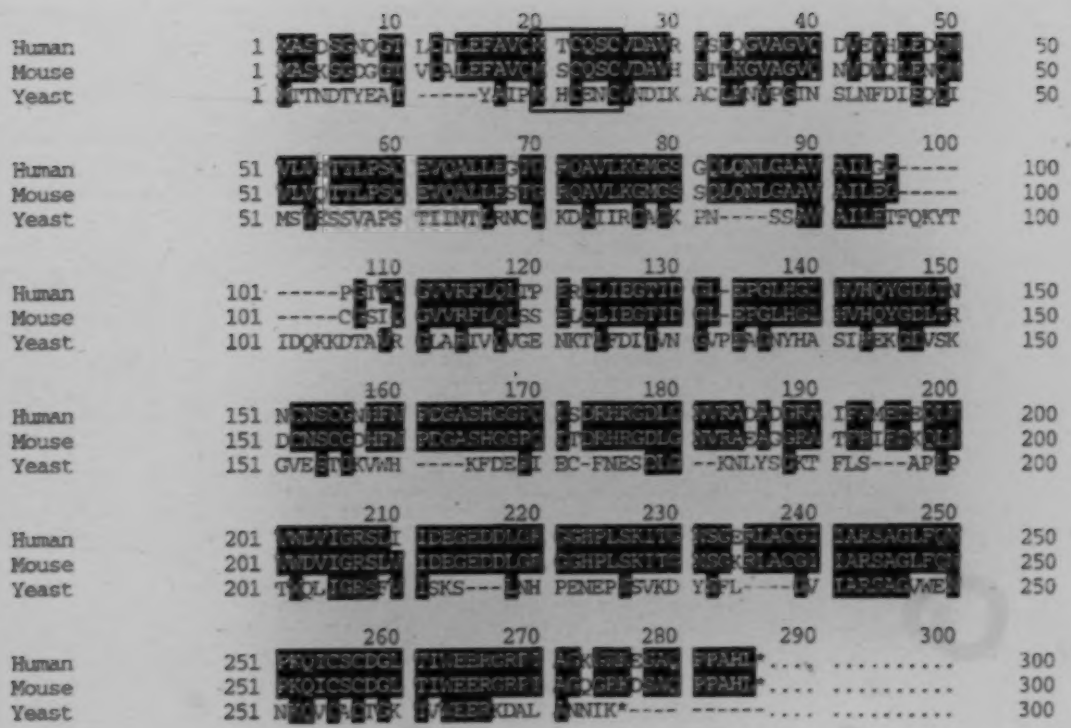

Figure 2-2: *Ccsd/CCS* amino acid sequence alignment of copper chaperone for SOD1. The copper binding motif, MXCXXC (outlined in black box), is highly conserved among all three species. Mouse *Ccsd* has an 80.6% sequence identity and 86.9% amino acid identity to human. All three species also show several additional regions of conservation. Identical amino acids are highlighted.

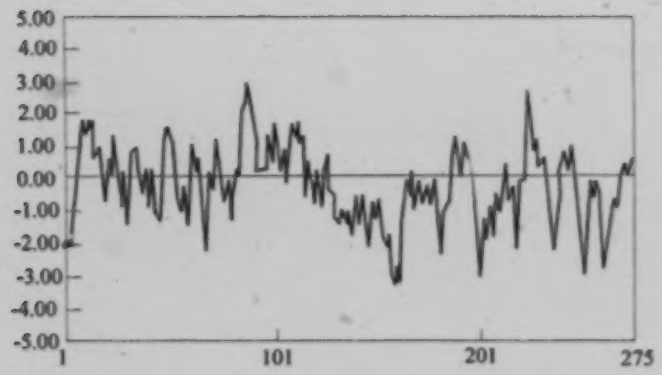

Human CCS

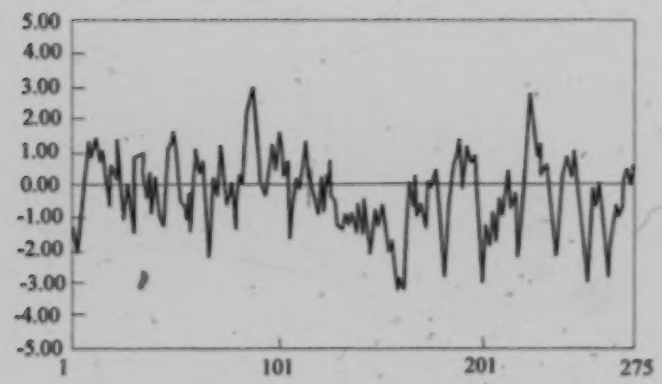

Mouse Ccsd

Figure 2-3: Hydrophobicity plots of mouse Ccsd and human CCS. Analysis of the plots did not reveal any extensive hydophobic regions (typically 18-33 residues over +1.6) suggestive of a membrane protein. Y axis indicates score and X axis indicates residue position.

2.3.2) Mapping CCS/Ccsd

Mapping results from the radiation hybrid panel, calculated by Jackson laboratory, showed linkage of the mouse gene, *Ccsd,* to D19Mit29 with a lod score of 20.4 and to D19Mit109 with a lod score of 16.1. This placed mouse *Ccsd* in the proximal part of chromosome 19, 4.0 cM from the centromere, most likely centromeric to D19Mit29 and D19Mit68 (Figure 2-4).

Results from the panel for human CCS (submitted to the Whitehead Institute [http://www-genome.wi.mit.edu]) confirmed that the gene is on human chromosome 11 and is placed 8.56 cR from D11S913, with a lod score of 9.65 in the region 11q13 (Figure 2-5).

2.3.3) Mouse/Human expression pattern

To determine tissue expression patterns for the copper chaperone in human and mouse, species-specific clones were used to probe human and mouse multiple tissue northern blots. The mouse RNA demonstrated a single band ~ 1.1 kb in length in all tissues; however, liver and skeletal muscle had additional bands that were longer than the expected transcript (Figure 2-6). Human brain, heart, kidney, spleen, liver, and leukocytes all showed significant levels of expression (Figure 2-6). However, additional bands were also detected in kidney, liver, and leukocytes, which are only faintly seen in mouse skeletal muscle. These additional bands ranged from approximately 1.7 kb to 6 kb.

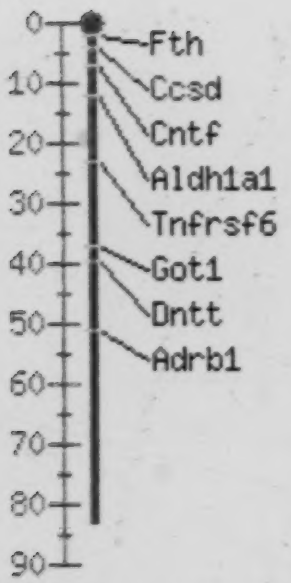

Figure 2-4: Mapping Ccsd to mouse chromosome 19. The locus is located at the proximal position 4.0 cM from the centromere (diagram from Jackson Laboratory). Numbers on the left indicate cM from the centromere.

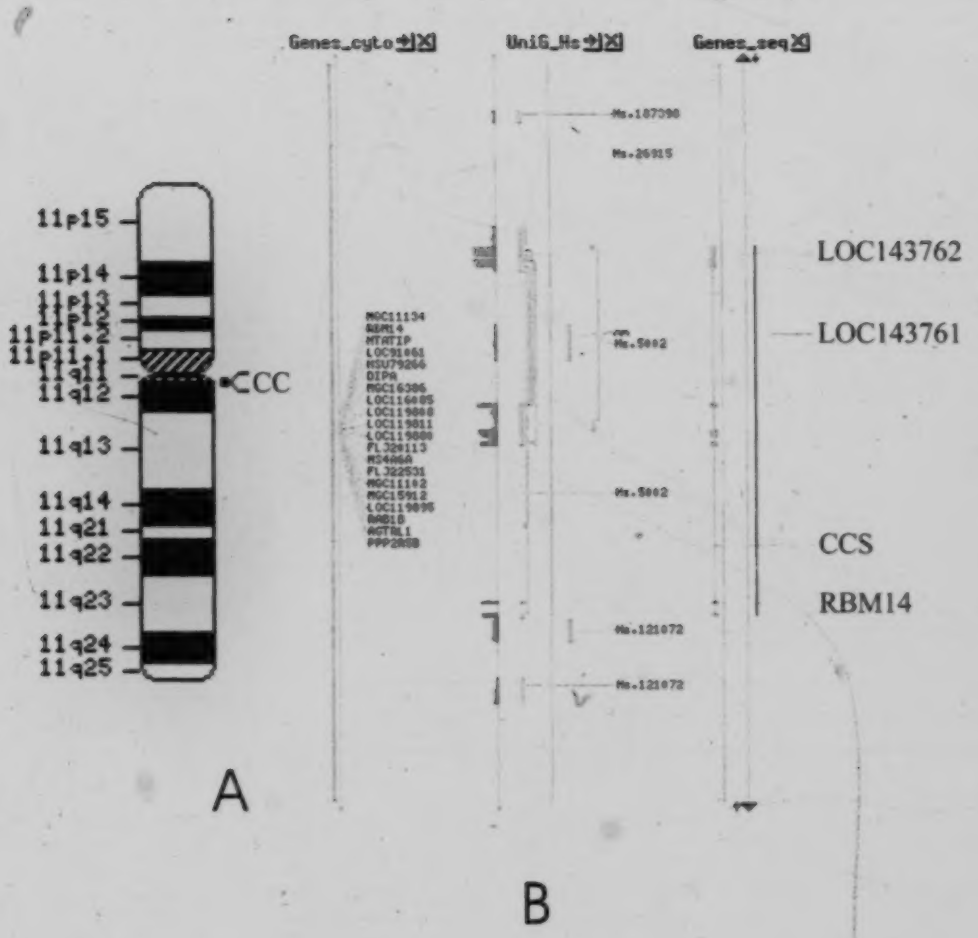

Figure 2-5: Chromosomal location of CCS. (A) Ideogram of chromosome 11 indicating approximate location of CCS locus. (B) Genetic annotation in chromosomal region demonstrating genomic structure of CCS (information from NCBI).

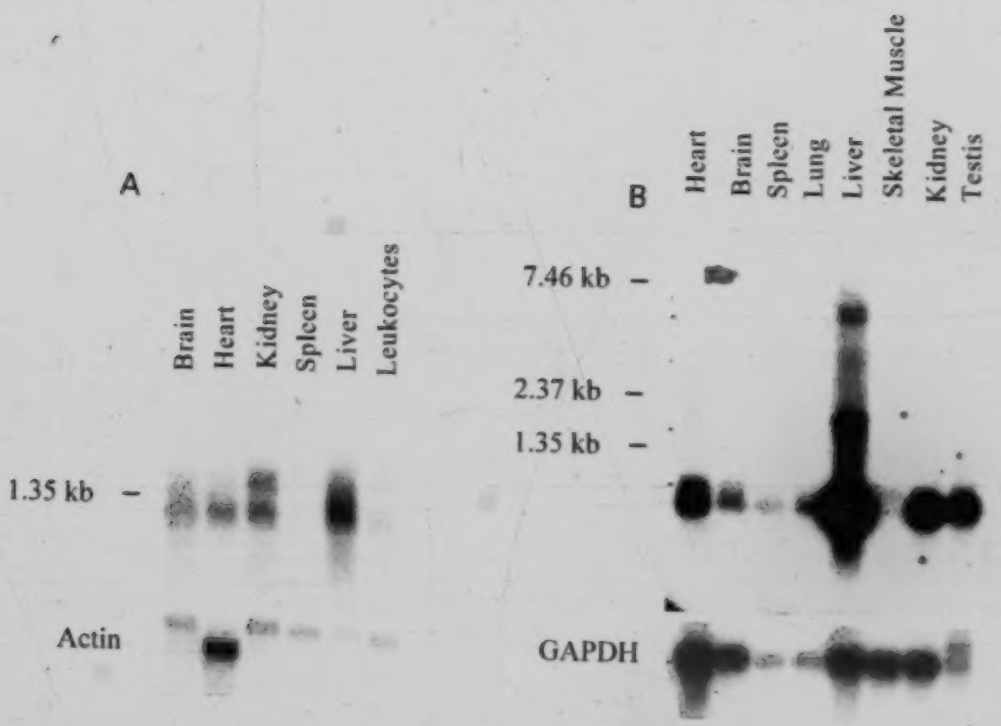

Figure 2-6: Expression of mouse and human copper chaperones. The human poly-A RNA multiple tissue northern (A) was probed with partial Ccsd (365 bp) and actin. The lanes are in the following order: brain, heart, kidney, spleen, liver, and leukocytes. A poly-A RNA mouse multiple tissue northern (B) probed with complete Ccsd and GAPDH. The corresponding lanes represent heart, brain, spleen, lung, liver, skeletal muscle, kidney, and testis, respectively. The mouse northern blot was purchased from Clontech and the human northern blot was purchased from Origene.

2.4) DISCUSSION

In the case of yeast Lys7p (a homolog of CCS), the metallochaperone has been shown to maintain copper in a readily accessible state for transfer to SOD1 (Rae et al., 1999). The delivery of copper from the copper chaperone to the mutant "gain of function" SOD1 is essential for the mutant SOD1 phenotype to manifest (Hottinger et al., 1997; Casareno et al., 1998; Corson et al., 1998). Further characterization of both the mouse and human copper chaperone for SOD1 should aid in studying familial amyotrophic lateral sclerosis.

The complete cDNA sequence that we identified was mapped to mouse chromosome 19, 4.0 cM from the centromere. The region of a cluster of syntenic genes in the human genome is on chromosome 11q13. Therefore, our data support syntenic gene regions described in Genbank between human 11q13 and the proximal region on mouse chromosome 19.

The expression pattern of the copper transporter is a key factor in a more detailed understanding of the global regulation and function of the protein. *Ccsd* is expressed in the same tissues as the antioxidant protein, SOD1, in mice (de Haan et al., 1994). Since *Ccsd* is the copper chaperone for SOD1, this is an expected result; however, our northern blots reveal additional fragments. These bands could either be an artifact or represent alternative transcripts. It is possible that there are alternative tissue-specific transcripts that have either multiple start sites or an alternative poly-adenylation termination site, which could indicate species differences for alternative transcripts. The function and significance of these alternative transcripts is not yet known.

2.5) REFERENCES

Amaravadi,R., Glerum,D.M., and Tzagoloff,A. (1997). Isolation of a cDNA encoding the human homolog of COX17, a yeast gene essential for mitochondrial copper recruitment. Hum. Genet. *99*, 329-333.

Casareno,R.L., Waggoner,D., and Gitlin,J.D. (1998). The copper chaperone CCS directly interacts with copper/zinc superoxide dismutase. J Biol Chem *273*, 23625-8.

Corson,L.B., Strain,J.J., Culotta,V.C., and Cleveland,D.W. (1998). Chaperone-facilitated copper binding is a property common to several classes of familial amyotrophic lateral sclerosis-linked superoxide dismutase mutants. Proc Natl Acad Sci U S A *95*, 6361-6.

Culotta,V.C., Klomp,L.W., Strain,J., Casareno,R.L., Krems,B., and Gitlin,J.D. (1997). The copper chaperone for superoxide dismutase. J Biol Chem *272*, 23469-72.

de Haan,J.B., Tymms,M.J., Cristiano,F., and Kola,I. (1994). Expression of copper/zinc superoxide dismutase and glutathione peroxidase in organs of developing mouse embryos, fetuses, and neonates. Pediatr Res *35*, 188-96.

Hottinger,A.F., Fine,E.G., Gurney,M.E., Zurn,A.D., and Aebischer,P. (1997). The copper chelator d-penicillamine delays onset of disease and extends survival in a transgenic mouse model of familial amyotrophic lateral sclerosis. Eur. J. Neurosci. *9*, 1548-1551.

Klomp,L.W., Lin,S.J., Yuan,D.S., Klausner,R.D., Culotta,V.C., and Gitlin,J.D. (1997). Identification and functional expression of HAH1, a novel human gene involved in copper homeostasis. J Biol Chem *272*, 9221-6.

Rae,T.D., Schmidt,P.J., Pufahl,R.A., Culotta,V.C., and O'Halloran,T.V. (1999). Undetectable intracellular free copper: the requirement of a copper chaperone for superoxide dismutase . Science *284*, 805-8.

CHAPTER 3

EXPRESSION IN MOUSE KIDNEY OF MEMBRANE COPPER TRANSPORTERS Atp7a and Atp7b

Methods and data discussed in this chapter have been published in part in the following publication:

Moore, S.D.P and Cox, D.W. (2002). Expression in mouse kidney of membrane copper transporters Atp7a and Atp7b. *Nephron* (In Press)

3.1) INTRODUCTION

Within the kidney, copper is normally present in the proximal tubules, distal tubules, and glomeruli (Yoshimura, 1994). In animal models for Wilson disease, copper accumulation occurs in the proximal tubules but not in the distal tubules or the glomeruli (Yoshimura, 1994). In Wilson disease patients, this accumulation is suggested to be the cause of tubular dysfunction (Elsas et al., 1971). In addition to tubular dysfunction, glomerular dysfunction is also a characteristic of Wilson disease; however this dysfunction is suggested to be linked to D-penicillamine treatment. Wilson disease patients characteristically show a large increase of copper in the urine of >100 μg/day compared with the normal value of <40 μg/day (Table 1-2). Increased copper in the urine is presumed to be associated with the relatively high copper levels in the serum. However, the re-absorption of iron occurs in the loops of Henle and it has been suggested that copper re-absorption also occurs in this region (Wareing et al., 2000).

In humans, the increased copper level in the kidney of Menkes disease patients is similar to or higher than that of Wilson disease patients (Kodama et al., 1992). As in Wilson disease patients, the macular mouse, allelic mutation of the mottled locus, demonstrates copper accumulation in the proximal convoluted tubules (Kodama et al., 1993). However, there is no renal tubular dysfunction in Menkes disease patients. The accumulation of copper could be the result of a localized disruption of copper transport in the proximal convoluted tubules or a secondary downstream effect from a global problem with copper regulation.

The focus of this study is to compare the specific localization of the transporters Atp7a and Atp7b within mouse kidney. Clarification of the specific localization pattern

of the copper transporters in this tissue may help to provide a molecular explanation for clinical features observed in Wilson and Menkes disease patients.

3.2) METHODS AND MATERIALS

3.2.1) Construction of Atp7a and Atp7b probes

Reverse transcriptase products from total kidney RNA were used to obtain a 751 base pair fragment of *Atp7b* (Atp7b.i) derived using primers Atp7b.A1 (5'- TTC TCT CAG TGT TGG TCG C -3') and Atp7b.A2 (5'- GTG TCA AAG AAG GTC ACG G - 3'). A 724 base pair fragment of *Atp7a* (Atp7a.iii) was obtained by using primers Atp7a.A11 (5'-GGA AAA CGC TGG GGA AGG-3') AND Atp7a.A22 (5'-CAG CCA TCG TCC TAG TGC G-3'). Because *Atp7a* and *Atp7b* are paralogues (highly similar genes within the same organism) fragments were selected to minimize cross-hybridization of probes. RT-PCR products were cloned into pGEM-T Easy vector (Promega) using the manufacture's protocol. Ligated products were transformed into XL-1 blue competent cells and white colonies containing inserts were identified by plating on IPTG and X-Gal LB plates. Positive clones were screened by restriction digest for the proper fragment size and were sequenced to confirm identity. Atp7b.i was labeled using random T7 quickprime kit and used as probes on a multiple tissue northern blot (Clontech) to confirm that the correct size transcript were recognized.

Digoxygenin (DIG)-labeled RNA was made by *in vitro* transcription (Roche RNA DIG-labeling kit) using the characterized plasmid clones. To produce RNA from *Atp7b* in opposite orientations, the plasmid was first linearized on either the 5' or 3' side of the insert utilizing the multiple cloning sites, followed by transcription using the corresponding promoter. Purity, size, and DIG incorporation into the RNA products

were confirmed by running the products in a denaturing gel by electrophoresis. The separated RNA products were then transferred onto an N^+ nylon membrane (Amersham) by capillary transfer. RNA products were detected using anti-DIG antibodies conjugated to alkaline phosphatase (AP) using 5-bromo-4-chloro-3-indolyl-phosphate (BCIP)/ 4-nitroblue tetrazolium chloride (NBT) (Roche).

3.2.2) Probe Characterization

After linear run-off transcription for generation of RNA probes, DIG labeled transcripts were run on 0.6% formaldehyde denaturing gel and transferred to a nylon N^+ membrane by a capillary transfer apparatus. The membrane was washed with buffer (0.1 M Tris and 0.15 M NaCl) and then blocked with 2% skim milk powder and washed again. The membrane was then incubated with anti-DIG antibody conjugated to alkaline phosphatase for 30 min followed by two 10 min washes. Buffer containing 0.1 M Tris pH 9.5 in combination with 5-bromo-4-chloro-3-indolyl-phosphate (BCIP)/ 4-nitroblue tetrazolium chloride (NBT) was placed over the membrane for 10-30 min for the alkaline phosphatase reaction to proceed. The reaction was stopped by washing with water and allowing the membrane to dry. Confirmation of promoter orientation relative to insert was determined by designing primers that flanked the T7 promoter, thereby allowing the sequencing product to encompass the vector, promoter, and insert sequentially. These primers were SM-PGEM2732 (HSC #2482) (5'-AGG GAA GAA AGC GAA AGG AG-3') and SM-PGEM27111 (HSC #2481) (5'-GGC GAA CGT GGC GAG AAA GG-3').

3.2.3) Preparation of tissue sections

Mouse perfusions were initiated while the balb/cCr//AltBM mice were sedated and in surgical plane. Surgical plane was induced by using Methoxifane as an inhalant. When the mouse no longer responded to pinching stimulus it was considered to be in surgical plane and ready for surgery. The mouse was placed on its back with the front limbs secured with tape. The abdominal cavity was opened by a transverse incision just below the rib cage. Using forceps, the xyphoid process was clamped and curled back to expose the diaphragm. The diaphragm was pierced and cut following the rib cage. Using scissors, the rig cage was peeled back while being cut along both sides of the body. The mouse was now prepared for commencing injections.

A 26 gauge needle was inserted into the left ventricle pointing straight up so the flow from the needle led directly into the aorta. Once the needle was in place, saline was injected at a rate of 300 ml/hr. Using scissors, the right ventricle was cut to promote drainage of excess fluid. It was imperative that the left ventricle was not pierced while cutting the right ventricle. In addition, the larger the excision made to the right ventricle, the better the blood drained and therefore the better the perfusion. After approximately 10 min, 50 ml saline, or complete discoloration of liver, saline injections were discontinued. A paraformaldehyde mixture (4% paraformaldehyde and 0.05% gluteraldehyde) was injected at a rate of 350 ml/hr immediately following saline injections. The paraformaldehyde mixture was made fresh each day. The kidney required approximately 80-100 ml of paraformaldehyde mixture to be injected for proper fixation. Each tissue had a unique consistency and tenderness so trial and error was necessary to obtain the appropriate firmness or fixation. Once the tissue received the proper amounts of fixative, the kidney was removed and placed in 4% paraformaldehyde

fixative for 30 min. For the liver, after removal from the mouse, the tissue was immediately placed in 1 X PBS. Both the kidney and the liver were left in 1 X PBS overnight and embedded the next day.

Embedding tissue in paraffin required a heated chamber (fitted with a vacuum). All solutions were preheated to 40°C. The kidney and liver were removed from 1 X PBS and place in preheated 1 X PBS for 2 min under vacuum. Again, the kidney and liver were then placed in 70% ethanol for 6 min under vacuum. Then in 95% ethanol for 12 min, 100% ethanol for 6 min, 100% ethanol for 6 min, and 100% ethanol for 12 min under vacuum. Next the kidney was placed in a 50:50 mixture of paraffin:xylene for 2-5 min prior to using pure paraffin. The liver was placed in pure paraffin without the 50:50 paraffin:xylene mixture. The tissue remained under a vacuum at 60°C for 30 min. The paraffin was refreshed and the kidney continued to be incubated overnight to allow more equal penetration into the dense tissue. For the liver, the second paraffin incubation was only 30 min in duration. Once the tissues were ready to embed in solidified paraffin, they were placed in a molding block with molten paraffin and positioned with forceps until the paraffin solidified enough to maintain the orientation.

During sectioning, if the kidney crumbled and/or morphology was lost following subsequent manipulations, the tissue was over-fixed. If the tissue shrank or was soft in the paraffin block, the tissue was under-fixed. The procedure was repeated using a fresh kidney until suitable samples were obtained.

3.2.4) In Situ Hybridization

Xylene was used to remove paraffin from kidney sections followed by re-hydration in a graded ethanol series. Sections were incubated with 6% hydrogen

peroxide to remove endogenous peroxidase activity. Freshly made proteinase K was added to the sections at a concentration of 60 µg/ml and incubated at 37°C for 10 min followed by one minute incubation in 70°C 2 X SSC to inactive residual proteinase K. 0.25% acetic anhydride in 0.1 M triethanolamine was used to reduce positive charges of proteins in the tissue, thus preventing charge interactions with probe. After two five minute washes with 2 X SSC, sections were incubated in a humidity chamber at 45°C for two hours in hybridization solution (50% formamide, 5 X SSC, pH 5.0, 1% SDS, 50 mg/ml heparin (Sigma), 50 mg/ml yeast RNA (Roche), in DEPC treated ddH_2O). After pre-hybridization, DIG labeled RNA was added to fresh hybridization solution and left in a humidity chamber overnight at 4°C. The next day, excess probe was removed by washing in 50% formamide based in a 2 X SSC solution at 70°C. Sections were then equilibrated in TBST (TBS and 0.1% Tween 20) and blocked in TBST with 10% sheep serum for 2 hours. After blocking, anti-DIG antibody conjugated to alkaline phosphatase, preabsorbed with kidney acetone powder (Roche), was incubated with the sections overnight at 4°C in a humidity chamber. Non-specific antibody was removed with extensive washing in TBST buffer. Anti-DIG-AP was detected by 5-bromo-4-chloro-3-indolyl-phosphate (BCIP)/ 4-nitroblue tetrazolium chloride (NBT) (Roche) in alkaline phoshatase buffer (0.1 M Tris pH 9.5, 0.05 M $MgCl_2$, 0.1 M NaCl, 0.1% Tween 20, and 0.5 mg/ml of levamisole (endogenous AP inhibitor)). Sections were incubated overnight at 4°C in a humidity chamber prior to stopping the AP reaction.

3.2.5) Immunohistochemistry

Prepared paraffin embedded kidney and liver sections were dewaxed and rehydrated. Tyramide Signal Amplification (TSA) biotin system NEL 700A (Life

Sciences) kit was used to detect Atp7b protein. Primary antibodies of polyclonal anti-ATP7B.N60 (Forbes and Cox, 2000) were pre-absorbed in acetone powder derived from HeLa cells. HeLa cells do not express ATP7B and therefore were used to remove non-specific background. Antibodies were used at a concentration of 1:1000. Due to possible endogenous peroxidase activity, tissues were treated with 3% H_2O_2 for 30 min during the procedure. To increase antigenic response of primary antibody, kidney sections were incubated with 60µg/ml of proteinase K for 10 min at 37°C followed by 1 min with 70°C of TNT buffer (0.1 M Tris, 0.15M NaCl, and 0.05% Tween 20) prior to incubation with primary antibody. Secondary antibodies were detected using the 3-3'-daminobenzidine (DAB) protocol (Vector).

3.3) RESULTS

3.3.1) RNA probes

Probe specificity was confirmed by northern blot hybridization (Figure 3-1). Atp7b.i recognized a 7.5 kb transcript and Atp7a.iii recognized an 8.0 kb transcript. RNA *in vitro* transcripts were the correct size (no aberrant bands) and had proper DIG incorporation as detected by alkaline phosphatase reactions (Figure 3-2).

3.3.2) Non-radioactive in situ hybridization of Atp7a and Atp7b in mouse kidney

In situ hybridization, using the anti-sense RNA strand (plasmid linearized by NcoI and transcribed with T7 RNA polymerase, see Figure 3-3) for *Atp7a*, was clear with neither background nor localized signal. Using *Atp7a* sense RNA probes, (plasmid linearized by SpeI and transcribed with Sp6 RNA polymerase, see Figure 3-3) signal was

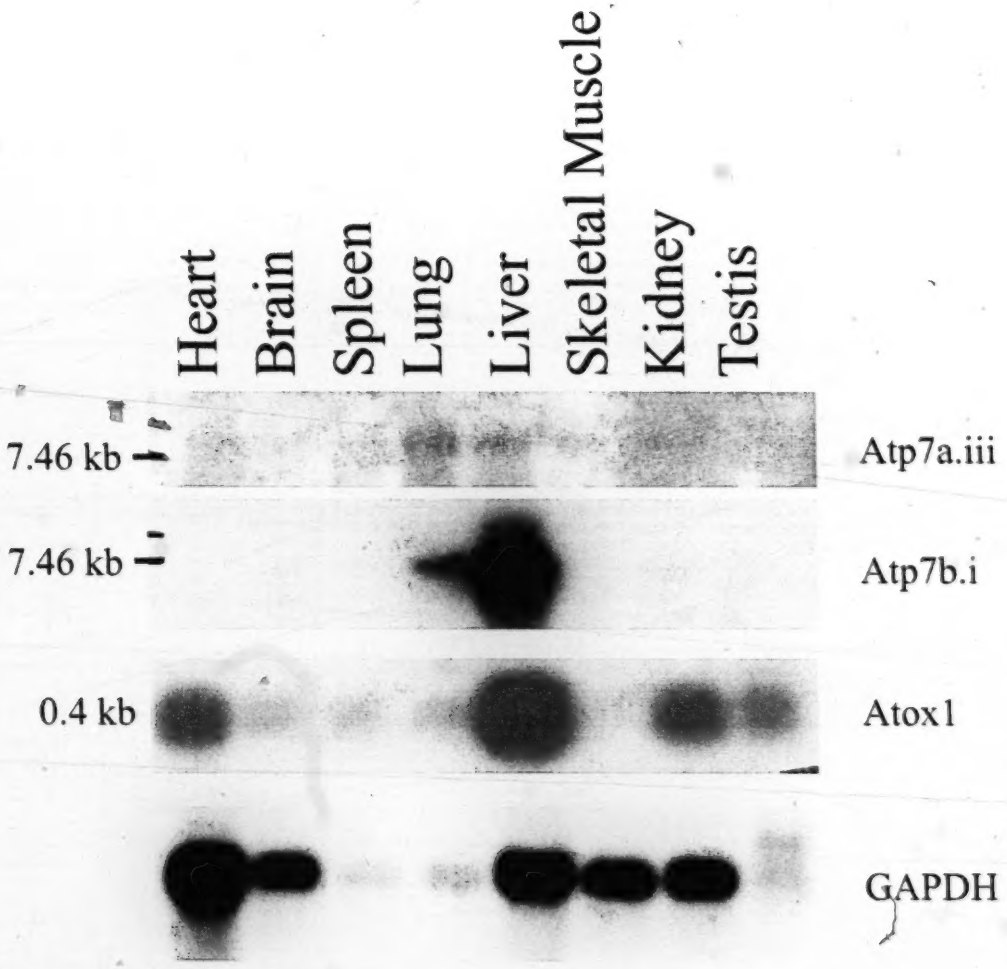

Figure 3-1: Mouse multiple tissue northern blots (obtained from ClonTech) probed with radiolabelled Atp7a.iii, Atp7b.i and Atox1. GAPDH was used as a control for lane loading.

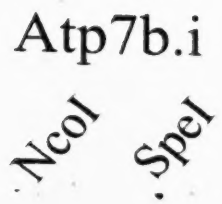

750 bp –

Figure 3-2: RNA probes produced from in vitro transcription from the Atp7b.i clone, either from a NcoI linearize plasmid or a SpeI linearized plasmid, were electrophoresed on a denaturing gel and transferred to a nylon membrane. The membrane was then incubated with anti-DIG antibodies conjugated to alkaline phosphatase, and labeled probes were detected using NBT/BCIP.

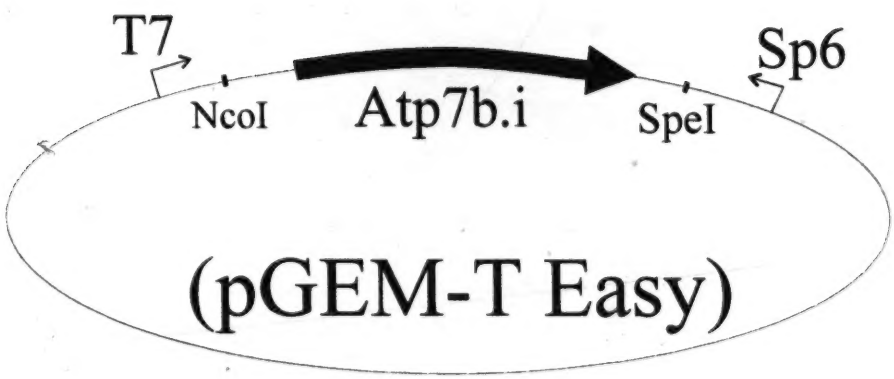

Figure 3-3: The pGEM-T Easy vector system shown with T7 and Sp6 promoters, restriction enzymes used for linearization, and orientation of Atp7b.i insert relative to vector.

produced in glomeruli (Figure 3-4). Slight signal was shown in the interior of various tubules; however, the strongest signal was shown in the glomeruli.

For *in situ* hybridization with the anti-sense RNA probe (plasmid linearized by NcoI and transcribed with Sp6 RNA polymerase, see Figure 3-3) for Atp7b, except for a slight edge effect, no signal was detected. *In situ* hybridization studies using the *Atp7b* sense probe (plasmid linearized by SpeI and transcribed with T7 RNA polymerase, see Figure 3-3) demonstrated localized signal in two specific regions of the mouse kidney: in the cortex, especially in the glomeruli, and in the inner and outer zone of the medulla (Figure 3-5), implicating the loops of Henle. The inner zone of the medulla was more heavily stained than the outer zone. The inner zone consists of a higher density of thin portions of the loops of Henle. Within the cortex, very slight tubular signal was observed. This may be an artifact since no pattern can be detected and slight background along edges, called edge effect, is quite common (personal communication with Dr. D. Rayner).

These data are peculiar since the anti-sense RNA should have produced a signal rather than the sense RNA. To determine if these results are interpretable, various experiments were conducted. The orientation of the cDNA insert with respect to flanking promoters was determined by sequence analysis, PCR primer orientation, restriction digests analyses, and RNA protection assays. In these experiments each result indicated the pGEM-Easy vector's T7 promoter produced sense and Sp6 promoter produced anti-sense RNA as predicted theoretically. Human error was eliminated as a possibility by obtaining identical results after confirming the experiments in triplicate, each time initiating from the glycerol stock and using different mice. Identical linearized templates were used both for transcription and sequencing thereby eliminating the possibility of

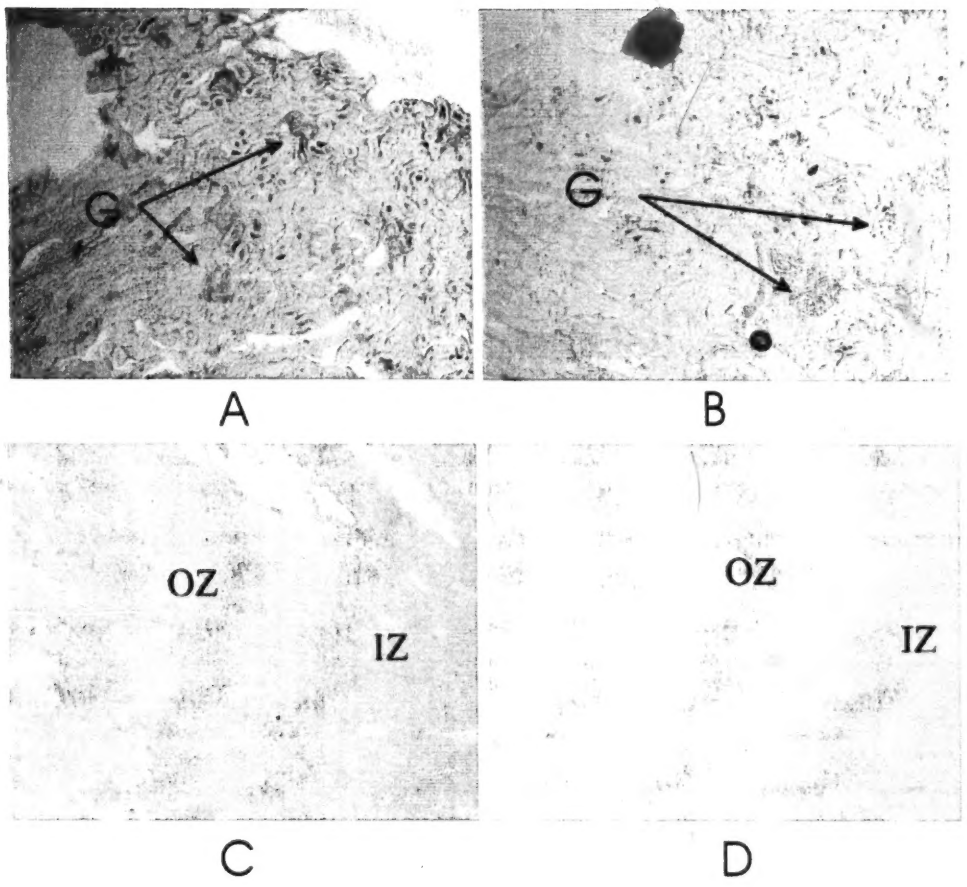

Figure 3-4: In situ hybridization of Atp7a in mouse kidney. Blue alkaline phosphatase precipitate observed using DIG labelled RNA probe. (A&C) The RNA probe used was created by run-off transcription from a linear pGEM plasmid digested with SpeI containing the Atp7a.iii fragment and transcribed with T7 RNA polymerase (Figure 3-2). (B & D) An RNA strand of the complementary strand was made by excising the pGEM vector (Figure 3-2) with NcoI and transcribed with Sp6 RNA polymerase. This RNA probe was hybridized in an adjacent kidney section. G: glomeruli. IZ: inner zone of medulla. OZ: outer zone of medulla. All pictures were taken at a magnification of 200 X.

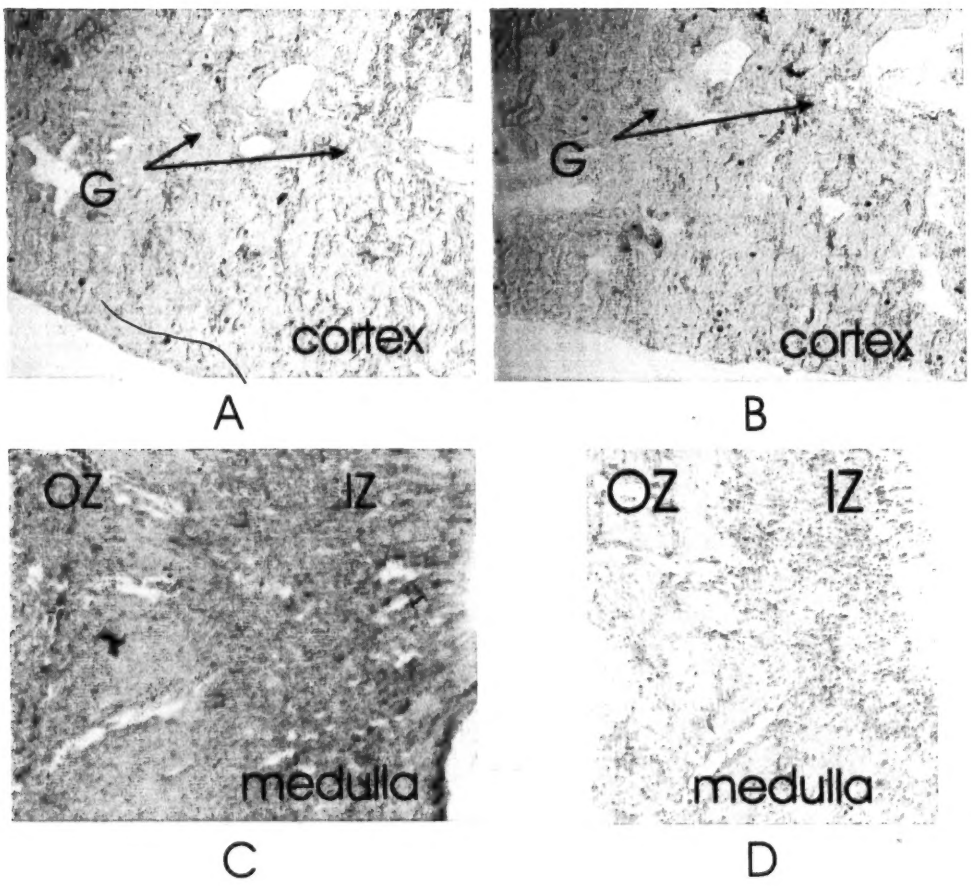

Figure 3-5: In situ hybridization of Atp7b in mouse kidney. Blue precipitate from the DIG labelled RNA probes was detected in the glomeruli within the renal cortex (A) and in the inner (IZ) and outer zone (OZ) of the medulla (C). The probe was synthesized by in vitro run-off transcription from a linear pGEM plasmid containing the Atp7b.i fragment digested with SpeI (see Figure 3-2). An RNA strand synthesized in the opposite direction was made by linearizing the same pGEM plasmid with NcoI (B and D represent adjacent kidney sections indicating the same regions as A and C, respectively). All pictures were taken at a magnification of 200 X.

differences between templates. To confirm that the plasmid Sp6 and T7 promoters flanking the insert were in the correct orientation, vector primers were designed to flank the promoter sites. Results indicated that the promoter and the insert were oriented correctly.

3.3.3) Immunohistochemistry with ATP7B.N60 in mouse kidney

Pre-absorbed antibodies specifically recognized a protein product approximately 165 kDa in size (Figure 3-6), which corresponds to the predicted size of Atp7b.

Interestingly, immunohistochemistry revealed Atp7b to be localized to the same two structures as shown by *in situ* hybridization results. Expression was localized to the glomeruli and the inner and outer zone of the medulla involving the loops of Henle indicated by the dark brown stain (Figure 3-7). Denser staining patterns were seen in the inner zone of the medulla that primarily consists of thin loops of Henle. Staining of collecting ducts is not likely since the ducts are also located in the cortex and little to no staining of tubules occurred in the cortex.

3.4) DISCUSSION

Copper excretion through the kidney is tightly regulated by various copper transporting proteins. Based on copper distribution studies, metal ions are normally observed in the proximal and distal tubules as well as the glomeruli (Kirby et al., 1998; Kodama et al., 1993). In patients with Menkes disease, copper accumulates in the proximal tubules; although, urinary copper levels remain normal. Untreated Wilson disease patients also demonstrate copper accumulation in the proximal tubules but these patients also have an increase in urinary copper levels, a reflection in part of increased

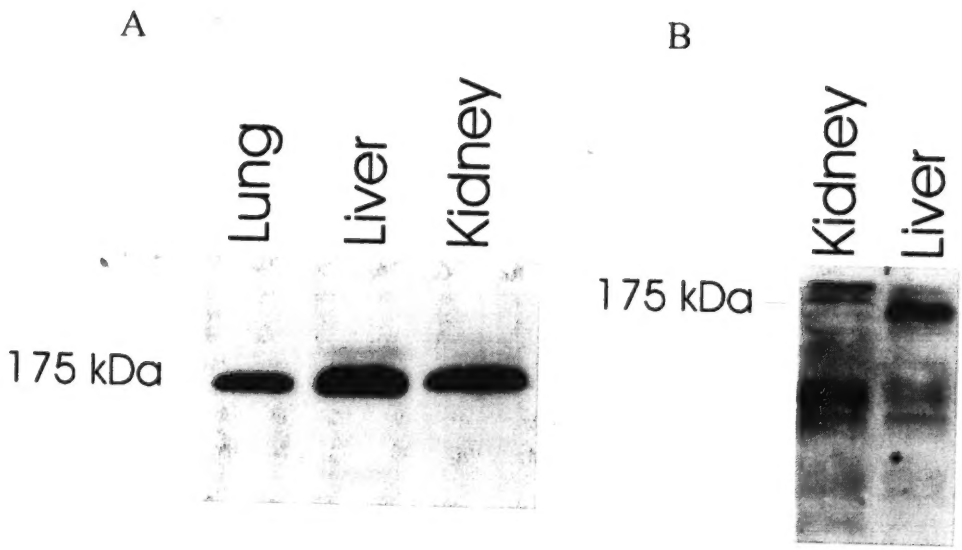

Figure 3-6: (A) Western blot analysis of mouse tissue lysates, using HeLa protein powder to preabsorb antibody ATP7B.N60. (B) Western blot analysis using ATP7B.N60 prior to preabsorption with HeLa protein powder.

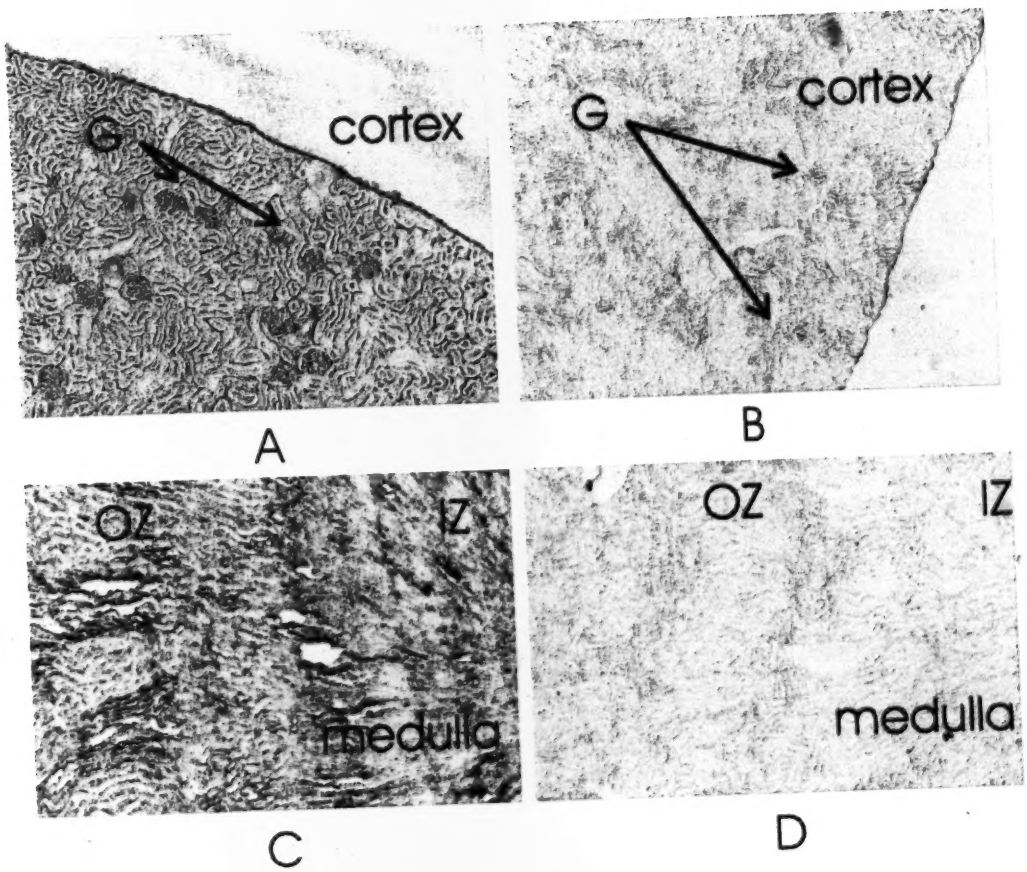

Figure 3-7: Immunohistochemical detection of Atp7b in mouse kidney. Pre-absorbed anti-ATP7B.N60 detected proteins in the glomeruli (G) (A) and in the inner (IZ) and outer zone (OZ) of the medulla (C). Pre-injection serum showed no signal in either the cortex (B) or the medulla (D). All pictures were taken at a magnification of 200 X.

non-ceruloplasmin bound copper in the plasma. The localized expression pattern of copper transporter ATP7B may elucidate its specific role in renal copper transport.

The signals detected with the sense RNA probes and the lack of signals detected with the anti-sense RNA probes are contrary to theoretical predictions. It is interesting however, that this apparent reversal of probe hybridization has previously been reported for *in situ* hybridization during a study on another kidney gene (Kestila et al., 1998). However, since no definitive explanation has been obtained as to the cause of the reversal, the *in situ* hybridization results are not interpretable. Based on experimental evidence, I have eliminated trivial explanations as to the cause, however, the frustrating issue still remains. This reversal in signal would be a very interesting problem to address since there is anecdotal evidence from other laboratories regarding this trying predicament. Some possible explanations for the cause of this peculiar finding are addressed below.

Within the mouse brain, the hippocampus has been shown to have a high affinity for RNA probes creating localized background that appears as a true signal for both sense and anti-sense RNA. Glomeruli are not structures that preferentially bind RNA since signal was not seen with the anti-sense RNA probe nor was it seen with probes for another gene, *Ccsd* (data not shown). To dismiss possible differences between labeling and quality each probe was verified to be of a single length and have adequate DIG incorporation (Figure 3-2). In addition, the RNA transcripts were likely not the result of an aberrant 3'-OH RNA polymerase initiation. If there was RNA polymerase initiation at the linearized end of the plasmid then there would be varying lengths of RNA products depending upon the processivity of the polymerase along the linearized plasmid. This was seen in some RNA preparations but the preparations were never used unless there

was a single 750 base pair product. To date, no detailed gene mapping, including genomic structures, has been completed for this region in the mouse. However, by analyzing sequence data from NCBI, one Expressed Sequence Tag (EST) (AK002066) was detected within the first intron of *ATP7B* that is predicted to transcribe in the opposite orientation. However, this sequence was not in the region chosen to create the *Atp7b* fragment. No additional ESTs or genes have been discovered in the opposite orientation for either *Atp7a* or *Atp7b*. Given the synteny between the chromosomal regions surrounding the human and mouse loci, there is a low probability that a gene producing transcripts in the opposite orientation is a concern. However, it is still possible that in the regions I selected for both genes in question, unidentified genes or pseudogenes may exist that are transcribed in the opposite orientation. Another suggestion is that neighboring genes, in opposite orientations, have a relatively large 3' or 5' UTR that extend into *Atp7a* and *Atp7b*. This would produce complementary RNA products that can hybridize the sense RNA and thereby produce a signal.

Since the purpose of the thesis was to address the expression pattern of genes involved in copper transport, an additional method was used to identity cells in the kidney that expressed Atp7b. ATP7B.N60, a polyclonal antibody for ATP7B, was used for immunohistochemical detection on mouse kidney. Interestingly, the immunohistochemical signal stained the identical structures to those seen by *in situ* hybridization for *Atp7b*.

Atp7a expression studies shown the gene is active in the proximal and distal tubules of the kidney by utilizing immunohistochemistry (Grimes et al., 1997) and *in situ* hybridization techniques (Murata et al., 1997). Signal from *in situ* hybridization studies of *Atp7a* from this chapter show slight tubular staining (undetermined tubules), but the

majority of signal was in the glomerulus. Unfortunately, *in situ* studies from this thesis can not add any new information into the localized expression of Atp7a in the kidney.

In the kidney, steady state levels of copper are distributed within the glomerulus, proximal and distal tubules (Kodama et al., 1993) indicating a possible transport mechanism in each of these locations. Based on expression of Atp7b in the glomeruli, the glomeruli may have a role in regulating the amount of copper in the filtrate. Since Atp7b has been shown to have a role in copper efflux, it is possible that copper is retained in the serum by being actively transported back in to the serum rather then progressing through into the filtrate. Copper is not free within cells, but is protein bound; therefore a specific active transport mechanism likely exists within the glomeruli. The cause of proximal tubular copper accumulation in Wilson disease may be a secondary effect resulting from either a higher concentration of low molecular weight substances associated with copper penetrating the glomerular sieve or it may be linked to a disruption in the active transport of copper back into the serum for retention. The copper transporter CTR1 has been shown to localize within the tubules of mouse kidney and could be responsible for copper uptake downstream of the glomeruli (Kuo et al., 2001).

Atp7b expression in the loops of Henle suggests that once in the filtrate, Atp7b is responsible for copper re-absorption. Previous data suggest that copper may be reabsorbed by the same pathway as that involved in iron re-absorption (Wareing et al., 2000), which occurs between the proximal and distal convoluted tubules, interpreted as the loops of Henle. The presence of high amounts of copper in the urine may be explained not only by the higher serum levels but possibly by a deficiency in copper re-absorption from the filtrate.

In Wilson disease patients, kidney dysfunction can involve both tubular and glomerular dysfunction. Untreated patients typically have a higher impairment in tubular function than in glomerular function (Sozeri et al., 1997). Pathogenesis of proximal tubular dysfunction is likely linked to the localized accumulation of copper in the proximal tubules (Elsas et al., 1971). Tubular dysfunction can also lead to Fanconi syndrome in Wilson disease patients, with in tubular necrosis and degeneration (Tabet, 1969). Penicillamine, a copper chelator used to treat Wilson disease, leads to an increase in glomerular dysfunction (e.g. proteinuria) in approximately one third of patients studied, while tubular function is restored within two years of therapy (Sozeri et al., 1997). After Wilson disease patients have received penicillamine treatment, the chelator accumulates in the proximal tubules but not the glomeruli nor the distal tubules. Interestingly, this accumulation is consistent with the Heymann's nephritis model suggested by Bacon as a pathogenetic model for penicillamine-induced nephropathy (de Angelis et al., 1984). Glomerular dysfunction, however, also occurs in patients suffering from rheumatoid arthritis who are treated with D-penicillamine (Almirall et al., 1993). Therefore, the majority of glomerular damage is likely due to penicillamine treatment rather than a consequence of disrupted copper transport.

In summary, the glomeruli and the loops of Henle appear to be central components in kidney copper homeostasis (Figure 3-8). When glomerular copper transport is disrupted by mutations in *Atp7b*, copper accumulates downstream in the proximal tubules. In Wilson disease patients, excess copper in the urine may result from disruption of copper re-absorption in the loops of Henle, as well as the increased levels of copper in the serum.

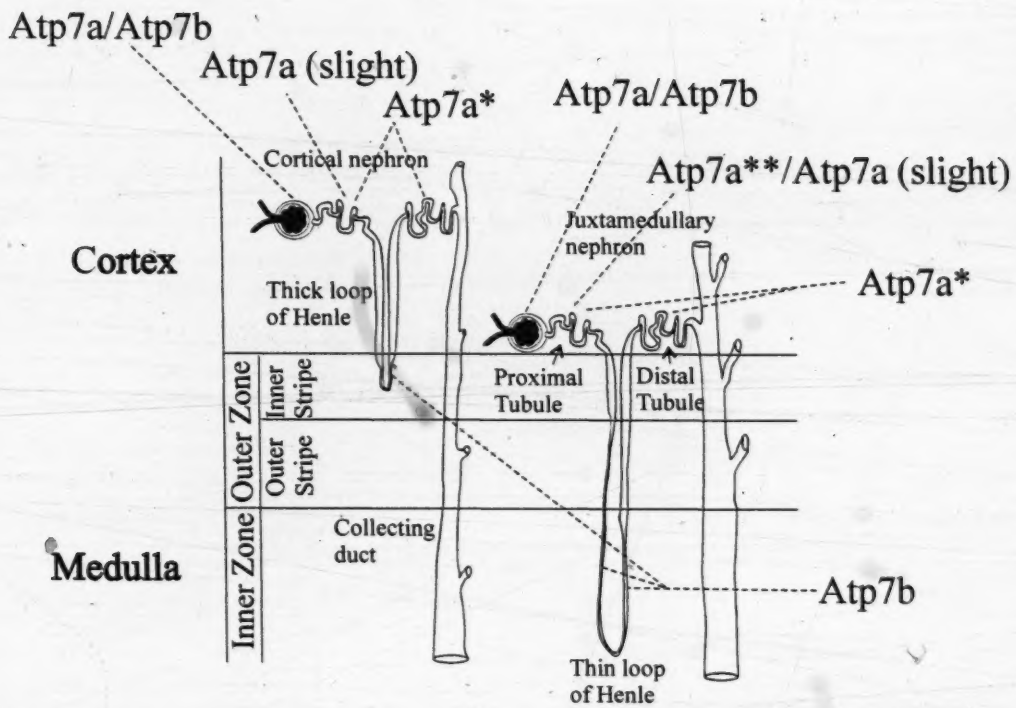

Modified from Guyton (1990)

Figure 3-8: Schematic representation of the relative expression patterns of Atp7a and Atp7b. Expression of Atp7a is from Grimes et al. (*) and Murata et al. (**). No asterisk indicates work presented in Chapter 3 of this thesis.

3.5) REFERENCES

Almirall,J., Alcorta,I., Botey,A., and Revert,L. (1993). Penicillamine-induced rapidly progressive glomerulonephritis in a patient with rheumatoid arthritis. Am. J. Nephrol. *13*, 286-288.

de Angelis,E., Lombardi,M.L., and Ruocco,V. (1984). Distribution of [3H]-D-penicillamine in mouse kidney. An autoradiographic study. Rheumatol. Int. *4*, 183-186.

Elsas,L.J., Hayslett,J.P., Spargo,B.H., Durant,J.L., and Rosenberg,L.E. (1971). Wilson's disease with reversible renal tubular dysfunction. Correlation with proximal tubular ultrastructure. Ann. Intern. Med. *75*, 427-433.

Forbes,J.R. and Cox,D.W. (2000). Copper-dependent trafficking of Wilson disease mutant ATP7B proteins. Hum Mol Genet *9*, 1927-35.

Grimes,A., Hearn,C.J., Lackhart,P., Newgreen,D.F., and Mercer, J.F. (1997). Molecular basis of the brindled mouse mutant (Mo(br)): a murine model of Menkes disease. Hum. Mol. Genet. *6*, 1037-1042.

Guyton,M.D. (1990). Textbook of Medical Physiology. HBJ College & School Division.

Kestila,M., Lenkkeri,U., Mannikko,M., Lamerdin,J., McCready,P., Putaala,H., Ruotsalainen,V., Morita,T., Nissinen,M., Herva,R., Kashtan,C.E., Peltonen,L., Holmberg,C., Olsen,A., and Tryggvason,K. (1998). Positionally cloned gene for a novel glomerular protein--nephrin--is mutated in congenital nephrotic syndrome. Mol. Cell *1*, 575-582.

Kirby,B.J., Danks,D.M., Legge,G.J., and Mercer,J.F. (1998). Analysis of the distribution of Cu, Fe and Zn and other elements in brindled mouse kidney using a scanning proton microprobe. J. Inorg. Biochem. *71*, 189-197.

Kodama,H., Abe,T., Takama,M., Takahashi,I., Kodama,M., and Nishimura,M. (1993). Histochemical localization of copper in the intestine and kidney of macular mice: light and electron microscopic study. J. Histochem. Cytochem. *41*, 1529-1535.

Kodama,H., Okabe,I., Kihara,A., Mori,Y., and Okaniwa,M. (1992). Renal tubular function of patients with classical Menkes disease. J. Inherit. Metab Dis. *15*, 157-158.

Kuo,Y.M., Zhou,B., Cosco,D., and Gitschier,J. (2001). The copper transporter CTR1 provides an essential function in mammalian embryonic development. Proc. Natl. Acad. Sci. U. S. A *98*, 6836-6841.

Murata,Y., Kadama,H., Abe, T., Ishida,N., Nishimura,M., Levinson,B., Gitschier,J., and Packman,S. (1997). Mutation analysis and expression of the mottled gene in the macular mouse model of Menkes disease. Pediatr. Res. *42*, 436-442.

Sozeri,E., Feist,D., Ruder,H., and Scharer,K. (1997). Proteinuria and other renal functions in Wilson's disease. Pediatr Nephrol *11*, 307-11.

Tabet,M. (1969). [De Toni-Debre-Fanconi syndrome in Wilson's disease]. J. Med. Liban. *22*, 55-65.

Wareing,M., Ferguson,C.J., Green,R., Riccardi,D., and Smith,C.P. (2000). In vivo characterization of renal iron transport in the anaesthetized rat. J. Physiol *524 Pt 2*, 581-586.

Yoshimura,N. (1994). Histochemical localization of copper in various organs of brindled mice. Pathol Int *44*, 14-9.

CHAPTER 4

STUDIES OF THE COPPER CHAPERONE ATOX1

Methods and data discussed in this chapter have been published in part in the following publication:

Moore S.D.P., Helmle, K., Prat L., Cox, D.W. (2002). Localization of the copper chaperone ATOX1 in the liver and kidney and its potential role in disease. *Mamm. Gen.* **13**: 1-6.

Karmen Helmle, undergraduate summer student, performed immunohistochemistry for two of the three placental stages.

Lisa Prat, technician, was involved in the publication but not with data from this chapter.

4.1) INTRODUCTION

As outlined in Chapter 1, Atx1p, a yeast copper chaperone, is necessary for the intracellular copper transport pathway and is indirectly required for high affinity iron uptake (Lin et al., 1997). In higher organisms, ATOX1, the mammalian homologue of Atx1p, is hypothesized to be the only copper transporter that delivers copper to the P-type ATPase copper transporter paralogues, ATP7A and/or ATP7B, defective in Menkes and Wilson disease respectively. Examination of tissue specific expression patterns for the chaperone in mice can help elucidate tissue specific functions.

Tissue specific localization patterns for the membrane copper transporters have been investigated in the rat liver (Schaefer et al., 1999a) and the mouse kidney (Grimes et al., 1997). Within the human liver, Atp7b is localized to unspecified regions and regions suspected to be localized in the pericanalicular area (Schaefer et al., 1999b). Renal expression of *Atp7b* is localized both to the glomeruli and the thin portions of the loops of Henle (Chapter 3). In contrast, Atp7a expression has been shown previously to be in the proximal and distal tubules of the nephron (Grimes et al., 1997; Murata et al., 1997).

Typically, mouse pups and new born humans have high hepatic copper levels. In contrast, *toxic* milk mouse pups have low hepatic copper levels subsequent to birth and only begin hepatic accumulation in the third postnatal week (Rauch, 1983). Interestingly, this copper deficiency in *tx* pups mimics symptoms in Menkes disease patients and does not have the high copper levels found in Wilson disease. One possibility for the copper deficiency in mice may be differences in the placental transfer of copper between humans and rodents. Placental localization of Atp7b in rat showed the transporter to be expressed in the maternal portion and not in the fetal-derived tissue (Muramatsu et al., 1998). We therefore wanted to continue investigations into the placental localization of copper

transporting proteins by analyzing the expression of Atox1 during mouse development, to determine if a maternal or fetal expression bias exists as it does for *Atp7b* in rat.

To compare the expression pattern of the copper chaperone with the copper transporters Atp7a and Atp7b, polyclonal antibody derived against ATOX1 was used for immunohistochemistry on mouse liver, kidney, and placental tissues.

4.2) MATERIALS AND METHODS

4.2.1) ATOX1 cDNA construction

Total human liver RNA was isolated using TRIzol reagent and the manufacturers protocol (GibcoBRL). RT-PCR was performed with the isolated RNA. Total RNA was incubated at 37°C for 20 min in the presence of DNase I-RNase Free (Roche). DNase I was inactivated by incubating at 70°C for 10 min. Oligo-T primer was added and the solution was cooled to 55°C. A mixture of First Strand Buffer, DTT, dNTP's, and Superscript II were added and the temperature was brought to 42°C for 45 min. *ATOX1* RT products were amplified using PCR with primers Atox1.3 (5'-TGA CGA ATT CTC AGT CAT GCC GAA GCA CGAG-3') and HAH1.R1 (5'-CCA AGT CCC AGG TCT GTC TG-3'), based on sequence data obtained from NCBI Genbank (Accession number: U70660). PCR amplified fragments were cloned into pGEM using Promega TA pGEM Easy-cloning kit according to the manufacturer's instructions. Transformed cells were plated on IPTG and X-Gal plates allowing for selection of white colonies that contained inserts, checked for size of insert by restriction digestion, and sequenced for fragment confirmation.

4.2.2) Antibody production

The ATOX1 human cDNA construct was expressed in bacteria and the resulting protein was purified, using methods as described for ATP7B (DiDonato et al., 1997). Purified lyophilized protein was generously provided by Dr. Bibudendra Sarkar's group after providing him with the ATOX1 cDNA construct. Purified protein was re-suspended in PBS containing 2% SDS. Two New Zealand White (NZW) rabbits (Vandermeer Rabbitry, Edmonton, AB) were injected with ATOX1 purified antigen in Freund's adjuvant three times at three-week intervals. Titre for one rabbit (H184) was sufficient after the third injection as tested by western blot of mouse liver homogenate, at which time serum containing ATOX1 antibody was collected. All animal procedures were approved by the University of Alberta Health Sciences Laboratory Animal Services Committee.

Antibody specificity was demonstrated by western blot analysis. Flash frozen mouse liver was homogenized in buffer (20% glycerol, 4% SDS, 0.13M Tris at pH 6.8). DNA was sheared by needle injection and centrifuged at 14,000 rpm for 10 min to remove cellular debris. Protein concentrations of the resulting cytosolic fraction were estimated by using the Bradford Assay (Pierce Chemical). Western blotting was performed as previously described for ATP7B (Forbes and Cox, 1998), using a 1:1000 dilution of antiserum with 100 ng of purified ATOX1 and 1:750 dilution with 10 μg of cytosolic protein.

4.2.3) Tissue section preparation and immunohistochemistry

Sedated Balb/cCr//AltBM mice (six weeks old) were perfused by injecting fixative (4% paraformaldehyde and 0.05% gluteraldehyde, Korvonsky's mixture) into the

left ventricle of the heart while the right ventricle was cut to drain the circulatory system. Mice were euthanized by cervical dislocation. Harvested tissues were then removed and soaked overnight in water. The next day, kidney, liver and placenta were dehydrated in an ethanol series and embedded into paraffin. Paraffin blocks were sectioned and stored at 4°C for up to 3 weeks (see Chapter 3 for details).

ATOX1 protein was detected by alkaline phosphatase reactions using the Vector *Elite* ABC kit with a 1:500 dilution of antiserum. To exclude possible endogenous peroxidase activity, tissues were treated with 3% H_2O_2 for 15 min during the procedure. To increase antigenic response of primary antibody, sections were incubated with 60 µg/ml of proteinase K for 10 min at 37°C followed by 1 min at 70°C with TNT buffer (0.1 M Tris, 0.15M NaCl, and 0.05% Tween 20) prior to incubation with primary antibody. Secondary antibodies were detected using the DAB protocol (Vector). Fluorescent detection of anti-ATOX1 was performed by using 1:200 dilution of rhodamine labeled streptavidin (KPL) in conjunction with biotin conjugated to the anti-rabbit antibody from the ABC kit from Vector. Where indicated, periodic acid Schiff (PAS) staining was used to identify glycogen, which is present in the proximal convoluted tubules.

Atp7b protein was identified in hepatic tissue by using polyclonal antibody ATP7B.N60, previously described (Forbes and Cox, 1998). Mouse liver sections were treated as described above and incubated with 1:750 of preabsorbed ATP7B.N60 (described in Chapter 3.2.5) and detected using an ABC kit from Vector (described above).

4.2.4) Tissue expression during mouse development

Gene expression during stages of mouse development was assessed by northern blot analysis (Seegene). The expression of Atox1 and Atp7b were assessed from gestational stages E4.5 through E18.5. For Atox1, a probe was created using primers Atox1.3 (HSC#1036) (5'-TGA CGA ATT CTC AGT CAT GCC GAA GCA CGAG-3') and Atox1.4 (HSC#1037) (5'-TGA CGA ATT CCT GGA CTG GAC TGA GCA GTT GG-3'). For *Atp7b*, the fragment Atp7b.iii (Chapter 3.2.1) was used to investigate the gene expression pattern. GAPDH was used as a control for lane loading. All probes were radiolabeled by ^{32}P using random primer labeling (Amersham).

4.3) RESULTS

4.3.1) ATOX1 Antibody

Antibody derived from human ATOX1 successfully cross reacted with the orthologous mouse protein, Atox1. A single band of approximately 7 kDa was detected using western blot analysis with ATOX1 anti-serum on mouse liver and kidney cytosolic protein fractions (Figure 4-1). Since the rabbit anti-serum alone gave no additional bands on either mouse kidney or liver cytosolic protein preparations, the antiserum was used for immunohistochemistry without additional purification.

4.3.2) Immunohistochemistry

Liver

Within the liver, portal veins bring blood from the digestive tract and other organs; central veins lead into hepatic veins that deliver blood out of the liver. Portal and central (hepatic) veins and their branches may be morphologically similar. A direct and

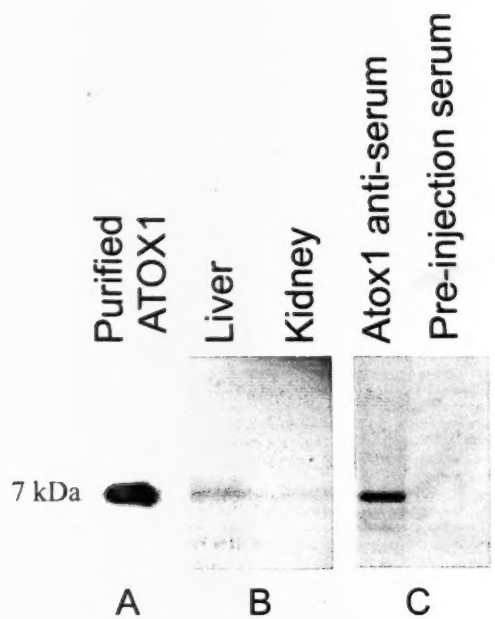

Figure 4-1: Western blot detection of ATOX1/Atox1 protein detected with anti-serum L184. (A) Purified antigenic protein ATOX1, molecular mass approximately 7 kDa. (B) A single band was detected in cytosolic mouse liver and kidney protein preparations. (C) The pre-injection serum was compared with the anti-serum showing that Atox1 was only detected from mouse liver protein preparations when using the anti-serum.

simple approach to determine the difference between portal and central (hepatic) veins was made by morphology of hemotoxylin-eosin (H&E) stained sections demonstrating that portal veins run in association with hepatic artery branches and bile ducts (Figure 2A, D and G). Bile ducts are the only cells in the liver lined by cuboidal epithelium. H&E staining is a simple low-technology approach that allows completely reliable differentiation of hepatic (central) veins from portal veins. Central veins were identified as the center of a lobule by the presence of portal triads on the periphery of the lobule.

Immunostaining on mouse liver sections localized Atox1 to hepatocytes surrounding hepatic (central) vein branches but not portal vein branches (Figure 4-2). The diffuse intracellular immunostaining is consistent with a cytoplasmic protein that is distributed throughout the intracellular matrix (Figure 4-2J). Some zone 3 hepatocytes surrounding central vein branches were also positive. Slight nuclear staining in hepatocytes was seen throughout the liver. The nuclear signal could be an artifact of alkaline phosphatase detection however it was not seen in the negative control. No immunostaining of hepatocytes was observed using pre-injection serum (Figure 4-2C, F and I). An identical expression pattern was observed when the anti-ATOX1 antibody was detected with fluorescence rather than alkaline phosphatase (Figure 4-3).

ATP7B was detected by immunohistochemistry in mouse liver sections. Punctate staining in hepatocytes surrounding a central vein corresponded to a vein that also had surrounding hepatocytes expressing *ATOX1* (Figure 4-4). Additional regions within the liver demonstrated punctate staining of ATP7B. ATP7B is a membrane protein that, under low copper levels, is localized to the *trans*-Golgi apparatus. Therefore, unlike ATOX1, which is a cytoplasmic protein, we do not expect to see diffuse cytoplasmic

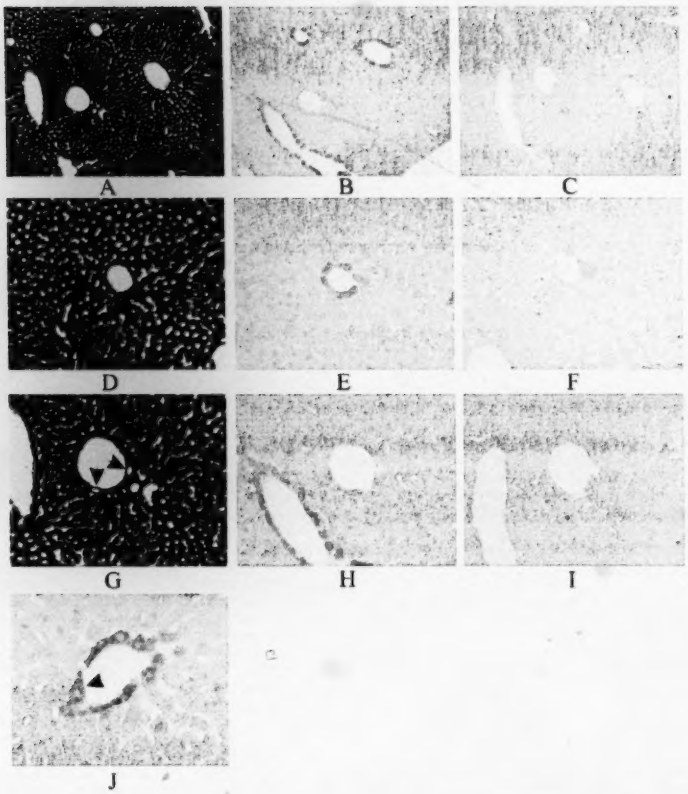

Figure 4-2: Detection of Atox1 in whole mouse liver. (A, B and C) Adjacent liver sections (100X) show liver structures. (A) Hematoxylin-eosin (H&E) staining indicates hepatic (H) and portal (P) veins. (B) Atox1 was detected using ATOX1 anti-serum and found to be in hepatic veins. (C) Pre-injection serum was negative. (D, E and F) Higher magnification (200X) shows a hepatic vein. (D) Hepatic veins are identifiable on the adjacent H&E section (E) ATOX1 anti-serum produced a signal in hepatocytes surrounding the hepatic vein. (F) Pre-injection serum was negative. (G, H and I) Higher magnification (200X) demonstrates a portal vein. (G) Portal veins are identifiable by epithelial tissue lining indicated by arrows in adjacent H&E section. (H) A portal vein has no localized signal using ATOX1 antiserum while an adjacent hepatic vein does. (I) Pre-injection serum was negative. (J) Immunostaining of a cell lining a central vein is indicated by an arrow (400X).

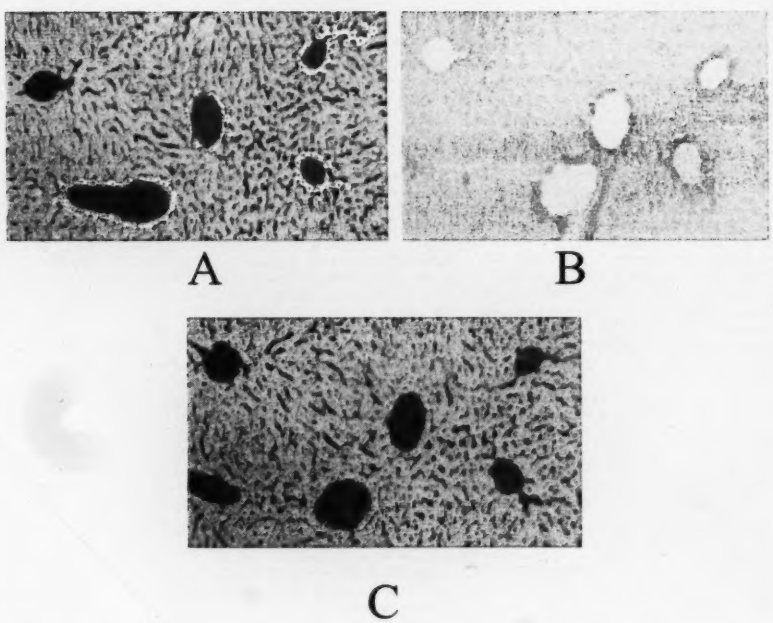

Figure 4-3: Fluorescent detection of hepatic Atox1. Anti-Atox1 antibody detects ATOX1 antigen and is detected by either (A) fluorescence or (B) alkaline phosphatase in adjacent sections. (C) Pre-bleed serum on an adjacent section provides a negative control for the experiment. All pictures were taken at a magnification of 200 X.

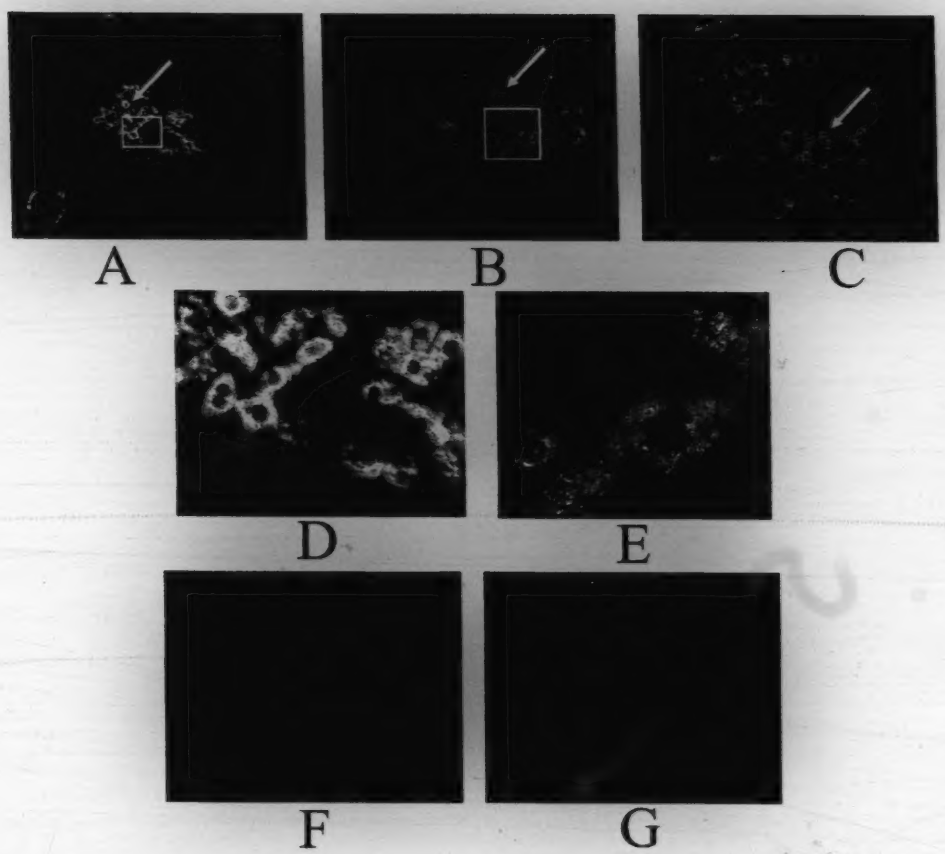

Figure 4-4: Immunohistochemistry on mouse liver using ATOX1 anti-serum and antibody ATP7B.N60. (A) ATOX1 anti-serum detected antigen in hepatocytes surrounding a central vein. (B) ATP7B.N60 antigen is detected in an adjacent section that corresponds to the same vein shown in A. (C) ATP7B.N60 also detects hepatocytes in specific regions in the liver section. Arrows indicate hepatocytes that show localized signal from antibody of interest. (D and E) Highlighted boxes in A and B are magnified (approximately 30 X) to demonstrate hepatocytes with diffuse cytoplasmic immunostaining using ATOX1 anti-serum and punctate immunostaining using antibody ATP7B.N60, respectively. (F and G) Pre-injection serum from the same rabbit used to derive ATP7B.N60 was used as a negative control in adjacent sections. A, B, C, F and G are taken at 200 X magnification.

immunostaining. The lower staining intensity of Atp7b relative to Atox1 may be attributed to differences in affinity between the two polyclonal antibodies.

Kidney

Within the kidney, Atox1 was detected in the medulla inner and outer zones (Figure 4-5). Staining was observed well into the tips of the renal papillae. Signal localized in the medulla is consistent with expression in the loops of Henle. Localization within the cortex was limited to the glomeruli and epithelial tissue adjacent to the glomerulus. Positive PAS staining allowed identification of proximal tubules near the glomerulus; serial sections used for immunohistochemistry showed that these tubules do not contain Atox1 protein. No signal was detected for the pre-injection serum negative control.

Placenta

Localization of Atox1 in placental tissue from stages E12.5, E15.5, and E18.5 showed expression in both fetal and maternal portions (Figure 4-6). Although both the maternal and fetal portions of the placenta showed expression, the fetal portion apparently has a more intense immunostaining signal.

4.3.2) Mouse developmental northern blot

Expression of *Atp7b* by northern blot analysis in the mouse developmental stages at days E4.5 to E18.5 showed a single product approximately 7.5 kb in length (Figure 4-7). Expression is seen in stages E6.5 and E7.5 but by E8.5 levels decrease to a relatively low level until E13.5, where expression begins to increase until birth. *Atox1* detects two

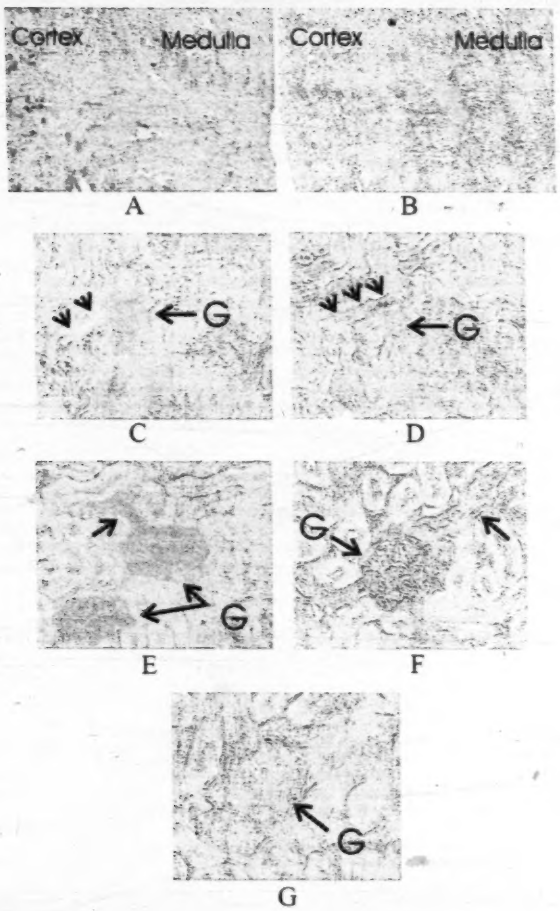

Figure 4-5: Localization of Atox1 protein in mouse kidney. (B) hemotoxylin/PAS staining of the mouse kidney (25X) demonstrates the overall architecture. (A) Horseradish peroxidase staining indicates Atox1 is localized in the medulla and the cortex (25X). Higher magnification of the cortex (C) (200X) indicates immunostaining in glomeruli but not the proximal tubules, indicated by red PAS tubular staining identified by arrows in an adjacent section (D). (E) Epithelial tissue adjoining glomeruli stained positive for anti-Atox1 serum (200X) (F) hemotoxylin staining of epithelial tissue adjoining the glomerulus. (G) Kidney sections incubated with pre-injection serum from antigenic rabbits were used as a negative control (200X). Glomerulus: G

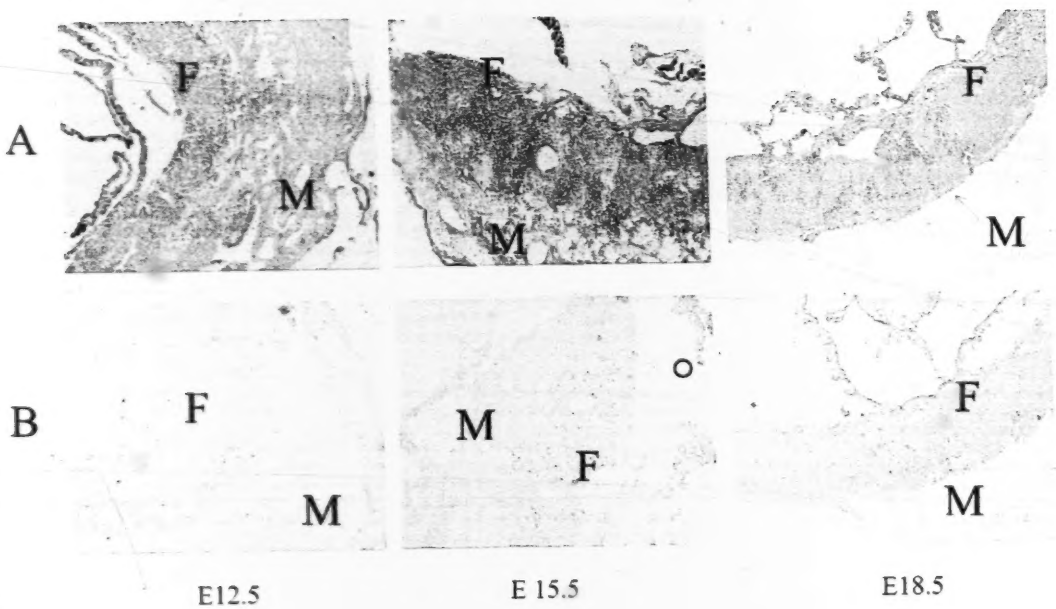

Figure 4-6: Localization of Atox1 protein in mouse placenta during various gestational stages. (A) Anti-ATOX1 detected Atox1 in developing mouse placenta. (B) Pre-injection serum in corresponding developmental stages serve as a negative control. The maternal portion of the placenta is indicated by M and the fetal portion is indicated by F. All pictures were taken at a magnification of 200 X.

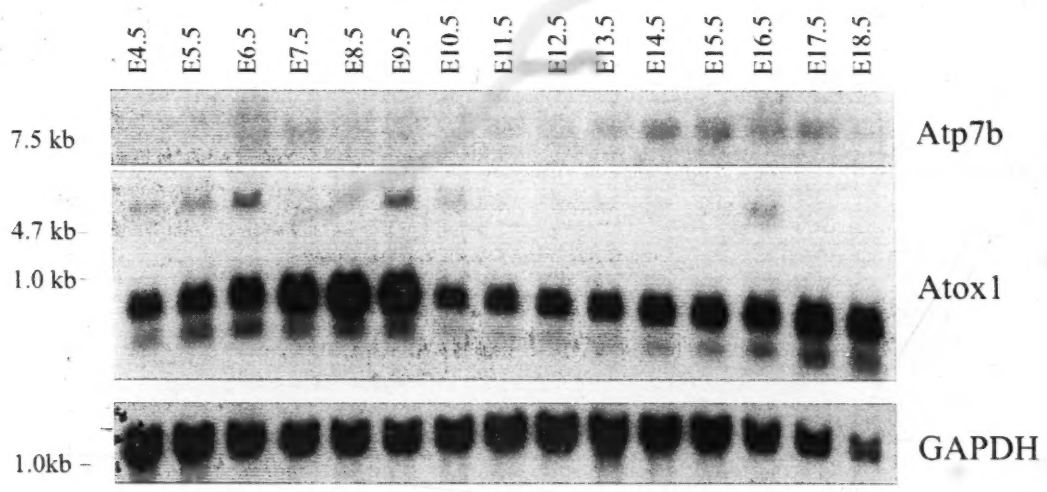

Figure 4-7: Mouse developmental northern blot (Seegene). Northern blot was probed with radiolabeled Atp7b.i and Atox1. GAPDH was used as a control for lane loading.

bands. The first is approximately 500 bp, as expected, and a putative minor alternative transcript is approximately 6 kb. *Atox1* is expressed throughout mouse developmental stages E4.5 to E18.5. The alternative product is seen at E4.5 and continues until E10.5. At E11.5 the alternative product significantly decreases in expression but is temporarily seen again at higher levels during E16.5.

4.4) DISCUSSION

Liver

Expression of Atox1 has been examined in the liver, kidney and placenta. In mouse liver, Atox1 was localized to hepatocytes surrounding central veins. The diffuse intracellular pattern is consistent with a cytoplasmic protein that is not localized to organelles within the cell, but is distributed throughout the intracellular matrix. Immunohistochemistry studies using antibody against the N-terminal copper binding domain, ATP7B.N60, on mouse hepatic tissue indicated that ATP7B was localized to central veins. Adjacent sections demonstrated Atox1 expression in identical central veins that expressed ATP7B. In addition to this co-localization, previously published studies described punctate expression in unspecified regions of the liver. ATP7B.N60 also identified punctate expression in regions of the liver, however, these regions appear to be zone 3 hepatocytes. Localization to zone 3 hepatocytes and the epithelial lining of central veins adds a new complexity to the function of the liver in copper transport. Nutrient rich blood is supplied to the liver by the portal vein system and has a sequential decrease in oxygen and nutrients from zone 1 through to zone 3. Oxygen and nutrient rich blood move through different zones of hepatocytes until eventually entering the central veins for delivery back into the circulatory system. Atox1 is suggested to be

expressed in zone 3 hepatocytes and therefore in addition to central vein co-localization, the chaperone co-localizes with Atp7b in these regions.

Kidney

Within the mouse kidney, immunological localization of Atox1 was observed in the inner and outer zones of the medulla and in specific regions within the cortex. Since there is little to no tubular expression in the cortex, expression in collecting tubules is unlikely. Medullar localization is consistent with presence in loops of Henle from either cortical nephrons or juxtamedullary nephrons. Since localization was seen in the medulla, and the thick portions of loops of Henle from cortical nephrons reside in the cortex, this suggests that expression is limited to the thin portions of the loops of Henle. Within the cortex, glomerular expression indicates that Atox1 has a role in a copper pathway involving Atp7b (and possibly Atp7a) at the initial site of filtration. There was little to no detection of Atox1 within the proximal and distal tubules, where Atp7a has been previously reported (Grimes et al., 1997; Murata et al., 1997). This alludes to the possibility that there is an alternative copper chaperone for Atp7a present in the proximal and distal convoluted tubules. However, there are expression data that suggest a copper transporter may function independent of the chaperone as first described in *C. elegans* (Wakabayashi et al., 1998). Atox1 expression co-localizes with Atp7b as both are localized to the glomeruli and the thin portions of the loops of Henle.

Placenta

Immunohistochemical localization of Atox1 in the placenta demonstrates its presence in both the maternal and fetal portions, particularly intensely in the latter. The

darker immunostaining in the fetal portion may represent either a greater concentration of Atox1 in fetal cells or may be a reflection of the fetal tissue being more dense that the maternal tissue. This localization of ATOX1 in both regions of the placenta indicates its probable involvement in copper transport in both maternal and embryonic regions. Therefore, Atox1 is associated with the nutritional transfer of copper between the mother and embryo during mouse development. In rat, Atp7b protein is localized only to the maternal portion of placenta (Muramatsu et al., 1998). This may suggest two possibilities: first Atox1 has a function independent of Atp7b, or second, another protein such as Atp7a, is expressed in the fetal portion of the placenta which utilizes Atox1 for copper transport.

During Development

By comparing the developmental expression of Atp7b with Atox1 during mouse embryonic growth, an interesting pattern is observed. Northern blot analysis indicates that the up-regulation of *Atp7b*, beginning at developmental stage E14.5, coincides with the up-regulation of *Atox1* prior to birth. Although these expression patterns are very different, it is interesting that they are both up-regulated to some extent prior to birth because both of these proteins are thought to be involved in the same pathway.

The alternative product detected by the *Atox1* probe may be derived from extra-embryonic tissue. The purchased northern blot combined both extra-embryonic and embryonic tissue RNA for developmental stages 4.5 through to 9.5. The alternative product noticed from developmental stages 4.5-10.5 and then again in 16.5 may be extra-embryonic tissue that was present due to preparation method prior to stage 9.5 or present due to contamination. This extra embryonic tissue may also explain the higher levels of

transcription product prior to gestation day 9.5. If the extra embryonic tissue highly expresses Atox1, it would mask the lower levels in the embryonic tissue.

4.5) REFERENCES

DiDonato,M., Narindrasorasak,S., Forbes,J.R., Cox,D.W., and Sarkar,B. (1997). Expression, purification, and metal binding properties of the N- terminal domain from the wilson disease putative copper-transporting ATPase (ATP7B). J. Biol. Chem. *272*, 33279-33282.

Forbes,J.R. and Cox,D.W. (1998). Functional characterization of missense mutations in ATP7B: Wilson disease mutation or normal variant? Am J Hum Genet *63*, 1663-74.

Grimes,A., Hearn,C.J., Lockhart,P., Newgreen,D.F., and Mercer,J.F. (1997). Molecular basis of the brindled mouse mutant (Mo(br)): a murine model of Menkes disease. Hum. Mol. Genet. *6*, 1037-1042.

Lin,S.J., Pufahl,R.A., Dancis,A., O'Halloran,T.V., and Culotta,V.C. (1997). A role for the Saccharomyces cerevisiae ATX1 gene in copper trafficking and iron transport. J Biol Chem *272*, 9215-20.

Muramatsu,Y., Yamada,T., Moralejo,D.H., Suzuki,Y., and Matsumoto,K. (1998). Fetal copper uptake and a homolog (Atp7b) of the Wilson's disease gene in rats. Res. Commun. Mol. Pathol. Pharmacol. *101*, 225-231.

Murata,Y., Kodama,H., Abe,T., Ishida,N., Nishimura,M., Levinson,B., Gitschier,J., and Packman,S. (1997). Mutation analysis and expression of the mottled gene in the macular mouse model of Menkes disease. Pediatr. Res. *42*, 436-442.

Rauch,H. (1983). Toxic milk, a new mutation affecting cooper metabolism in the mouse. J Hered *74*, 141-4.

Schaefer,M., Hopkins,R.G., Failla,M.L., and Gitlin,J.D. (1999a). Hepatocyte-specific localization and copper-dependent trafficking of the Wilson's disease protein in the liver. Am J Physiol *276*, 639-46.

Schaefer,M., Roelofsen,H., Wolters,H., Hofmann,W.J., Muller,M., Kuipers,F., Stremmel,W., and Vonk,R.J. (1999b). Localization of the Wilson's disease protein in human liver. Gastroenterology *117*, 1380-1385.

Wakabayashi,T., Nakamura,N., Sambongi,Y., Wada,Y., Oka,T., and Futai,M. (1998). Identification of the copper chaperone, CUC-1, in Caenorhabditis elegans: tissue specific co-expression with the copper transporting ATPase, CUA-1. FEBS Lett. *440*, 141-146.

CHAPTER 5

SEQUENCE ANALYSIS FOR POTENTIAL ATOX1 MUTATIONS IN SELECTED PATIENTS

Methods and data discussed in this chapter have been published in part in the following publication:

Moore S.D.P., Helmle, K., Prat L., Cox, D.W. (2002). Localization of the copper chaperone ATOX1 in the liver and kidney and its potential role in disease. *Mamm. Gen.* **13**: 1-6.

Karmon Helmle was involved in tissue localization studies, which were included in the publication along with the studies in this chapter.

Lisa Prat sequenced approximately ten out of the twenty eight patients for exon 2 and 3 of ATOX1.

5.1) INTRODUCTION

ATOX1 delivers copper to both ATP7A and ATP7B. It is suggested that phenotypic findings in patients with ATOX1 mutations would be more similar to patients with Menkes disease verses patients with Wilson disease since copper deficiency is more severe and produces congenital clinical symptoms. However, a partially functional ATOX1 protein may provide adequate function in the intestine for copper to be delivered to ATP7A for secretion into the serum, thereby avoiding deficiency, as in Menkes disease. If ATOX1 is an essential protein in the pathway that results in the excretion of copper via ATP7B from the liver, mutations with a partially functional *ATOX1* may provide enough copper for ATP7A yet still lead to an accumulation of copper in the liver.

The usual cause of Wilson disease is the toxic accumulation of copper in the liver and brain. The hepatic copper accumulation could manifest much like the accumulation as seen in Wilson disease patients. Therefore we selected 27 patients with Wilson disease-like phenotypes in whom mutations in *ATP7B* have not yet been identified and screened them for mutations in *ATOX1*. In addition, since Atox1 null mutant mice demonstrate Menkes-like phenotypes, two patients with Menkes disease-like phenotypes were also screened for *ATOX1* mutations. The gene structure was not known at the time this study was initiated.

5.2) METHODS AND MATERIALS

5.2.1) ATOX1 BAC isolation and sequencing

Human BAC library, RPCI-11 (developed by Kazutoyo Osoegawa) was screened at The Hospital for Sick Children, Toronto, using the *ATOX1* cDNA construct (described in section 4.2.1). Isolated BACs (B173, B174 and B175) were digested with EcoR1 and

HindIII, blotted onto a nylon membrane and probed with radiolabeled cDNA. The resulting bands were compared with a published Southern blot of ATOX1 (Klomp et al., 1997) to confirm the presence of ATOX1 sequence in the isolated BACs. Human BACs containing ATOX1 were subcloned into plasmids. Subcloned plasmids were screened using colony lifts probed with radiolabeled ATOX1 cDNA. Positive plasmids were purified and sequenced to identify intron/exon boundaries. During our investigation the sequence of BAC contig AC0011374, containing genomic *ATOX1* became available and was used for completion of identification of intron/exon sequence boundaries by comparing genome sequence with cDNA sequence.

5.2.2) Sequencing of ATOX1 in Patients

Dideoxynucleotide sequencing, using both manual (Amersham), and LONG READER 4200 automated sequencer (Li-Cor), as described by the manufacturer, was used to sequence DNA from selected patients. Exon 1 was sequenced using primer HSC # 2385 (5'- GTT CTG AAA AAG GCC GAC AG -3') and HSC # 2388 (5'- CCT GAG CCC TTC AAG ATC AG -3'). Exon 2 was sequenced using primer HSC # 1942.2 (5'- CAC GAC GTT GTA AAA CGA CCA TGG TCC CCC TGT GTT TG -3') (M13 sequence tagged) and 1943.3 (5'- TCT CTCC TGC AAC ATC TGC –3'). Exon 3 was sequenced using HSC # 1378 (5'-CCC CAT ACC CCA TTT CCT C-3') and M13 sequence tagged # 1382 (5'-CCT ATT GTT AAA GTG TGT CCG AAT TCC AAG GTG TTC GCT CTG ATG-3') (appendix A.1).

Testing for *ATOX1* mutations was carried out on 27 patients that showed copper storage disorders phenotypically similar to Wilson disease, but not confirmed to have the condition by partial mutation analysis. Three different groups of patients were used for

the study (see appendix A.2). The first set included twenty four selected patients who had no identified mutations in *ATP7B* after sequencing at least five mutation rich exons. Sequencing of this limited number of exons should identify at least one mutation in 65% of Wilson disease patients (Cox, unpublished). Ethnic origins included four Asians, one Pakistani, three Saudi Arabians, one First Nations, and the remainder European. Patients included 19 with hepatic onset of symptoms (six under 14yrs, thirteen from 18 to 66 years of age) and five with neurological onset (one at nine years, one at 10 years, and three between 21 and 35 years of age). Three patients had both neurological and hepatic manifestations. Set two consisted of three patients with hepatic onset (two of them Saudi) that could not have ATP7B mutations as the cause of copper storage because they did not share marker haplotypes with their affected sibs. The last set was comprised of two patients with Menkes-like features (low ceruloplasmin and either seizures or a connective tissue disorder) but without typical impaired efflux of copper from fibroblasts (H. Vallance, personal communication).

5.3) RESULTS

5.3.1) BAC isolation

Three BACs containing ATOX1 were identified (B171, B173, B174, and B175). Southern blot analysis showed all contained *ATOX1* genomic sequence by comparing banding pattern with previously published results (Figure 5-1). Resolution of intron/exon boundaries demonstrated that ATOX1 is composed of four exons, with exon 1, 2 and 3 containing the entire coding region (Figure 5-2).

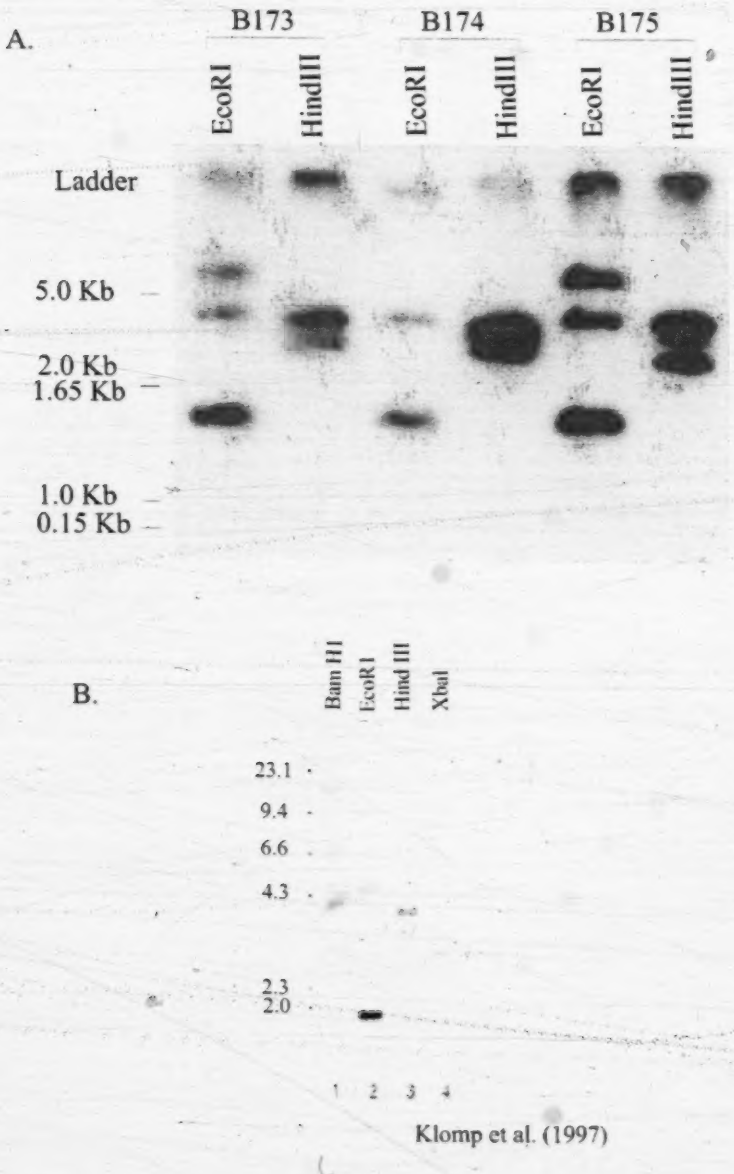

Figure 5-1: Human BACs containing genomic ATOX1 sequence. (A) Digested BACs (B171, B173, B174, and B175) obtained from screening BAC library RPCI-11 probed with ATOX1. (B) Southern blot from genomic DNA probed with ATOX1 from Klomp et al. (1997).

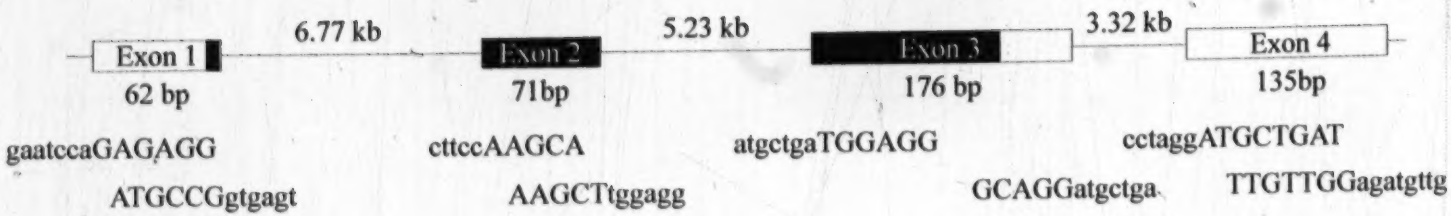

Figure 5-2: Genomic structure of ATOX1. Open boxes represent untranslated cDNA sequence and closed boxes represent translated sequence. Upper case sequence represents exon sequence and lower case sequences represent intronic sequence.

5.3.2) Sequencing of ATOX1 in selected patients

The entire coding region within the three exons containing coding sequence for ATOX1 was sequenced in all twenty-nine patients. No alterations in sequence were identified.

5.4) DISCUSSION

Toxic hepatic copper accumulation is typically due to Wilson disease. Wilson disease is caused by a mutation in the copper transporter ATP7B, a P-type ATPase transporter involved in bile copper excretion. However, some patients with a clinical diagnosis of Wilson disease have yet to have a molecular confirmation by mutation detection. ATOX1 is known to be involved in the copper transport pathway in yeast and chapter four provides supporting evidence that Atox1 and Atp7b co-localize within both the liver and kidney. A mutation in ATOX1 could lead to a disruption in hepatic copper transport, which may be linked to an increase in hepatic copper levels. We sequenced *ATOX1* in DNA from patients with evidence of a copper transport defect. In DNA from twenty-seven selected patients, including three excluded from having Wilson disease by haplotype analysis, no mutations were identified after sequencing the entire coding region of *ATOX1*.

Alternatively, the phenotype resulting from a complete disruption of both functional alleles of *ATOX1* could result in a copper deficiency, as seen in Menkes disease patients and the *Atox1*$^{-/-}$ knockout mouse. We therefore tested two patients with clinical symptoms similar to Menkes disease, who did not show the typical impairment in copper efflux from fibroblasts (Dr. Nina Horn, personal communication). No mutation of *ATOX1* was identified.

The lack of identified *ATOX1* mutations does not exclude the possibility that patients exist with the noted clinical features, but they are not present in our series. Mutations with partial function would likely not have as severe consequences as in the knock-out mouse. The phenotype of patients with ATOX1 mutations could be entirely different. Based on crystal structures it is predicted that this protein acts as a monomer. However, crystallography does indicate the protein can crystallize as a homodimer suggesting that a stable structure is formed when two CXXC motifs interact with a Cu(I) ion. This may functionally represent the CXXC motif of ATOX1 interacting with one of the six CXXC motifs in the N-terminal domain of the transporters ATP7A and ATP7B. Copper is easily transferred in two-coordinate geometry (two Cys residues) from one subunit to another. If present as a homodimer it would suggest copper is typically associated with two ATOX1 molecules in three-coordinate geometry. This three-coordinate geometry would be less conducive to the transfer of copper from the chaperone to a metal binding domain of the transporters and therefore less likely to occur *in vivo*. In heterozygous individuals, if ATOX1 functions as a monomer, 50% of the functional pool would be unable to transfer copper to the transporters. Unless there is a dosage effect, phenotypic consequences will likely not be noticed in heterozygous individuals. This is supported by finding no phenotypes in the *Atox1*$^{-/+}$ mouse model (Hamza et al., 2001). If ATOX1 functions as a dimer, heterozygous individuals will have a 75% reduction in functional homodimer products. This decreased dosage may or may not produce a disease phenotype. Heterozygous individuals will produce symptoms if ATOX1 dosage is critical, suggesting the disorder is dominant.

Additional findings from the knock-out mouse phenotype indicate patients may have neurological manifestations and connective tissue defects. However, since ATOX1

is believed to deliver copper to ceruloplasmin (Fet3p homologue) (Culotta et al., 1999), then patients with a deficiency of ATOX1 would also be predicted to have a decreased level of holoceruloplasmin in the serum.

5.5) REFERENCES

Culotta,V.C., Lin,S.J., Schmidt,P., Klomp,L.W., Casareno,R.L., and Gitlin,J. (1999). Intracellular pathways of copper trafficking in yeast and humans. Adv Exp Med Biol *448*, 247-54.

Gitlin,J.D. (1998). Aceruloplasminemia. Pediatr. Res. *44*, 271-276.

Hamza,I., Faisst,A., Prohaska,J., Chen,J., Gruss,P., and Gitlin,J.D. (2001). The metallochaperone Atox1 plays a critical role in perinatal copper homeostasis. Proc. Natl. Acad. Sci. U. S. A *98*, 6848-6852.

Klomp,L.W., Lin,S.J., Yuan,D.S., Klausner,R.D., Culotta,V.C., and Gitlin,J.D. (1997). Identification and functional expression of HAH1, a novel human gene involved in copper homeostasis. J Biol Chem *272*, 9221-6.

Shiono,Y., Wakusawa,S., Hayashi,H., Takikawa,T., Yano,M., Okada,T., Mabuchi,H., Kono,S., and Miyajima,H. (2001). Iron accumulation in the liver of male patients with Wilson's disease. Am. J. Gastroenterol. *96*, 3147-3151.

CHAPTER 6

GENERAL DISCUSSION AND CONCLUSIONS

The general goal of this thesis was to identify the expression pattern of genes involved in copper transport to help make inferences about their function. The identification of copper transport proteins in yeast has helped provide information on mammalian copper transport, however, much remains to be investigated. Given the complexity of the mammalian system over the single celled yeast, the role of the copper chaperones relative to their putative targets may be more complicated. Organs are separated into various regions each of which can potentially have separate functions and therefore have different expression profiles. Therefore, by analyzing the tissue specific expression pattern, we may determine if a chaperone co-localizes with its putative target as predicted from copper pathway investigations in yeast.

When the experiments for this thesis were initiated, the mammalian expression patterns of proteins involved in copper homeostasis were largely unknown. Some of the chaperones were described in yeast, however their functional role in the copper transport pathway were not yet fully elucidated (Lin and Culotta, 1995; Culotta et al., 1997; Culotta et al., 1995). Mouse orthologues for the copper transporters ATP7A and ATP7B had been identified. Within the mammalian system, the *tx* mouse mutant had recently been discovered to be the result of a mutation within the orthologue of *ATP7B* (Theophilos et al., 1996). In addition, the mottled mouse was determined to be a model system for Menkes disease by having mutations in the orthologue gene *Atp7a* (Levinson et al., 1994).

In order to study the expression patterns of the genes, technical difficulties had to be overcome and protocols developed. Expertise on various protocols, including protocols for non-radioactive probe construction, histology, perfusion, *in situ* hybridization, and immunohistochemistry were very limited on campus. Based on the

protocols I developed for *in situ* hybridization, histology and perfusions, other laboratories on campus (H. McDermid, R. Wevrick and M. Walter laboratories) adapted these protocols for their own purposes. In addition, my cDNA constructs for ATOX1 have been used by Dr. B. Sarkar's laboratory at The Hospital for Sick Children for biochemical analysis of the chaperone.

6.1) COPPER CHAPERONE FOR SUPEROXIDE DISMUTASE

The free radical scavenger superoxide dismutase (SOD1) requires both copper and zinc for functional activity. In yeast, copper is delivered to Sod1p via the copper chaperone Lys7p (Rae et al., 1999). One of the aims of this thesis was to identify mouse homologues to either human or yeast proteins involved in copper movement. Based on work from this thesis the mouse copper chaperone for superoxide dismutase was identified (*Ccsd*). The predicted protein was found to have significant identity with the human protein (86.9%) which included the highly conserved copper binding motif.

In addition to ascertaining the complete cDNA sequence for *Ccsd*, I mapped the mouse gene to mouse chromosome 19 proximal to the centromere and mapped the human orthologue, *CCS*, to 11q13. The proximal region on mouse chromosome 19 and human 11q13 were already known to have conserved synteny. The mapping results did not associate these genes with any region linked with a disorder in either mouse or human relating to predicted effects from copper.

Data for *Ccsd/CCS* in mouse and humans indicate that this chaperone is expressed in many tissues. SOD1 expression in mice is seen in the same array of tissues (de Haan et al., 1994). Similarities in expression between the cytoplasmic target, SOD1, and the chaperone itself provide support that in the mammalian system, *Ccsd/CCS* is a chaperone

that transports copper to superoxide dismutase. Additionally, this mammalian pathway was supported by the observation that the *Ccsd* knockout mouse has oxidative damage similar to that seen in SOD1 deficient mice (Wong et al., 2000).

6.1.1) Future directions

Mapping genes is an important step that may assist investigators in the selection of candidate disease genes. For instance, if positional cloning suggests that either a human or mouse phenotype results from a region where I have mapped *Ccsd/CCS*, these genes may be considered as candidates for the disorder.

The cDNA sequence for *Ccsd* (Genbank accession #AF173379) enables the complete genomic structure for the chaperone to be elucidated. Since genomic sequence was not available, the complete annotation of intron/exon boundaries could be predicted using internet sites such as BCL search launcher to scan the cDNA for possible boundary sites. Alternatively, the mouse genomic database can be compared with the cDNA sequence which would identify an intron sequence that would not be present in the cDNA. After *in silico* predictions of intron/exon boundaries were completed, molecular characterization involving PCR from genomic or BAC DNA would be needed to confirm assumptions. When boundaries have been identified, patients can be screened more easily for mutations if a phenotype or positional cloning study suggests *Ccsd/CCS* as a candidate for a disorder.

The alternative bands identified by northern blot analysis should be investigated. As a first step toward understanding their functional significance, these alternative bands can be isolated and sequenced.

Based on northern blot analysis and phenotypes seen in mouse knockouts for *Ccsd* and *Sod1*, it is predicted that this chaperone could have a sole function for copper delivery to SOD1 in the mammalian system. Therefore, more detailed investigations into tissue expression patterns should demonstrate a co-localization of the chaperone with its target. Because of the importance of SOD1 in neuronal tissue, expression studies in the brain would be an excellent tissue on which to begin this inquiry.

6.2) ATOX1 EXPRESSION

The copper chaperone Atox1 is expressed in most tissues (Hamza et al., 2000; Naeve et al., 1999). This protein, initially discovered in yeast, was also found to be involved in the transport pathway associated with the eventual delivery to the yeast copper dependent oxidase Fet3p, via the membrane P-type ATPase transporters (Lin and Culotta, 1995). The mammalian orthologue of Fet3p is the serum copper protein ceruloplasmin. An additional aim of this thesis was to investigate the expression pattern of proteins involved in copper transport. Based on investigations of mammalian expression from this thesis, *Atox1* has been found to be expressed in specific structures throughout the liver, kidney, and placenta during mouse development.

6.2.1) Liver

The portal veins within the liver contain blood flowing from the intestine, and are full of nutrients absorbed from ingested food. Blood then passes over the various zones of the liver, then collects in central veins that feed into hepatic veins and eventually into the heart for delivery to the body. Ingested copper, after initial absorption, is released

back into the blood stream from the liver, in part incorporated as a component of ceruloplasmin (Weiss and Linder, 1985).

The expression of *Atox1* in the mouse liver indicated localization to hepatocytes surrounding central and hepatic veins and the zone 3 (nutrient poor) hepatocytes. The presence of Atox1 in hepatocytes surrounding the central and hepatic veins suggests copper is actively transported in these cells.

6.2.1.1) Future directions

Ceruloplasmin is a minor source, if at all, for the delivery of copper to tissue. Since Atox1 is believed to deliver copper to ceruloplasmin via the P-type ATPase transporter, I hypothesized, based on my work, that within the liver, ceruloplasmin is expressed in hepatocytes surrounding the hepatic and central veins. If ceruloplasmin is expressed in these veins, it would support the function of Atox1/ATOX1 in the pathway responsible for delivering copper into ceruloplasmin. In addition, if Atox1 was instrumental in indirectly delivering copper to ceruloplasmin, it would be predicted that holoceruloplasmin levels in the serum of the *Atox1*$^{-/-}$ mouse would be below normal.

6.2.2) Kidney

The kidney plays an important role, not only in copper absorption, but in copper excretion. The first wave of ingested copper is delivered to the liver and kidney, which effectively remove all traces from the plasma (reviewed in Linder et al., 1998). The kidney is a complex organ. Regions involved in copper transport should be identified in part by identifying where Atox1 is expressed.

Within the kidney, Atox1 is expressed both in the glomeruli and the medulla. Glomeruli are the initial site of blood filtration. There are three major layers comprising the glomerulus. The first layer is composed of endothelial cells, the second layer is a basement membrane and the third layer is composed of epithelial cells on the outer surfaces of the glomerular capillaries. The glomerulus has an extremely high degree of selectivity for molecular size. High molecular weight components are excluded from entering the filtrate by the glomerular sieve (Figure 6-1) and remain in the serum. Typically, proteins, or amino acids, of molecular weight less than 69 kDa (e.g. insulin and metallothionein) pass through the sieve while proteins with a molecular weight of 69 kilodaltons are largely maintained in the plasma. The smaller the protein, the more easily it can penetrate the sieve. After the initial ingestion of copper, copper associates with high molecular weight proteins in the blood that deliver copper to the kidney and liver. Copper binding proteins such as albumin (69 kDa), and possibly transcuprein (270 kDa), are both high molecular weight compounds that carry ingested copper to the kidney during the first wave of absorption, however they do not penetrate the glomerular sieve. Copper may be actively transferred from these high molecular weight proteins in the glomerulus. The presence of Atox1 in the glomeruli suggests that the chaperone has a critical role in renal copper transfer and supports the hypothesis that the glomeruli are involved in renal copper retention.

However, after the first wave of copper absorption, copper is typically thought of as being bound to histidine or other small molecular complexes in physiological fluids that enter the glomerular filtrate without mediation by an active transport.

Once copper enters the filtrate, it progresses through the proximal convoluted tubules and later to the loops of Henle. One study found that the loops of Henle are

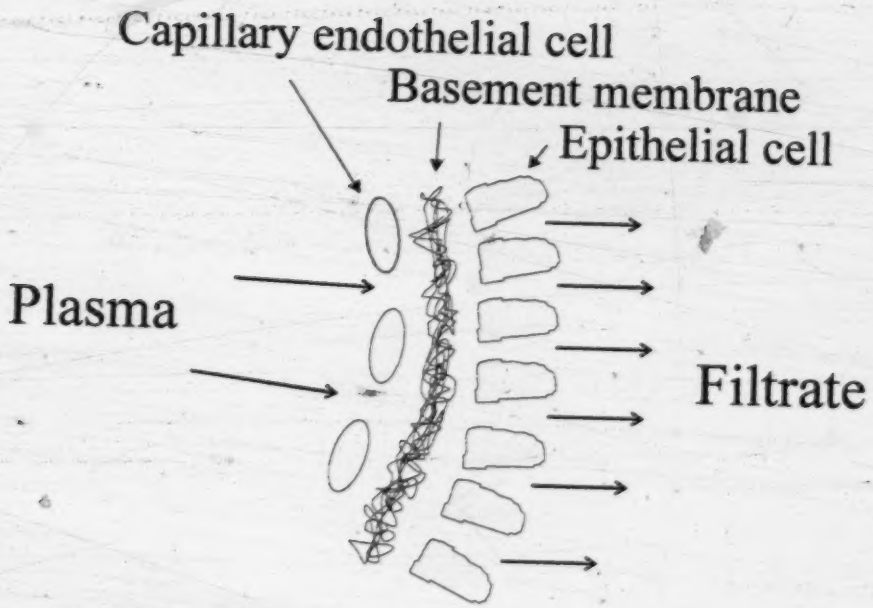

Modified from Guyton (1990)

Figure 6-1: Schematic of glomerular sieve.

functionally involved in the re-absorption of iron (Wareing et al., 2000). Their results also indicated that copper successfully competed against iron for absorption, suggesting that copper is also absorbed in the loops of Henle. The localization of Atox1 to the loops of Henle suggests this region also has a critical role in renal re-absorption of copper.

6.2.2.1) Future directions

The importance of Atox1 in the kidney could also be studied in the mouse knockout. If Atox1 is critical for the initial entry of copper into the filtrate it would be predicted that in the absence of the chaperone, copper would accumulate in the glomerulus. In addition, the involvement of Atox1 in the kidney may be very similar to the presumed function in the liver. Ceruloplasmin has been shown to be expressed to some degree in the kidney (Gaitskhoki et al., 1990). Investigations into possible co-localization of Atox1 with ceruloplasmin may provide additional evidence supporting the importance of Atox1 in the mammalian copper transport pathway involving ceruloplasmin.

6.2.3) ATOX1 co-expression with ATP7A and ATP7B

Yeast two hybrid interaction studies involving the copper chaperone have shown that Atx1p interacts with the copper transporter Ccc2p (Pufahl et al., 1997). The human orthologue of Atx1p, ATOX1, has also been shown to interact with the Ccc2p orthologues, ATP7A and ATP7B, by yeast-two-hybrid studies, mammalian-two-hybrid studies (Larin et al., 1999), and co-immunoprecipitation (Hamza et al., 1999). In addition, crystal structures suggest a molecular mechanism for protein recognition and metal ion exchange between the chaperone and the copper transporters (reviewed in

Rosenzweig, 2001). These mammalian studies suggest that Atox1 acts as a copper chaperone for the copper transporters Atp7a and Atp7b. I therefore hypothesized that the expression for the chaperone would co-localize with the expression of the transporters in the mammalian system. To address this hypothesis, cell specific expression of Atox1 in liver, kidney and placenta was compared with the expression patterns of Atp7a and Atp7b in the same tissues.

Immunohistochemical localization of Atp7b within the liver was compared with the localization of Atox1 in adjacent sections. Atp7b and Atox1 were both found in zone three hepatocytes and central veins. To date, neither data from this thesis nor previously published data for Atp7b in human and rat show expression in the bile epithelial tissue (Schaefer et al., 1999a; Schaefer et al., 1999b).

The kidney is particularly interesting because both Atp7a and Atp7b are expressed there. Copper has been found to have a regulated steady state level within the glomeruli, proximal and distal tubules; however, copper is not typically seen at any significant level within the loops of Henle (Kodama et al., 1993). Initial studies localized the expression of Atp7a to the proximal and distal convoluted tubules of the mouse kidney (Figure 6-2). Grimes et al. (1997) showed localized expression of Atp7a in both the proximal and distal tubules but the distal tubules showed significantly darker staining. If Atp7a transporter activity was responsible for copper accumulation, then accumulation would also be expected in the distal convoluted tubules since Atp7a is expressed there as well, but this is not the case. However, in mottled mice, it is possible that copper does not accumulate in the distal tubules because Atp7b, in the loops of Henle, is capable of removing all excess copper from the filtrate. However, this dependence in Atp7b activity in the loops of Henle to alleviate distal tubule accumulation would not explain why in

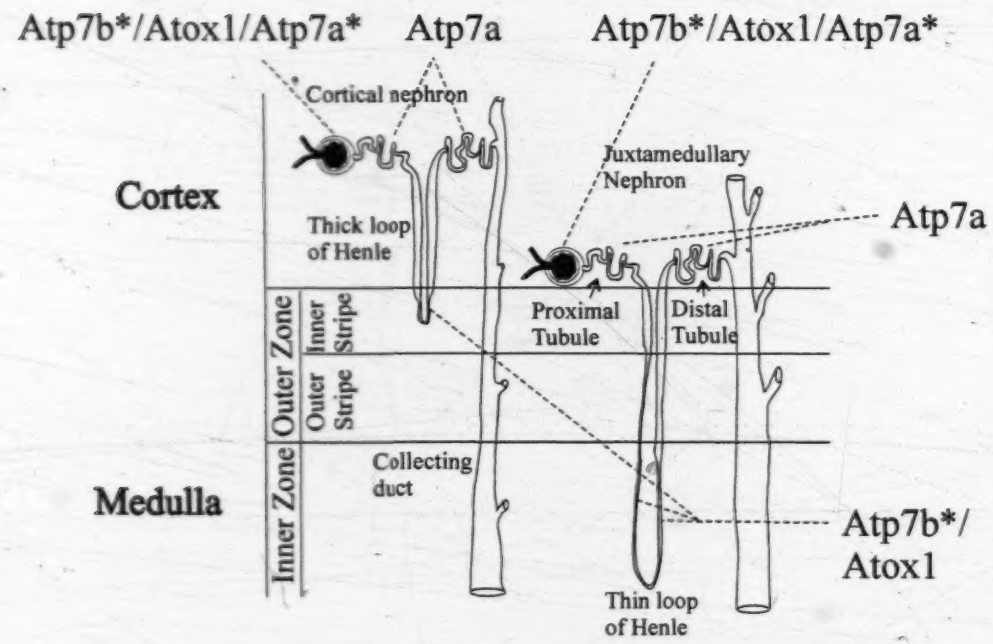

Figure 6-2: Schematic representation of the expression patterns of Atp7a, Atp7b, and Atox1. Expression of Atp7a (Grimes et al) and Atp7b from the present thesis (Chapter 3). Atp7a* signal suggested in Chapter 3, but not confirmed. Asterisks indicates signals shown in Chapter 3.

Wilson disease patients, where Atp7b is dysfunctional in the loops of Henle, elevated levels of copper are not found in the distal tubules. Atox1 expression was seen in the glomeruli and the loops of Henle, unlike the expression of Atp7a shown in the proximal and distal tubules (Figure 6-2). These differences in localization raise the possibility that there may be another chaperone that functions in association with Atp7a in the distal and proximal convoluted tubules. This is also a possible explanation for why northern blot analysis demonstrates that skeletal muscle does not express Atox1 but does express Atp7a.

Studies from this thesis localized expression of Atp7b, the paralogue of Atp7a, to the glomeruli and the loops of Henle. This renal localization completely overlaps with the localization of Atox1 supporting my hypothesis that the chaperone will co-localize with the copper transporter.

6.2.3.1) Future directions

This thesis supports the hypothesis that, as in the liver, Atp7b in the kidney requires Atox1 for its role in the copper transport pathway. Co-localization studies from additional tissues will support the role Atox1 has with Atp7b and the possible lack of a functional role with Atp7a. However, the expression patterns in the kidney neither confirm nor deny this possibility. Immunohistochemical investigations with Atp7a may provide interpretable results as to the renal expression of this transporter.

The glomerulus is highly structured and is composed of endothelial and epithelial cell types. Since Atox1 and Atp7b are localized to the glomerulus, a higher resolution study may indicate which cell types within the glomerulus express each protein.

6.3) MODELS FOR RENAL COPPER HOMEOSTASIS

I originally hypothesized that proteins involved in copper homeostasis, namely Atox1, Atp7a and Atp7b, would be expressed in the proximal tubules because copper accumulates in these tubules and Atp7a has been demonstrated to express there. Evidence from this thesis does not support my initial hypothesis. I discovered that Atp7b and Atox1 are expressed in the glomeruli and loops of Henle and not the proximal convoluted tubules. To explain the difference between the renal localization of the copper transport proteins and the renal accumulation of copper, I suggest two different models.

The first model assumes that the role of the kidney is in the retention of copper (Figure 6-3). Copper deficiency is not well tolerated, so over the evolutionary time scale, mechanisms to avoid copper loss would be advantageous. Since copper is seen in cells of the glomerulus, and the kidney is known to be involved in removing the initial wave of ingested copper, copper is likely actively removed from high molecular weight albumin and transcuprein and transported into the glomerular cells. Both copper transporters Atp7a and Atp7b have been demonstrated to have roles in copper efflux (Nagano et al., 1998; Petris et al., 1996). The absorbed copper would be actively released back into the serum, explaining the necessity of having transporters involved in copper efflux within the glomerulus. In the absence of these transporters, copper is not actively transported back into the serum but makes its way by an unknown mechanism into the filtrate, where it accumulates in the proximal tubules.

The cause of copper accumulation specific to the proximal tubules cannot be addressed by this study. However, localization studies involving MT-3 revealed expression in the kidney, specifically in cells in the proximal and distal tubules as well as

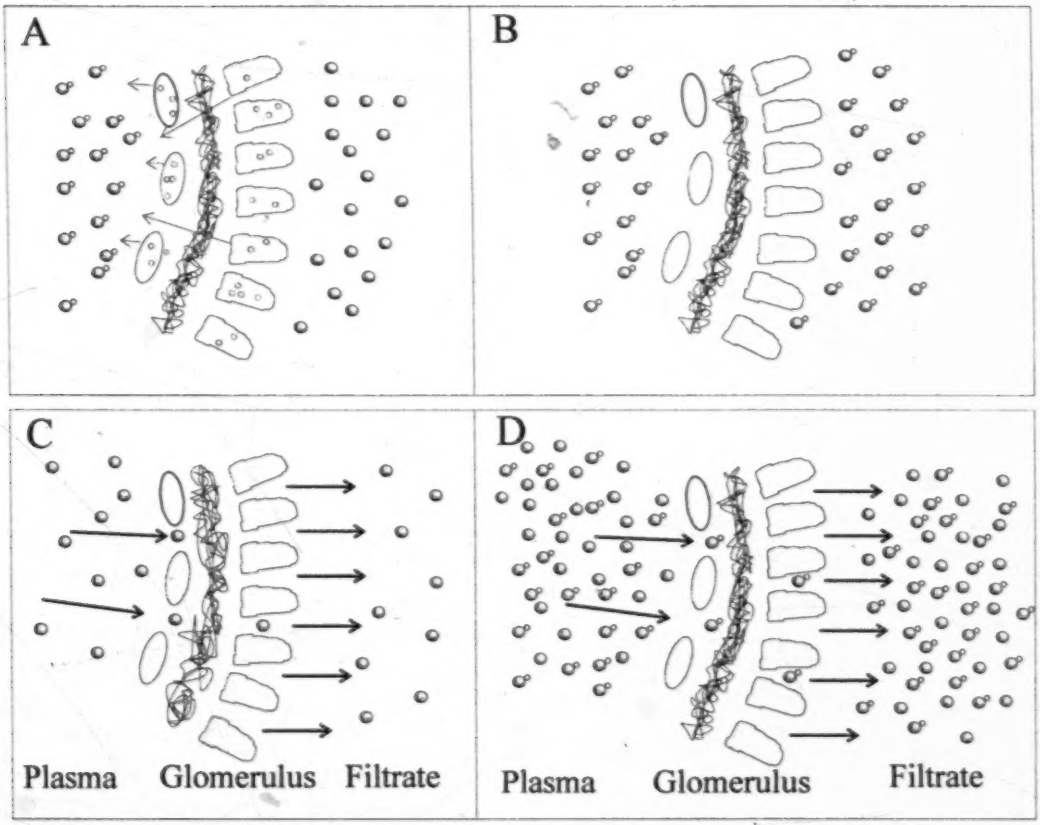

Figure 6-3: Models for renal copper homeostasis, excluding Atp7a signal data. Copper retention model (A&B) suggests that normally (A) copper is taken up by the glomerular cells from serum proteins and actively excreted back into the serum by copper transporter ATP7B. When ATP7B is dysfunctional (B), copper passes through sieve and enters the filtrate. The second model (C&D), is based on an increase of low molecular weight (LMW) substances associated with copper. (C) Under normal conditions, LMW substances in the serum are not associated with copper. (D) In Wilson disease, copper associated LMW substances increase in the serum and passively enter the filtrate. Both models assume that once copper is in the filtrate it is taken up and retained in the proximal tubules. Circles represent serum proteins. Double circles represent copper associated with serum proteins, copper being the smaller circle.

the glomeruli (Kim et al., 2002; Hoey et al., 1997; Garrett et al., 1999). Therefore, localized copper accumulation solely in the proximal tubules is not likely due to a site specific expression of MT-3. However, there are a total of five MT isoforms, four of which have not been investigated for renal specific expression.

As the filtrate emerges from the glomerulus, it progresses through the proximal convoluted tubule and enters the loop of Henle where Atp7b is expressed. The loops of Henle are known to function in the re-absorption of ions including iron (Wareing et al., 2000) and therefore suggest that Atp7b is involved in the re-absorption of copper in this region. In Wilson disease patients, the increase in copper within the urine may be related to two factors: first, the large increase of copper in serum overflows into the filtrate and/or second the inability for copper to be reabsorbed within the loops of Henle.

The second model is related to an increase, in serum of patients, of low molecular weight substances that can passively enter the glomerular sieve and deposit copper in the proximal tubules (Figure 6-3). Normally the small cysteine rich protein metallothionein (MT) is present within the serum (Mulder et al., 1991). In their cases of copper induced liver cirrhosis, MT levels in the serum increase as much as ten fold. In LEC rats, serum levels of the low molecular weight CuMT increase and are temporally linked to copper accumulation in the kidney (Nomiyama et al., 1999). They suggest that these elevated levels of CuMT in the serum are responsible for the copper accumulation in the proximal convoluted tubules. Additional studies with cadmium demonstrate that orally ingested cadmium induced intestinal metallothionein and is at least partially responsible for downstream renal accumulation in the proximal tubules (Elsenhans et al., 1992). In both Menkes and Wilson disease patients, CuMT accumulates in the intestine and liver respectively (Shiraishi et al., 1991). Therefore, renal copper accumulation could be

coupled with the accumulation of CuMT in the intestine and the liver and its potential release into the serum (Figure 6-3).

To investigate the importance of metallothionein in copper deficient mice, one study crossed a mottled mouse mutant (Mo^{ma}) with a metallothionein deficient mouse, resulting in an embryonic lethality at gestational stage E11 (Shiraishi et al., 1987). Since metallothionein appears to be critical in mice, another approach is required to study the effect of elevated CuMT levels in the mouse. For example, the effect of elevated levels of CuMT in the serum could be studied by measuring the amount of radioactivity deposited within the proximal convoluted tubules after administering radiolabeled CuMT into the blood of mice.

6.4) PLACENTA AND DEVELOPMENT

6.4.1) Developmental expression

The mouse *Atox1* knockout model also demonstrates the importance of this chaperone during fetal development (Hamza et al., 2001). Northern blot analysis in my studies indicates that *Atox1* is up-regulated near the time of birth and also supports an earlier finding of a longer alternative transcript of approximately the same length (Naeve et al., 1999). This time, the alternative product is seen up to embryonic gestation stage of E10.5 and once again appears E16.5. The reason for *Atox1* up-regulation prior to birth and the function of the alternative transcript is not yet known.

6.4.2) Atox1 co-expression with ATP7B

Initial studies of the mouse *Atox1* knockout suggested the importance of the chaperone in the placental transfer of copper to the fetus (Hamza et al., 2001). Results

from this thesis show that during development, *Atox1* is expressed both in the maternal and fetal portion of the placenta. It appears that the fetal portion has a stronger signal than the maternal portion. This difference in signal may be a reflection of either a higher level of expression in the fetal portion or may be related to the greater tissue density in the fetal portion.

Some similar observations are made when the expression of Atp7b and Atox1 are compared in mouse embryonic development. Although Atox1 is expressed at high levels throughout development, as the embryo approaches maturity, the amount of Atox1 transcripts apparently increase. This increase could either be due to enhanced promoter activity, producing more mRNA transcripts, or conversely, may be caused by an increased stability of the mRNA. Interestingly, prior to birth, Atp7b is also up-regulated. Although the extent and patterns of increased transcript are different, it is interesting that both genes are up-regulated prior to birth.

One difference in the expression pattern between Atox1 and Atp7b was observed in the placenta. Studies from this thesis demonstrated Atox1 to be expressed in both the maternal and fetal portion of the placenta. Previous expression studies on Atp7b in the rat localize the transporter solely to the maternal portion of the placenta (Muramatsu et al., 1998). Although there is a co-localization of the chaperone with the transporter in the maternal portion, the apparent lack of Atp7b in the fetal portion raises some interesting possibilities about additional transporters with which Atox1 might associate within the fetal portion.

6.4.3) Future directions

Based on developmental northern blots from both this thesis and other work (Naeve et al., 1999), Atox1 appears to have an alternative transcript. Future investigations, directed at cloning and sequencing this longer transcript, may provide some insight into its function.

If the sole purpose of Atox1 is to deliver copper to the copper transporter Atp7b, the lack of expression in the fetal portion of the placenta poses an interesting dilemma. Either the rat expression pattern is different from that of the mouse and Atp7b is expressed in the fetal portion of the mouse placenta, or Atox1 has a function that is independent of its role for copper delivery to Atp7b. This can be addressed by trying to find additional transporters that are localized in the fetal portion. If Atp7a is expressed in the placenta, Atox1 may interact functionally with this transporter in the placenta.

Copper accumulates in the placenta of *Atox1* knock-out pregnant females. This accumulation was less marked in homozygous pregnant females ($Atox1^{-/-}$) than in heterozygous mothers ($Atox1^{-/+}$) (Hamza et al., 2001). I hypothesize that this difference in the amount of copper in the placenta is partially a result of the role of Atox1 in holoceruloplasmin biosynthesis. Investigations in the rat have indicated that holoceruloplasmin delivers copper to the placenta for eventual incorporation into the fetus via ceruloplasmin receptors in the placenta, however, holoceruloplasmin is not critical for fetal development (Lee et al., 1993; Sasina et al., 2000). If Atox1 is necessary for the incorporation of copper into apoceruloplasmin via a P-type ATPase transporter, a deficient pregnant female ($Atox1^{-/-}$) would be expected to have lower holoceruloplasmin level in the serum than a heterozygous pregnant female ($Atox1^{-/+}$).

6.5) FINAL CONCLUSION

My original hypothesis that Atox1 will co-localize with the transporters Atp7a and Atp7b is partly supported. The expression of the chaperone completely overlaps with that of Atp7b in liver and kidney. Within the placenta, Atox1 does co-express with Atp7b in the maternal portion, supporting the notion that the transporter requires copper from Atox1 for function. However, kidney expression data, indicate that Atp7a does not co-localize with its proposed mammalian copper chaperone Atox1. Data from the skeletal muscle also indicates that there are apparent differences in the chaperone and transporter expression patterns. This contradicts my original hypothesis that Atox1 will co-express with both Atp7a and Atp7b. Atox1 apparently co-expresses with Atp7b in each tissue examined, but does not co-express with Atp7a in each tissue. This suggests that an additional copper chaperone for Atp7a may exist in the mammalian system. However, after searching the database for proteins similar to ATOX1, sequences with significant homology to this chaperone have not yet been discovered. The highest conservation comes from a contig from chromosome 18 (RP11-734B5) that has a stretch of 20 identical nucleotides in a non-conserved region.

The general aim of this thesis was to study the tissue specific expression of genes, namely Atox1, Atp7a and Atp7b in an attempt to elucidate possible functions within specific organs and seek pathway interactions suggested by yeast studies. Based on co-localization of expression patterns in the kidney and liver, Atox1 seems to have a vital role in the mammalian copper transport pathway involving Atp7b. The role of Atox1 in the mammalian copper transport pathway involving Atp7a is not yet resolved. However, I provide evidence that in certain tissues, namely the placenta, Atox1 is expressed in the fetal portion previously indicated not to express Atp7b. This lack of co-localization is

not yet understood. In the liver, Atox1 appears to be important in hepatocytes surrounding the central and hepatic veins. These hepatocytes have not previously been implicated in copper transport. Within the kidney, the glomeruli and the loops of Henle express Atp7b and Atox1 suggesting that these regions of the organ are important in copper homeostasis.

Expression patterns from additional proteins, namely MURR1, ceruloplasmin and metallothionein isoforms, in these three organs may provide a more detailed understanding of organ functions in copper transport.

6.6) REFERENCES

Culotta,V.C., Joh,H.D., Lin,S.J., Slekar,K.H., and Strain,J. (1995). A physiological role for Saccharomyces cerevisiae copper/zinc superoxide dismutase in copper buffering. J Biol Chem *270*, 29991-7.

Culotta,V.C., Klomp,L.W., Strain,J., Casareno,R.L., Krems,B., and Gitlin,J.D. (1997). The copper chaperone for superoxide dismutase. J Biol Chem *272*, 23469-72.

de Haan,J.B., Tymms,M.J., Cristiano,F., and Kola,I. (1994). Expression of copper/zinc superoxide dismutase and glutathione peroxidase in organs of developing mouse embryos, fetuses, and neonates. Pediatr Res *35*, 188-96.

Elsenhans,B., Kolb,K., Schumann,K., and Forth,W. (1992). Endogenous intestinal metallothionein possibly contributes to the renal accumulation of cadmium. IARC Sci. Publ. 225-230.

Gaitskhoki,V.S., Voronina,O.V., Denezhkina,V.V., Pliss,M.G., Puchkova,L.V., Shvartsman,A.L., and Neifakh,S.A. (1990). [Expression of ceruloplasmin gene in various organs of the rat]. Biokhimiia. *55*, 927-937.

Garrett,S.H., Sens,M.A., Todd,J.H., Somji,S., and Sens,D.A. (1999). Expression of MT-3 protein in the human kidney. Toxicol. Lett. *105*, 207-214.

Guyton,M.D. (1990). Textbook of Medical Physiology. HBJ College & School Division.

Hamza,I., Faisst,A., Prohaska,J., Chen,J., Gruss,P., and Gitlin,J.D. (2001). The metallochaperone Atox1 plays a critical role in perinatal copper homeostasis. Proc. Natl. Acad. Sci. U. S. A *98*, 6848-6852.

Hamza,I., Klomp,L.W., Gaedigk,R., White,R.A., and Gitlin,J.D. (2000). Structure, expression, and chromosomal localization of the mouse Atox1 gene. Genomics *63*, 294-7.

Hamza,I., Schaefer,M., Klomp,L.W., and Gitlin,J.D. (1999). Interaction of the copper chaperone HAH1 with the Wilson disease protein is essential for copper homeostasis. Proc Natl Acad Sci U S A *96*, 13363-8.

Hoey,J.G., Garrett,S.H., Sens,M.A., Todd,J.H., and Sens,D.A. (1997). Expression of MT-3 mRNA in human kidney, proximal tubule cell cultures, and renal cell carcinoma. Toxicol. Lett. *92*, 149-160.

Kim,D., Garrett,S.H., Sens,M.A., Somji,S., and Sens,D.A. (2002). Metallothionein isoform 3 and proximal tubule vectorial active transport. Kidney Int. *61*, 464-472.

Kodama,H., Abe,T., Takama,M., Takahashi,I., Kodama,M., and Nishimura,M. (1993). Histochemical localization of copper in the intestine and kidney of macular mice: light and electron microscopic study. J. Histochem. Cytochem. *41*, 1529-1535.

Larin,D., Mekios,C., Das,K., Ross,B., Yang,A.S., and Gilliam,T.C. (1999). Characterization of the interaction between the Wilson and Menkes disease proteins and the cytoplasmic copper chaperone, HAH1p. J Biol Chem *274*, 28497-504.

Lee,S.H., Lancey,R., Montaser,A., Madani,N., and Linder,M.C. (1993). Ceruloplasmin and copper transport during the latter part of gestation in the rat. Proc. Soc. Exp. Biol. Med. *203*, 428-439.

Levinson,B., Vulpe,C., Elder,B., Martin,C., Verley,F., Packman,S., and Gitschier,J. (1994). The mottled gene is the mouse homologue of the Menkes disease gene . Nat Genet *6*, 369-73.

Lin,S.J. and Culotta,V.C. (1995). The ATX1 gene of Saccharomyces cerevisiae encodes a small metal homeostasis factor that protects cells against reactive oxygen toxicity. Proc Natl Acad Sci U S A *92*, 3784-8.

Linder,M.C., Wooten,L., Cerveza,P., Cotton,S., Shulze,R., and Lomeli,N. (1998). Copper transport. Am. J. Clin. Nutr. *67*, 965S-971S.

Mulder,T.P., Janssens,A.R., Verspaget,H.W., and Lamers,C.B. (1991). Plasma metallothionein concentration in patients with liver disorders: special emphasis on the relation with primary biliary cirrhosis. Hepatology *14*, 1008-1012.

Muramatsu,Y., Yamada,T., Moralejo,D.H., Suzuki,Y., and Matsumoto,K. (1998). Fetal copper uptake and a homolog (Atp7b) of the Wilson's disease gene in rats. Res. Commun. Mol. Pathol. Pharmacol. *101*, 225-231.

Naeve,G.S., Vana,A.M., Eggold,J.R., Kelner,G.S., Maki,R., Desouza,E.B., and Foster,A.C. (1999). Expression profile of the copper homeostasis gene, rAtox1, in the rat brain. Neuroscience *93*, 1179-87.

Nagano,K., Nakamura,K., Urakami,K.I., Umeyama,K., Uchiyama,H., Koiwai,K., Hattori,S., Yamamoto,T., Matsuda,I., and Endo,F. (1998). Intracellular distribution of the Wilson's disease gene product (ATPase7B) after in vitro and in vivo exogenous expression in hepatocytes from the LEC rat, an animal model of Wilson's disease. Hepatology *27*, 799-807.

Nomiyama,K., Nomiyama,H., Kameda,N., Tsuji,A., and Sakurai,H. (1999). Mechanism of hepatorenal syndrome in rats of Long-Evans Cinnamon strain, an animal model of fulminant Wilson's disease. Toxicology *132*, 201-214.

Petris,M.J., Mercer,J.F., Culvenor,J.G., Lockhart,P., Gleeson,P.A., and Camakaris,J. (1996). Ligand-regulated transport of the Menkes copper P-type ATPase efflux pump from the Golgi apparatus to the plasma membrane: a novel mechanism of regulated trafficking. EMBO J. *15*, 6084-6095.

Pufahl,R.A., Singer,C.P., Peariso,K.L., Lin,S.J., Schmidt,P.J., Fahrni,C.J., Culotta,V.C., Penner-Hahn,J.E., and O'Halloran,T.V. (1997). Metal ion chaperone function of the soluble Cu(I) receptor Atx1 . Science *278*, 853-6.

Rae,T.D., Schmidt,P.J., Pufahl,R.A., Culotta,V.C., and O'Halloran,T.V. (1999). Undetectable intracellular free copper: the requirement of a copper chaperone for superoxide dismutase . Science *284*, 805-8.

Rosenzweig,A.C. (2001). Copper delivery by metallochaperone proteins. Acc. Chem. Res. *34*, 119-128.

Sasina,L.K., Tsymbalenko,N.V., Platonova,N.A., Puchkova,L.V., Voronina,O.V., Gyulikhandanova,N.E., and Gaitskhoki,V.S. (2000). Isolation and partial characterization of cDNA clone of human ceruloplasmin receptor. Bull. Exp. Biol. Med. *129*, 491-495.

Schaefer,M., Hopkins,R.G., Failla,M.L., and Gitlin,J.D. (1999a). Hepatocyte-specific localization and copper-dependent trafficking of the Wilson's disease protein in the liver. Am J Physiol *276*, 639-46.

Schaefer,M., Roelofsen,H., Wolters,H., Hofmann,W.J., Muller,M., Kuipers,F., Stremmel,W., and Vonk,R.J. (1999b). Localization of the Wilson's disease protein in human liver. Gastroenterology *117*, 1380-1385.

Shiraishi,N., Kondoh,S., Hiraki,Y., Aono,K., and Taguchi,T. (1987). Metallothionein in kidney and liver of the macular mouse as an animal model of Menkes' kinky hair disease. Physiol Chem. Phys. Med. NMR *19*, 227-233.

Shiraishi,N., Taguchi,T., and Kinebuchi,H. (1991). Metallothionein messenger RNA levels in the macular mutant mouse: an animal model of Menkes' kinky-hair disease. Biol. Neonate *60*, 52-61.

Theophilos,M.B., Cox,D.W., and Mercer,J.F. (1996). The toxic milk mouse is a murine model of Wilson disease. Hum Mol Genet *5* , 1619-24.

Wareing,M., Ferguson,C.J., Green,R., Riccardi,D., and Smith,C.P. (2000). In vivo characterization of renal iron transport in the anaesthetized rat. J. Physiol *524 Pt 2*, 581-586.

Weiss,K.C. and Linder,M.C. (1985). Copper transport in rats involving a new plasma protein. Am. J. Physiol *249*, E77-E88.

Wong,P.C., Waggoner,D., Subramaniam,J.R., Tessarollo,L., Bartnikas,T.B., Culotta,V.C., Price,D.L., Rothstein,J., and Gitlin,J.D. (2000). Copper chaperone for superoxide dismutase is essential to activate mammalian Cu/Zn superoxide dismutase. Proc Natl Acad Sci U S A *97*, 2886-91.

APPENDICES

A.1) PRIMERS

Primers used for sequencing of ATOX1

HSC #	Primer name	Primer Sequence
2388	E2-L2	5'-CCTGAGCCCTTCAAGATCAG-3'
2385	E2-R2	5'-GTTCTGAAAAAGGCCGACAG-3'
1942.2	HAH1.P1	5'-CACGACGTTGTAAAACGACCATGGTCCCCCTGTGTTTG-3'
1943.2	HAH1.P2	5'-TCTCTCCTGCAACATCTGC-3'
1378	ATOX1.E3F	5'-CCCCATACCCCATTTCCTC-3'
1382	ATOX1.E3R	5-CCTATTGTTAAAGTGTGTCCGAATTCCAAGGTGTTCGCTCTGATG-3'

Primers used for ATOX1 amplification (Human)

HSC #	Primer name	Primer Sequence
1036	Atox1.3	5'-TGACGAATTCTCAGTCATGCCGAAGCACGAG-3'
1375	HAH1.R1	5'-CCAAGTCCCAGGTCTGTCTG-3'

Primers used for Atox1 amplification (Mouse)

HSC #	Primer name	Primer Sequence
1036	Atox1.3	5'-TGACGAATTCTCAGTCATGCCGAAGCACGAG-3'
1037	Atox1.4	5'-TGACGAATTCCTGGACTGGACTGAGCAGTTGG-3'

Primers used for Atp7b amplification

HSC #	Primer name	Primer Sequence
1944	ATP7B.A1	5'-CACGACGTTGTAAAACGACTTCTCTCAGTGTTGGTCGC-3'
1945	ATP7B.A2	5'-GTGTCAAAGAAGGTCACGG-3'

Primers used for Atp7a amplification

HSC #	Primer name	Primer Sequence
1957	MNK.UP	5'-GGATGACCTGTGCTTCTTG-3'
1956	MNK.LP	5'-CAGCACAATCAGCACATC-3'

Primers used for Ccsd amplification (Human)

HSC #	Primer name	Primer Sequence
1413.2	CCS.R1	5'-GAAAGTGCTCGCCCTGGAGG-3'
1415.2	CCS.L1	5'-TGTCCGTGCTGTGCTGACG-3'

A.1) PRIMERS (continued)

Primers used for Ccsd amplification (Mouse)

HSC #	Primer name	Primer Sequence
-	MCCS.L1	5'-CTAGGAATTCTGATGGAGCATCTCATGGGG-3'
-	MCCS.R1	5'-CTAGGAATTCTTGGGCTGAGTCCTTTCGGC-3'

Primers used for Ccsd RH mapping

HSC #	Primer name	Primer Sequence
-	CCS.UP	5'-TCAGTTGGAGAACCAGATGG-3'
-	CCS.LP	5'-TTCTGTAATTGGCTACTGCCC-3'

A.2) Patient list for ATOX1 mutation screening

DNA #	Phenotype	Age	Ethnic	Disease phenotype
1192	N	9	It/It	Wilson disease
1647	N,P	20	Pak/Pak	Wilson disease
1897	H	58	Sicily/Sic	Wilson disease
1908	N,P	24	NFLD/NFLD	Wilson disease
1919	N	35	N. European	Wilson disease
1920	N	21	Brit/Germ	Wilson disease
1923	H	13	Saudi/Sau	Wilson disease
1926	H	6	Saudi/Sau	Wilson disease
1928	H	45	Vietnam/Viet	Wilson disease
1935	H	13	Saudi/Sau	Wilson disease
1992	H	3	SephJew/French	Wilson disease
2044	N	10	Asian	Wilson disease
2131	N,P	24	England/Eng	Wilson disease
2197	H	29	Greek/Germ	Wilson disease
2200	H	66	Brit/Brit	Wilson disease
2202	H	10	Siox/FrPQ-Sic	Wilson disease
2215	H	49	Brit/Brit	Wilson disease
2260	H	65	Vietnam/Viet	Wilson disease
2261	H	12	FirstNation/FN	Wilson disease
2271	H	NA	NA	Wilson disease
2277	H	38	ChinCanto/ChC	Wilson disease
2283	N	35	Brit/Brit-Russ	Wilson disease
2314	H	40	China/China	Wilson disease
2330	N	31	N. European/N. Eu	Wilson disease
2409	H	47	German/Germ	Wilson disease
2442	H	61	Brit/Brit	Wilson disease
2524	H	18	Hung/Germ/Fr	Wilson disease
2850			NA	Menkes disease
2851			NA	Menkes disease

H= Hepatic
N= Neurological
P= Psychiatric
NA= Not available